

CONTRACT N°: FIKW-CT-2001-00179

ISSUE CERTIFICATE

# PDS-XADS

## Preliminary Design Studies of an Experimental Accelerator-Driven System

**Workpackage N°: 3****Identification N° : DEL/02/009****Revision : 0**


### REQUIREMENTS FOR THE XADS ACCELERATOR & THE TECHNICAL ANSWERS

**Dissemination level: PU****Issued by: CEA****Reference: DAPNIA - 02 - 302****Status: Final****Summary:**

This deliverable (D9) describes the basic accelerator requirements of a proton accelerator needed for the XADS project. After indicating the most important parameters (beam energy and intensity, time structure), some features specific to the XADS are highlighted (reliability, operational procedures). Interface with other elements (beam dump, spallation target and reactor core) is analyzed.

Although the cyclotron option has been addressed, it is shown that the preferred solution for the accelerator is the linac. Each section of the linac (injector, intermediate energy, high energy) is described in quite a detailed manner with complete beam dynamics calculation. The RF structure for the intermediate section is still an open choice.

Finally, some recommendations are given for future R&D work.

	Henri SAFA CEA	Alex MULLER CNRS	Bernard CARLUEC FRAMATOME
24/10/2002			
DATE	RESPONSIBLE Name/Company Signature	WP LEADER Name/Company Signature	COORDINATOR Name/Company Signature

# **PDS-XADS : WP3**

## **Deliverable D9**

### **REQUIREMENTS FOR THE XADS ACCELERATOR & THE TECHNICAL ANSWERS**

#### **PDS-XADS : DELIVERABLE D9**

<b>1. INTRODUCTION.....</b>	<b>3</b>
<b>2. BASIC ACCELERATOR REQUIREMENTS FOR XADS.....</b>	<b>5</b>
2.1. ENERGY .....	5
2.2. INTENSITY .....	5
2.3. TIME STRUCTURE.....	6
2.4. RADIATION PROTECTION .....	8
2.5. AVAILABILITY & RELIABILITY .....	9
2.6. DIAGNOSTICS .....	10
2.7. OPERATIONAL PROCEDURES.....	13
<b>3. SPECIFIC INTERFACE REQUIREMENTS.....</b>	<b>15</b>
3.1. OPERATION OF THE ACCELERATOR.....	15
3.2. BEAM INJECTION INTO THE REACTOR .....	17
3.3. OPTICAL DESIGN OF A VERTICAL BEAM INJECTION FOR THE GAS-COOLED SYSTEM.....	18
3.4. THE SPALLATION TARGET .....	23
<b>4. PROPOSED TECHNICAL SOLUTIONS.....</b>	<b>35</b>
4.1. LINAC OPTION.....	35
4.2. CYCLOTRON OPTION.....	63
<b>5. TECHNICAL FEATURES .....</b>	<b>65</b>
5.1. ASSESSMENT OF AVAILABILITY/RELIABILITY .....	65
5.2. ASSESSMENT OF INVESTMENT COST.....	68
5.3. POTENTIAL FOR OTHER APPLICATIONS .....	71
<b>6. PRELIMINARY REQUIRED R&amp;D .....</b>	<b>72</b>
<b>7. CONCLUSION.....</b>	<b>74</b>

# 1. INTRODUCTION

The aim of this deliverable is to define the features of the accelerator needed for an eXperimental Accelerator Driven System (XADS). The accelerator is basically a high intensity proton machine, delivering beam on a spallation target to provide an external neutron flux source for a sub-critical core. The deliverable will summarize the accelerator parameters as required by the WP1 group [1] and describe then discuss the technical solutions that can meet those requirements.

Two accelerator options will be presented: The cyclotron and the linear accelerator (Linac). Although the cyclotron could probably fulfill the demonstrator needs, more emphasis will be put in the detailed description of the different linac options. The main reason is that a high power cyclotron will be closely approaching its technological limits. For future industrial high power ADS systems, it will therefore be unavoidable to use linacs. Consequently, it makes more sense to favor the demonstration of the linac accelerator that offers much more capability for future upgrade and extension to higher energies and to higher current beams.

Any high intensity linear proton accelerator can be divided in three main parts. The first one is the *injector* including the source (usually delivering a continuous current) followed by a bunching structure like a RadioFrequency Quadrupole (RFQ). The beam comes out from the injector at energies between 2 to 10 MeV. The second part, labeled here "*Intermediate Part*", brings up the beam to energies in the vicinity of 100 MeV. At that energy, although the proton is not yet fully relativistic ( $\beta = v/c = 0.428$ ), its speed is high enough to use elliptical cavities. The final (and most efficient) part of the linac using these elliptical cavities is the *high-energy section*. It starts from around 100 MeV up to any desired final energy.

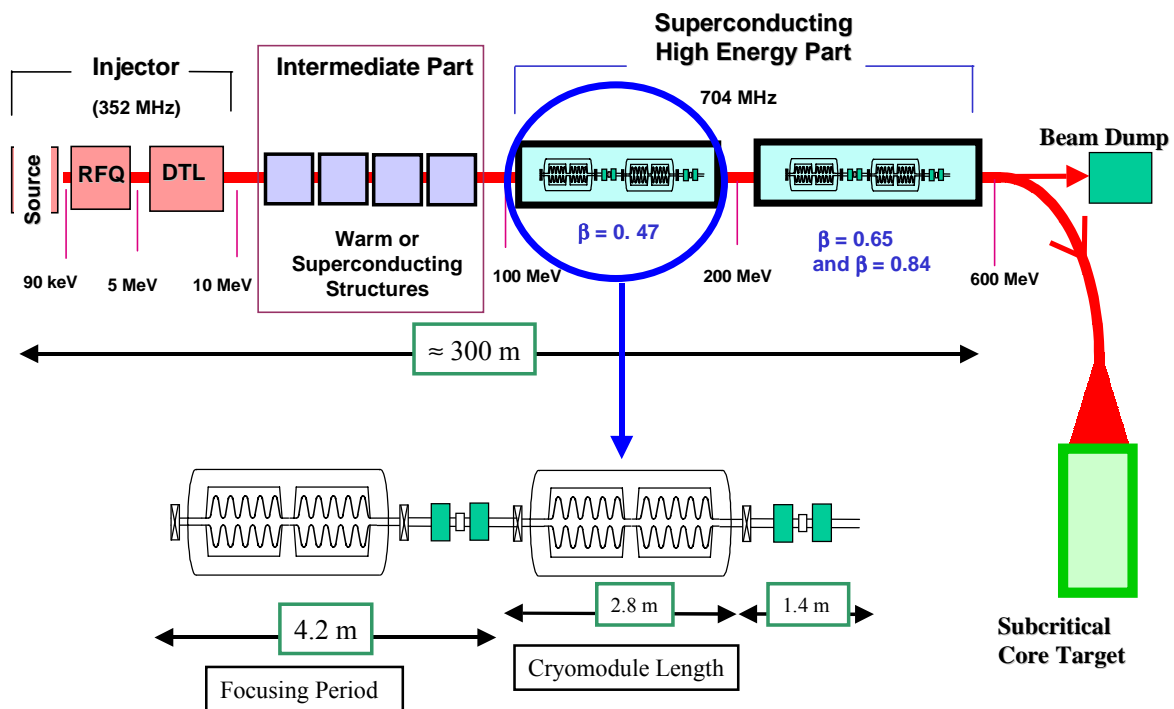


Figure 1 – Schematic layout of the XADS accelerator in the linac option.

Both the injector section and the high-energy section are quite straightforward. The source is usually an Electron Cyclotron Resonance (ECR) ion source based on the experience accumulated in many laboratories around the world [2,3]. ECR sources have demonstrated delivering reliable proton beams exceeding 100 mA, an order of magnitude higher than the requirements needed for the XADS. The source is followed by an RFQ that has two main functions: It prepares the particles in bunches separated by the RF period (the beam is now microscopically pulsed<sup>1</sup> in burst of particles flowing at the rate of the RFQ frequency) and it accelerates the beam to an energy of a few MeV while maintaining a strong confinement. In a similar manner, there is a general agreement that the high-energy section should be made of superconducting elliptical cavities. These have been demonstrated to be extremely effective (accelerating fields exceeding 25 MV/m have been experimentally obtained in many laboratories) and a lot of experience and knowledge has been accumulated. Moreover, large size machines using Superconducting RF Cavities (SCRF) have been constructed or are currently under construction (like the Spallation Neutron Source, SNS at Oak Ridge, USA) that may bring some confidence in the achievable performance for a XADS type accelerator.

However, at that time, there is still no consensus in the linac community on the best radiofrequency (RF) structures to use in the intermediate section (from 5 MeV to 100 MeV). There is some debate still open concerning the best structure to choose. This is why many different options are presented here including a "warm option" (i.e. room temperature RF structure) and two superconducting options (crossbar and spoke cavity). Advantages and disadvantages of these different structure types can be compared, especially regarding the XADS specific requirements (reliability and tuning). But it is clear at this point that no definite solution will be firmly given for this intermediate section until some particular R&D has been finalized, laboratory performance demonstrated and a thorough comparison performed. This is the reason why in this deliverable the intermediate section, although representing a modest part of the linac, might look overweighed in comparison to the other sections (injector and high energy). At this point, the document can be considered as showing the actual work going on in the main European laboratories involved rather than giving a streamline for an actual XADS design report. Therefore, due to the so many various people contribution, some discrepancy may be noticed in the average content.

The interface between the accelerator and the sub-critical core and spallation target is a rather important point that may impact the whole system. It has to be addressed at a fairly early stage of the design in order to give some idea on the matching device and requirements (beam profile, operation mode, failure scenarios). As a starting point, an optical design including two 45 degrees last bending magnets and a rastering scheme is presented with an injection scheme from the top lid of the reactor assembly. That should serve to initiate pending questions concerning the accelerator/reactor interface like the window separating the accelerator vacuum (how many, where to place) or the neutron leakage due to the beam line insertion. It could also serve as basis for initiating failure scenarios that could eventually lead to develop additional specific diagnostics there.

Some basic issues particularly relevant to this accelerator class type will be addressed, highlighting for example the extremely stringent reliability. These technical features have been estimated to be important enough to be addressed in a separated chapter. Some preliminary estimated cost figures and the synergy with other possible applications using the same accelerator will be equally discussed.

Finally, although no showstopper has been identified for the feasibility of such a XADS accelerator, some required research and development prior to the construction phase is

---

<sup>1</sup> Note that this is still considered as a Continuous Wave (CW) beam, because the RF frequency is quite high. A pulsed beam will be referred to whenever an additional time structure (ms range) will be superimposed to this beam. That will be discussed in section 2.3.

certainly needed. The most important technical points or performance demonstration that have to be worked out during the R&D phase are stressed. The success of the XADS will rely on the achievement of that R&D work.

## 2. BASIC ACCELERATOR REQUIREMENTS FOR XADS

### 2.1. Energy

The proton energy is a trade-off between the spallation efficiency, the accelerator length and the target beam load. Neutron production per unit energy through spallation rises sharply with the incident proton energy and starts leveling off at energies around 1 GeV. But the higher the proton energy, the higher the irradiation damage in the subcritical assembly. Also high energy protons induce more high energy neutrons that require heavy and expensive shielding. Therefore, for the demonstration purpose, the proton final energy has been set to **600 MeV** [1]. This is a quite important figure as all subsequent component will be designed accordingly (target, core, shielding, magnets, dump, etc...).

The accelerator itself will be designed for that final energy. In particular, that will determine the radius and the magnet weight for the cyclotron option or the overall length for the linac option. Note that in the case of linac option, the final energy is less of importance for the design because the accelerator can be quite easily expanded, merely adding more identical cryomodules. While a future extension to 800 MeV or 1 GeV would mean a completely new cyclotron, it will be a quite cheap and straightforward operation in the case of a linear machine.

Due to the possible application in case of a windowless target design, it is highly recommended that the final proton energy could be arbitrarily set in the tuning range between 300 and 600 MeV.

The value of the final energy will have to be stable to within  $\pm 1\%$ , which should *a priori* be quite easy to achieve.

### 2.2. Intensity

The beam intensity is deduced from the required beam power on target. In order to ensure the lower effective multiplication factor of the subcritical assembly ( $k_{\text{eff}} = 0.90$ ), the maximum beam current asked for would be **10 mA** on average [1]. The maximum beam power delivered on the spallation target would then be of 6 MW.

As the accelerator average current (and consequently power) will be the main parameter that will determine the overall thermal power, it will have to be fully adjustable from zero to maximum full beam. This can be done at the source output and checked all along the linac up to the beam line delivery to the target. That will also help to determine whether some important beam loss may have occurred in between the source and the output.

The nuclear control of the core will ask for a beam intensity stability of  $\pm 2\%$ . This is a rather stringent requirement considering the actual fluctuations of nowadays ion sources. Although feedback techniques can help meeting that goal, it is however highly recommended to initiate some specific development on diagnostics (see section 2.6) to properly achieve that requirement.

Considering that the energy stability will be almost perfectly under control (which is a relatively fair assumption in normal operation when compared to intensity fluctuations), the

final beam power stability on target will be fully determined by the actual beam intensity stability that can be achieved.

### 2.3. Time Structure

Although the total beam power is mainly the most important point for the neutron source generation, the time structure is a very important issue for the accelerator design. From the point of view of the neutron core, the time structure of the beam will have a limited impact as long as the beam repetition rate is high enough not to induce large temperature differences and fatigue in the structures.

But from the accelerator point of view, it is an important design issue to decide between a Continuous Wave (CW) and a pulsed machine. First, one has to distinguish between a pulsed beam current and a Radiofrequency (RF) pulsing of the accelerating structures. It will be considered here that a machine is pulsed whenever the RF power is applied in repeated pulses, the duty factor being the percentage of time the power is on. On the other hand, when the RF field is continuously maintained in the accelerating structures, the machine will be considered as a CW accelerator, no matter what the beam time structure. As a matter of fact, the beam current may be pulsed (for example at the source) in either a CW or a pulsed machine (with the constraint that in a pulsed machine, the beam duty factor should always be lower than the RF one).

From the neutronics part, there is no specific requirement on the beam time structure. However, a continuous beam will be preferred for stability. There is also a requirement for very short pulses to enable continuous on-line measurements of subcriticality, shutting down the neutron power source from time to time. These are referred to as Beam Interruptions for Measurements Purpose (BIMP). Inserting short "holes" (with duration of for example 100  $\mu$ s) in a CW machine would fulfill the requirement while maintaining an almost continuous beam. Any desired frequency can be chosen for these BIMPs (a 10 to 100 Hz repetition rate could be adopted for a continuous on line monitoring). These holes in the beam time structure will impact neither the accelerator operation, nor the reactor part. So this issue will not determine the accelerator time structure needed. Therefore, the choice of the RF time structure will have to be determined only by the machine design itself.

A high power cyclotron is clearly a CW machine by construction because high beam loading in the RF cavities would make beam pulsing quite difficult to control. Linacs could be operated equally either in CW or in a pulsed mode. But there is also no doubt that even in the linac option, operation in a CW mode will be highly preferred to a pulsed one. There are many points that support that statement, especially:

- A pulsed operation requires a much higher instantaneous current beam than a CW one. For example, a 10% duty factor would lead to accelerating a 100 mA beam instead of 10 mA. This means all components (couplers, cavities, RFQ, etc...) will have to sustain this high beam current. This will have a tremendous impact on the reliability of the machine, as MTBF (Mean Time Before Failure) of all components will be seriously degraded with increasing power. As an example, the power coupler of a superconducting cavity will have to sustain over 1 MW of RF power (instead of 100 kW), which even make this item at the limit of the present technology and beyond the actual state of the art for safe and reliable operation. Extensive and expensive R&D would therefore be needed to achieve the desired goals for a pulsed linac.
- When using a superconducting cavity in pulsed operation, a change in the resonance frequency will appear each time the RF is changed. This is known as the

"Lorentz force detuning" effect. While this effect is of no importance in a CW mode, it will be crucial in a pulsed operation mode. That leads to additional mechanical stiffening of the cavities (feasibility and cost issues) and to extra RF power needed for the resonance control (again cost, complexity and reliability).

- The overall efficiency is not degraded in a CW machine. While a pulsed operation would minimize the static RF and cryogenic losses, it will increase the dynamic losses (high power regime, filling time of cavities, RF control issues). The overall balance would even turn out to be in favor of the CW mode.
- A CW machine is much more flexible than a pulsed one. While in a pulse mode, the beam power will have to be adjusted using only the pulse repetition rate (or duty factor) maintaining the beam current and energy at fixed values, a CW mode would quite easily enable any kind of adjustment (beam energy, beam current and/or duty factor). The duty factor can be changed upon using a pulsed beam in a CW machine. As a matter of fact, that will even be necessary in the commissioning phase of a CW accelerator.

A more thorough and quantitative analysis have been made for the EURISOL driver machine [4], leading to the very same conclusions.

In conclusion, it is highly recommended to choose a **CW operation mode** for the XADS accelerator, the RF remaining continuously applied on the RF structures, while the beam intensity could be arbitrarily shaped. In normal operation, the beam time structure could for example look like a continuous current beam with very short "holes" in it to allow for on-line subcriticality measurements.

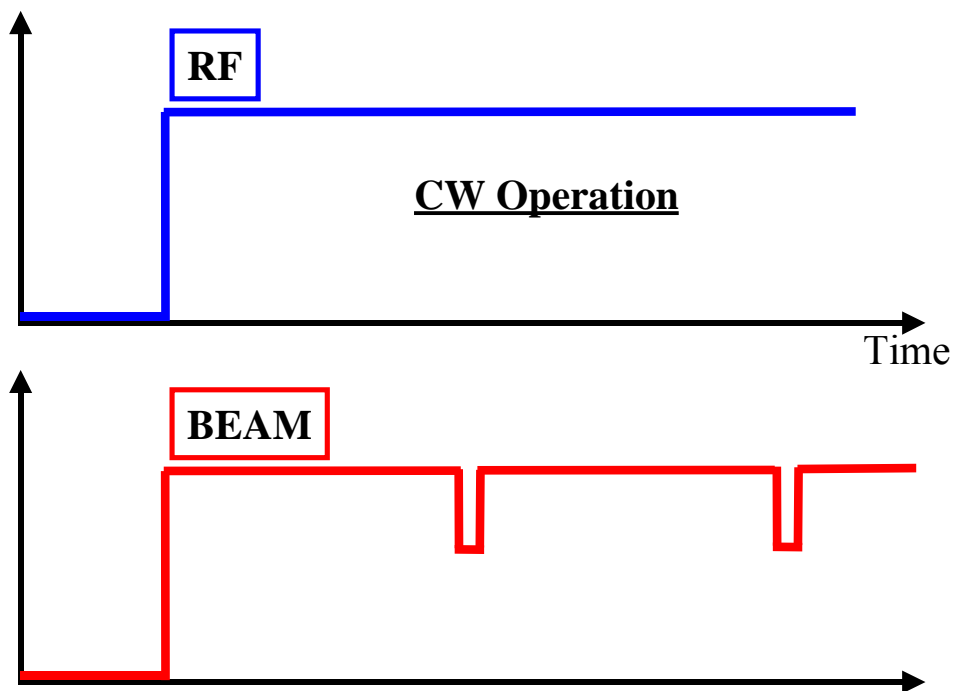


Figure 2 – Proposed beam time structure for the XADS accelerator.

## 2.4. Radiation Protection

The radiation protection of the personnel working in an XADS installation has to follow the international recommendations described in the ICRP-60. These recommendations are more specifically adapted to the European community in the 96/92/Euratom directive. Any radiation hazard has to be precisely evaluated and adequate shielding provided to comply with the ALARA (As Low As Reasonably Achievable) policy.

There are three main items where ionizing radiation should be estimated: the accelerator, the beam dump and the subcritical core.

Radiation from the proton accelerator can be considered of two different types. First, a continuous radiation is generally observed along the accelerator due to beam losses. These are either due to local defect points (mismatch, frequency jump, etc...) or to a homogeneous loss all along the machine (beam halo, interaction with residual gas). It is quite difficult to accurately predict the amount of radiation from these losses. Therefore, during operation, shielding must be adequately calculated in order to prevent excess radiation hazard (from neutrons and gammas). Concrete wall and earth shielding usually fulfill the requirements, namely ensuring that for example in the RF power hall next to the accelerator tunnel, people may work even though the accelerator is running. Wall shielding may be calculated in order to obtain an equivalent dose rate less than 1 mSv/year, which is similar to **0.5  $\mu$ Sv/hour**.

Interaction of the beam loss with the environment will mainly lead to activation of the accelerator material. When the beam is shut down, activation will gradually decrease with different constant times corresponding to the different radioactive species formed by the nuclear interactions. In order to allow hands on maintenance on some accelerator parts, it is generally admitted that the maximum allowed losses should be lower than **1 W/m**. The limit is a power limit because a high energy proton will induce much more activation than a low energy one. Consequently, beam loss at high energy should be lower than what is allowed at low energy. It turns out that the activation induced is more or less proportional to the power loss, justifying the beam loss limit.

In case of an accidental beam loss (for example, a complete loss of the beam in one point of the machine due to a failure), an equivalent instantaneous dose rate has to be evaluated. Of course, interlocks will operate (see section 3.1), but at a given speed depending on the detection time and the action command (beam shut down). One has to check that even in the accidental case, the integrated dose rate released during the shut down time is adequately shielded by the above normal operation shielding.

The beam dump will have to comprise its own shielding block. It should be treated separately from the accelerator, because it will have to handle a very high radiation dose in the running mode. The amount of radiation hazard from the beam dump will directly depend on the maximum beam power asked for in the design. The higher the power, the higher the radiation and consequently the higher the radiation hazard induced cost will be. Because of the extremely high activation foreseen, specific remote handling and specific storage for this beam dump will have to be installed, with the ability of automatically and remotely changing the beam dump in case of failure.

The accelerator part will mainly deal with activation (hopefully quite low after beam shutdown, at least low enough to allow hands on maintenance after a few hours). The beam dump, mainly also dealing with beam activation, will exhibit a much higher level of radiation hazard and should therefore justify a specific radiation procedure. But concerning the subcritical core, an additional radioactive hazard will have to be addressed, namely the use of nuclear material ( $\alpha$  emitters). Therefore, that part of the XADS project will have to comply with all nuclear facility regulations. It should be classified as a nuclear power plant and must follow the specific rules of any nuclear facility. These rules, for the time being, will depend



on the country where the nuclear installation will be sited. The radiation protection policy will have to be in accordance with the radiation legislation of the corresponding country.

## 2.5. Availability & Reliability

The ETWG report [5] and deliverable D1 [1] set the requirements for the availability and reliability of the accelerator. Namely, very short beam interruptions (with duration with less than a second, leading to insignificant transient) will not be accounted to the allowed beam trip budget, whereas the number of beam interruptions with duration  $> 1$  s (which lead to the plant shutdown) should be limited to a few (5 in D1) per year. Since the availability and reliability of a system strongly depends also on the (proactive) maintenance strategy of its components, Deliverable 1 pointed also out that the accelerator scheduled maintenance plan should be compatible with the existing maintenance policy of Nuclear Power Plants. Thus the “long” maintenance period will be scheduled after an operational period ranging from three months to a full year. It is therefore clear that the accelerator, in the absence of short and frequent (weekly) maintenance stops (as in most accelerator facilities), should be capable of operating with some faulty components, and its design needs to take into account criteria for derating of components, redundancy and spare on-line strategies. The long maintenance periods will be devoted to the proactive maintenance activities and to the replacement of faulty components.

To summarize, the machine needs to be designed with enough redundancy to guarantee, as a final goal, only a few unscheduled failures per year, leading to beam interruptions longer than one second. All failures that can be handled by diagnostic devices and control electronics in less than a second are not counted.

The system design needs also to follow the widely known criteria used to meet the reliability requirements. In particular the most important guiding criteria are:

1. **Derating of critical components** (or component over-design). All of the critical components need to operate below their nominal specifications, in order to benefit from an increase in their lifetimes.

2. **Component redundancy and spares on line.** It is important to include in the design redundant components, either in parallel or in series, which could take over the function of the failing components. The nature of the component connection (series or parallel, hot, cold, “k out of n”) strongly affects the system reliability and needs to be carefully investigated.

3. **Fault tolerance.** The proposed accelerator design needs to have some capabilities of functioning with a number of faulty components, meeting the nominal operational goals (energy, current, and stability). Automated procedures of the accelerator control system need to guarantee the prompt detection of faulty components and the consequent machine retune in a short time, with no beam interruptions. Only during the scheduled maintenance periods these components will be accessed and repaired or replaced. During the regular operation the faulty components need to be gracefully put in conditions not to jeopardize the system performance.

Besides these guidelines used for the design, formal standard methodologies for the assessment of the system availability and reliability can be used, as soon as a preliminary (“zeroth order”) design has been chosen for both the linac and cyclotron options. Among these we can mention two approaches:

1. **Top-down (deductive)** reliability analysis with the use of database of components. The accelerator configuration is schematically represented in a Reliability Block Diagram (RBD), where the nature of the connection between components is formally specified (components in series, parallel, hot, cold...). The information on the component operational (or design) characteristics (MTTF, MTTR...) are assembled in a database and the data is used to compute, through a formal mathematical analysis, the system reliability.

2. **Bottom-up (inductive)** approach. Techniques as the FMEA (Failure Modes and Effects Analysis) and FMECA (Failure Modes and Effects Criticality Analysis) try to identify the system failure modes from the failure modes of the single components.

These methodologies should be iterated in order to review the system (and components) design and achieve the desired availability and reliability (possibly under other constraints, e.g. total system cost).

From the considerations expressed above, one can however make a few statements regarding the different merits of the possible accelerator options.

First, the high degree of modularity of the superconducting linac under consideration (and described elsewhere in this deliverable, see section 4.1) seems to be particularly suited for the implementation of the redundancy/spare-on-line and fault tolerance criteria. The linac is split in sections, and each section is a sequence of nearly identical “cells” (an array of transversely focusing elements and accelerating sections). Each component, particularly the accelerating elements have been designed to operate at a very conservative level with respect to the state of the art of existing machines. The accelerating cavities are independently powered and phased. That enables, by means of a properly designed control system, the other remaining powered cavities to recover the failure of one of them. The present knowledge and technology seems able to fulfill the stringent demands of the ADS application.

On the other hand, the cyclotron is a single object that provides the beam focusing and acceleration. Here only a partial implementation of the redundancy criteria can be followed in some of the subsystem, but clearly the failure of critical components like the cavities or the sector magnets implies necessarily the system shutdown and the fault tolerance is limited. Conservative design criteria (over-design or derating) can be surely used in both cases to improve the components lifetime.

As a last comment, the component and beam diagnostics (that is, the capability to rapidly detect fault conditions and components), in conjunction with the control electronics and accelerator control software will play a critical role in the overall system reliability.

## **2.6. Diagnostics**

### **2.6.1 Introduction**

The design of a linear accelerator for the XADS plant will be based on techniques under operation or development at the present time in the fundamental research field. However, these techniques have to be pushed to higher limits in order to obtain the required characteristics and to bring into operation accelerators the reliability of which had never been considered.

Obviously, control of the running of those accelerators, beam breakdown prevention, beam monitoring under daily operation and beam losses prevention along the accelerating structure must be taken in account at the beginning of the design of the accelerator. Same considerations must be kept in mind for the beam transport from the accelerator to the target in the reactor.

Among the different systems which will contribute to the accelerator reliability, beam instrumentation will be a major component to obtain the nominal beam optic characteristics, a safe operation of the accelerator and a very high level of beam availability.

### **2.6.2 Beam Instrumentation Goals**

The linear accelerator is planned to deliver a 6 mA, 600 MeV proton beam. According to the different projects under consideration at the present time, it will be based on a low energy section including a proton source followed by a RFQ to accelerate the proton beam to several MeV, a Drift Tube Linac (DTL) to reach approximately ten MeV and the superconducting high energy section to accelerate the proton beam up to 600 MeV. Finally, a long beam transport line, including at least 5 achromatic beam deflection modules, will inject the beam vertically from above into the reactor. A raster scanning system located in the end of the beam line will assume a uniform painting of the target [See section 3].

#### **2.6.2.a Beam diagnostics requirements**

As far as it is possible yet to contemplate the design of the XADS plant, different types of specific beam measurement must take place to bring the accelerator and the beam transport line stage by stage into an “industrial way of operation” before the connection to the reactor.

First, beam instrumentation is needed for:

- Machine commissioning
- Beam dynamics calculation confirmation
- Help in understanding the beam behavior under normal and off normal conditions of operation of the accelerator.
- Beam loss control, monitoring and minimization.
- Improvements and validation of the raster scanning system performing the power distribution of the beam on the spallation target.

This step is essential to record as much as possible the different processes and ways of operation which may lead to the beam quality degradation. At the end of this experimental study period, one can define exactly “normal” conditions of further operation of the accelerator and high energy beam transport line.

A second type of measurement concerns the full power beam current establishment and normal daily operation:

- The beam instrumentation must then provide sufficient and necessary beam information to the accelerator and facility operators to operate the machine under normal and expected off-normal conditions.
  - In case of beam breakdown, beam instrumentation must minimize the time to identify the problem, to restart and to revalidate the beam characteristics.
  - In addition, measurements have to be carried and recorded in such a way that they may allow increase of knowledge about the operation of the accelerator after a failure. A powerful command and control system is of prime necessity.

#### **2.6.2.b General considerations on beam diagnostics**

- Even if some intrusive sensors may be used for specific measurements, the large quantity of beam energy deposited in any material, especially in the low energy sections of the accelerator, forces to use non-interceptive beam sensors. In addition to destroy the

sensor, the interception of some fraction of the beam will lead to a high activation level in the structure of the accelerator and its surroundings.

- The low energy section of the accelerator concentrates most of the difficulties for a complete characterization of the beam. There is a lot of work to do for designing operational and reliable beam diagnostics in this section. Non interceptive or at least minimally interceptive sensors are still under development.

- Special cares must be taken about the “radioactive environment”, especially above the target in the reactor, to select and define the beam diagnostics to be used. As a matter of fact, it is very attractive to dispose as close as possible to the target, beam diagnostics in order to achieve accurate beam parameter measurements.

### 2.6.3 Measurement Types

Beam diagnostics must work under various conditions:

- CW mode operation of the accelerator
- Low duty factor beam pulsed operation for commissioning and tests.

Several basic measurements may be pointed out.

#### **2.6.3.a Beam current measurements**

- DC and average-beam current measurements are useful during normal facility operation. Presently, specifications of industrial products exhibit a 100  $\mu\text{A}$  absolute accuracy on the measurement of the DC component of the current. Its resolution can reach 10  $\mu\text{A}$ .

- Pulsed beam current measurements provide information during startup, pulsed-beam commissioning, off normal events and restart procedures.

#### **2.6.3.b Transverse beam centroid measurements**

- Beam position diagnostics have to be put on operation in both transverse planes along the accelerating structure. These diagnostics must work under the different operation modes of the accelerator.

- These diagnostics are essential in the high energy transport beam line. They are vital for the raster scanning system.

- These diagnostics will be closely linked to the control and command system in order to achieve automatic beam alignment procedures. Half a mm for the absolute measurement on the beam position is possible and a tenth of mm for the resolution can be reached.

#### **2.6.3.c Transverse beam profiles measurements**

- These measurements are used to check that the beam is matched to the magnetic transport. These diagnostics will be mostly used during the commissioning period.

- It must be noticed that transverse profile monitors are not available at the present time under CW operation for high power beam in the low energy sections of the accelerator.

- Transverse beam profiles monitors will be needed to measure the expansion of the beam near the final target.

### **2.6.3.d Energy and phase measurements**

The beam energy and phase must be measured at many locations throughout the accelerator to properly set the accelerating cavities phases and amplitudes.

### **2.6.3.e Beam loss measurements**

- Beam loss measurements act as an input to the fast protection system that protects the components in case of failure.
- Beam loss measurements may also sense slightly off normal accelerator conditions such as mismatches.

### **2.6.4 Summary**

Most of the beam instrumentation for XADS may be based on the diagnostics used in the accelerator research field. However, a lot of work must be done to make them work in the expected harmful industrial environment of a reactor. A lack in the measurement of transverse beam profile is still existing. A non-interceptive transverse beam profiler must be then brought into operation [6].

At last, special procedures for accelerator commissioning and routine operation have to be defined in order to obtain the requested high level of reliability with the help of powerful beam instrumentation.

## **2.7. Operational Procedures**

### **2.7.1 Routine**

We only refer here activities involving the use of the beam. The XADS accelerator design goal, as defined by PDS-XADS Work Package 1, is the delivery of a 10mA / 600MeV beam [1].

The main concern during regular operation will be to avoid uncontrolled variations of beam energy and intensity, as well as to maintain extremely reliable operation and high availability, as a maximum limit of 5 trips per year is requested. Currently existing facilities operate only 30-75% of the year and are available 80-90% of that time [7]. This means frequent beam trips and many short interruptions, which are unacceptable for XADS (see section 2.6).

The design defines the maximum variation rates of energy  $|\Delta E|/E$  to be less than 1% and current  $|\Delta I|/I$  to be less than 2%. This being routinely achieved will mean very low loss levels and low radiation levels due to beam losses. Of concern will be sectors where radiation will be particularly high, causing possible damage to equipment and limiting access to those areas.

A critical step involved will be commissioning, during which a series of physics measurements, testing, check-up and tuning are required to characterize the actual operational parameters of the accelerator (magnetic fields, RF fields, Twiss parameters, etc) and to compare the output beam parameters to the beam reference values (energy, intensity). Full load as well as partial loads will have to be studied.

A detailed planning of the commissioning, with specific activities and measurements, will help to rapidly achieve the goals. This is true in particular, for a linac option, where modules can be more easily defined (source, cavities, beam lines, etc.) and commissioned in sequence as they become available, in a coordinated way.

Passive shielding and monitoring system attenuates the effects of routine and controlled beam losses, and defines the classification of areas near the beam enclosures. Interlocking radiation monitors assure classification compliance and the accelerator shutdown in case of large doses detection. The interlocking and classification systems define also access to the different areas. Areas with safe residual radiation will allow free access. Areas with higher doses will be through locked gates.

The exact conditions to be considered non-standard operation (besides large  $|\Delta I|$  and  $|\Delta E|$ ) and the exact steps to be taken by operators to respond to those conditions will have to be defined.

### 2.7.2 Accidental

As mentioned, routine beam parameter variations are very strict. This is due to the fact that larger variations have strong consequences on the target and the reactor, and thus, accelerator systems have to respond swiftly to those variations.

From other accelerators' experience [8], maximum credible fault and off-normal scenarios include magnetic failures, RF failures, control systems failures and operator errors.

Magnetic failures might lead to uncontrolled beam losses. For bending magnets, the losses will be local. Proposed layouts include wide-angle dipoles, and this most likely implies a total beam loss.

For focusing magnets, previous studies [9] suggest that beam losses can be quite limited: even if quad failures introduce perturbations in the focusing lattice, a single quad failure implies a very limited beam emittance growth. Eventually, sufficiently large physical apertures will prevent beam losses due to beam dynamic aperture growth. However, further studies are still required to understand possible consequences of nonlinear perturbations.

Small amplitude and short time power variations should not have significant effect, due to large rise and fall times of the magnetic fields.

RF systems failures mean variation of the beam energy, and might prove to be the most crucial aspect to be taken into account. Reliability and redundancy of the RF systems are already being taken into account, and are a central worry.

Control systems failures and operator errors are expected to have the same kind of consequences as magnetic and RF systems failures, not introducing new phenomena.

Fast accident recovery involves careful prediction of radiation levels at every sector of the accelerator and enclosures, as this might have implications for the recovery plans. Typically, most components can be considered cooled down after few hours [8]. This excludes parts like collimators and the dump.

Another factor crucial for fast recoveries will be the accelerator and building/tunnel layout, which will have to consider easy access to the involved sectors, and the existence and easy access to spare parts and tools.

During commissioning, all these factors will have to be tested, including verification of shielding, location of high radiation levels, and actual times to achieve residual radiation levels.

## 3. SPECIFIC INTERFACE REQUIREMENTS

### 3.1. Operation of the accelerator

#### 3.1.1 Commissioning

##### 3.1.1.a Accelerator Start-up

The accelerator should be able to run in two different modes. The first is the commissioning mode that will be mainly applied during the period of time immediately following the construction phase. During that commissioning time, which could last over a full calendar year, all the parts of the accelerator should be individually tested prior and after bringing them on line. For example, in the linac option, the source, the RFQ and each cryomodule will have to be successively installed and let the beam run through, step by step. For each step, the beam parameters should be completely evaluated and checked for. Of course, during that period, the current will be pulsed at extremely low duty cycle (less than 1%) in order not to induce any damage or excessive radiation if the beam were to be lost. Here, the accelerator will be operated as a stand-alone equipment, independently of the nuclear core part. Therefore, the beam at the output will be directed to a specific beam dump that would be designed to handle a small fraction of the total accelerator power. The full maximum beam power will not be available and tested until the target completion and installation. In the commissioning phase, the beam power will be limited to the maximum power allowable by the beam dump design.

Apart from beam power, all other parameters could be tested in the commissioning phase. In particular, beam energy can be established in the required range and checked for stability. Although the maximum average beam current will not be attainable, the maximum peak current will be. So, except for the thermal issues, that would allow to set all conditions for a proper operation of all components (RF power, RF feedback, couplers, cavities, etc...) as if the beam were at full power.

##### 3.1.1.b Accelerator Set-ups

The commissioning is a very important phase for the accelerator operation. Not only it helps to qualify and debug all the equipment, either hardware or software but it is of prime importance for the knowledge of the beam parameters all along the linac. By using specific diagnostics (see section 2.6) (which could eventually be removed during routine operation), the beam would have to be fully characterized at any point of the linac. In fact, the influence of any parameter modification, like for example the value of the focusing magnetic fields or the quadrupoles misalignments, would have to be very precisely assessed and experimentally checked. While doing so, that would help establishing future operational procedures used whenever the linac will be in the running mode when additional diagnostics cannot be anymore installed.

These operational procedures are important to establish, because the machine has to be tuned each time a given basic parameter is changed. For example, assuming that in a running mode, the operator (or the corresponding automatic task system) asks for an increase in the beam current to raise the reactor thermal power. Then all the components will have to be re-tuned in order to deliver the proper beam to the target. Each RF input power in every superconducting cavity will have to be increased while adjusting at each time the amplitude, phase and cavity frequency in order to keep a clean beam through it. These operational procedures (like a complete machine tuning) are to be checked, automated, implemented and experimentally demonstrated during the commissioning phase. Also some specific component

failures could be simulated and mitigation procedures found that could maintain the beam through. That would be of prime necessity to achieve the tremendous reliability requirement asked for this accelerator (see section 2.5). Verifications of these fault scenarios are to be equally demonstrated on a low power beam.

### **3.1.2 Running**

#### **3.1.2.a Interface**

In the operating mode, the accelerator will be delivering beam to the spallation target inside the reactor vessel, through a bending magnet and the beam line and rastering magnets as described in section 3.3. While running, the accelerator will equally have to deal with additional constraints coming from the subcritical core. In particular, its operation will be directly coupled to the level of desired neutron flux inside the reactor. It may also act as an active safety equipment, because a beam shutdown is equivalent to an extremely fast negative reactivity insertion (almost instantaneous when compared to classical reactors).

Consequently, the reactor comprising the spallation target and the subcritical assembly will be the main interface driving the accelerator parameters. But two other important items will also be interacting with the machine operation. First, the injection beam line (bending magnet, beam line, rastering and focusing magnets, diagnostics, etc... see section 3.3) which actually makes the link between the accelerator and the reactor. As a matter of fact, this ensemble could be considered as well either part of the accelerator or of the reactor or eventually both. The second major interface is the overall safety hazards control, driving the complete installation. That will mainly happen in any incidental situation, where the accelerator could play the role of a "fuse" thanks to the easy and extremely fast reaction following a beam shutdown. In an accelerator, beam trips may even sometimes occur when not desired. These trips will be considered as "unwanted beam interruptions" and should be minimized (see section 5.1).

#### **3.1.2.b Operation procedures**

Operation procedures established in the commissioning phase will be used for any modification in the accelerator set-up. One of the first procedure to master will be the power turn on, initially starting from zero power and progressively increasing to reach a given power level. That should require a quite slow ramping phase increasing the beam duty cycle and/or the intensity step by step while adjusting all components at the same time. That procedure should be followed each time the beam is shutdown. Because of that, any "unwanted beam stop" will need a long recovery time and that will certainly induce a large power swing on the spallation target.

Conversely, other important operational procedures should give the ability to swiftly move from one set point to another without requiring a complete shutdown. As an example, a raise in beam power can be gradually and smoothly done by continuously tuning all the accelerator components without destroying the beam quality. An easy way to operate would be at a given energy to slowly raise either the duty cycle or the beam current. In any case, all operation procedures should be implemented in the accelerator control-command and should be completely automated in order to reduce any undesirable manual mis-operation.

#### **3.1.2.c Interlocks**

Basic safety hazards (radiation, contamination, power level, criticality, etc...) will induce either accelerator or reactor interlocks usually leading to a complete shutdown of the



beam. Resuming beam power will only be possible after the corresponding default is fully analyzed and the problem solved.

In parallel to safety interlocks, a proper operation of the accelerator will require its internal interlocks. Any abnormal operation resulting from the detection of a wrong parameter either in a hardware component or from a diagnostic item will generate a default. Analyzing this default would induce an interlock signal, usually leading to a beam stop order. If the default can be corrected without stopping the beam, then specific procedures can be followed to set-up the right process, resetting the default.

### 3.1.3 Summary

In conclusion, the accelerator operation has to be an integral part of the global operating system, including the nuclear core control and the overall safety management. At this point, two operating modes can be identified: the commissioning mode and the normal running mode. In each mode, operating procedures should be established and automatically implemented together with specific interlocks. The general operation of the accelerator is schematically described in the following simplified block diagram (Figure 3).

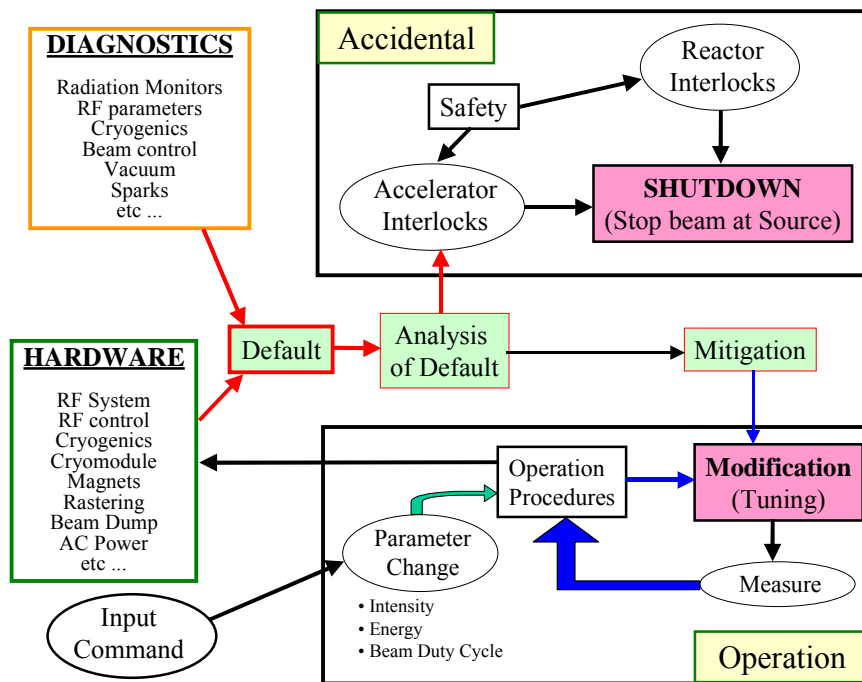


Figure 3 – Schematic of the accelerator overall operation.

## 3.2. Beam injection into the reactor

### 3.2.1 General Considerations

So far, no attempt has been made to define a general layout of the XADS plant. Nevertheless, the necessity of a high power beam dump capable of taking the beam during the commissioning phase of the accelerator or in case of emergency during normal operation with the reactor has been pointed out. As a consequence a beam switchyard is needed downstream of the accelerator to transport the beam either to this dump or to the reactor. For safety reasons, it seems preferable to direct the beam through a straight channel to the dump and to

deflect the beam serving the reactor, because in case of a fault condition, the beam goes directly to the dump. A very schematic view of such a configuration is shown in Figure 4.

In the absence of a more detailed description of this general layout, it is not possible to define the optics of the whole beam transport system between the accelerator and the reactor, but this is straightforward to be done once this overall layout has been assessed. This is the reason why the study presented here is limited to the critical design of the last part of the transport line used to inject the beam into the reactor.

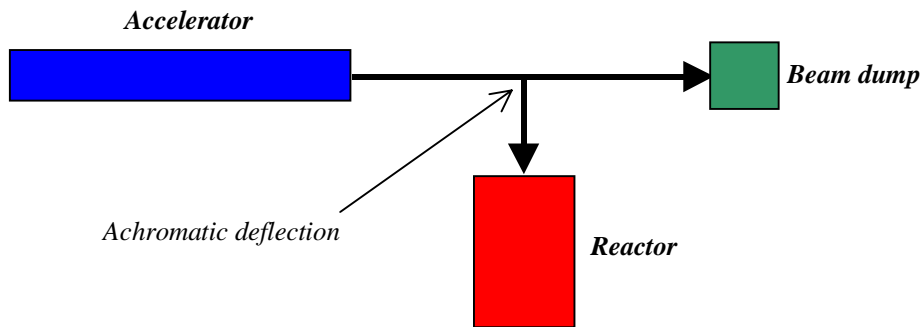


Figure 4 - Conceptual view of the XADS plant.

### **3.2.2 Beam penetration directions for the target unit**

In principle, the beam can be injected vertically from above, vertically from below or horizontally into the reactor. These different proton beam penetration directions for reactor vessel, core and target unit have been evaluated and compared in terms of advantages and disadvantages in order to identify the preferable arrangement for the two reference XADS concepts selected and defined by Ansaldo (LBE-cooled primary system) and Framatome ANP (gas-cooled primary system).

Although large bending magnets have to be placed in the upper region of the reactor building, the preferable configuration identified for both concepts of primary cooling system is a vertical beam line injecting the beam from above the reactor [10]. A vertical target unit with a beam line penetration from below seems also to fit to the gas-cooled primary system, but is excluded for the LBE-cooled primary system.

As a result of these conclusions, an optical design of the last part of the beam transport line in the reactor surroundings has been studied and is proposed for the case of the reactor scheme defined by Framatome ANP [11] (section 3.3) and by Ansaldo (section 3.4).

## **3.3. Optical design of a vertical beam injection for the gas-cooled system**

### **3.3.1 Constraints and design choices**

The distance between the last bending magnet and the target unit is one of the conditions that influence strongly the whole beam line design. In order to accommodate the layout of fuel, manipulator and target handling flasks in the above reactor roof area, while limiting the beam line elevation above the reactor (and therefore the height of the building), the principle of a removable and disconnectable magnet located above the fuel assembly area has been adopted (see Figure 5). With this system, the distance between the target and the dipole has been fixed to 16 m. Another important parameter is the beam footprint at the target, which has to be circular with a diameter of 16 cm.

To limit the size and the weight of the last bending magnet, a deflection angle of only 45 degrees has been chosen (it is 64 degrees for the spallation neutron facility SINQ at PSI

Switzerland [12]). A second dipole placed at a distance of 10 m from the last dipole restores the beam in the horizontal direction. Three quadrupole lenses are inserted in this drift space to control the beam envelopes and to cancel the dispersion function at both extremities of this 90 degrees deflection module.

The choice of such an achromatic optical system has interesting consequences. It has been made to eliminate beam size enlargement and beam position motion at the target due to possible energy spread changes and central energy fluctuations induced by the RF system of the accelerator.

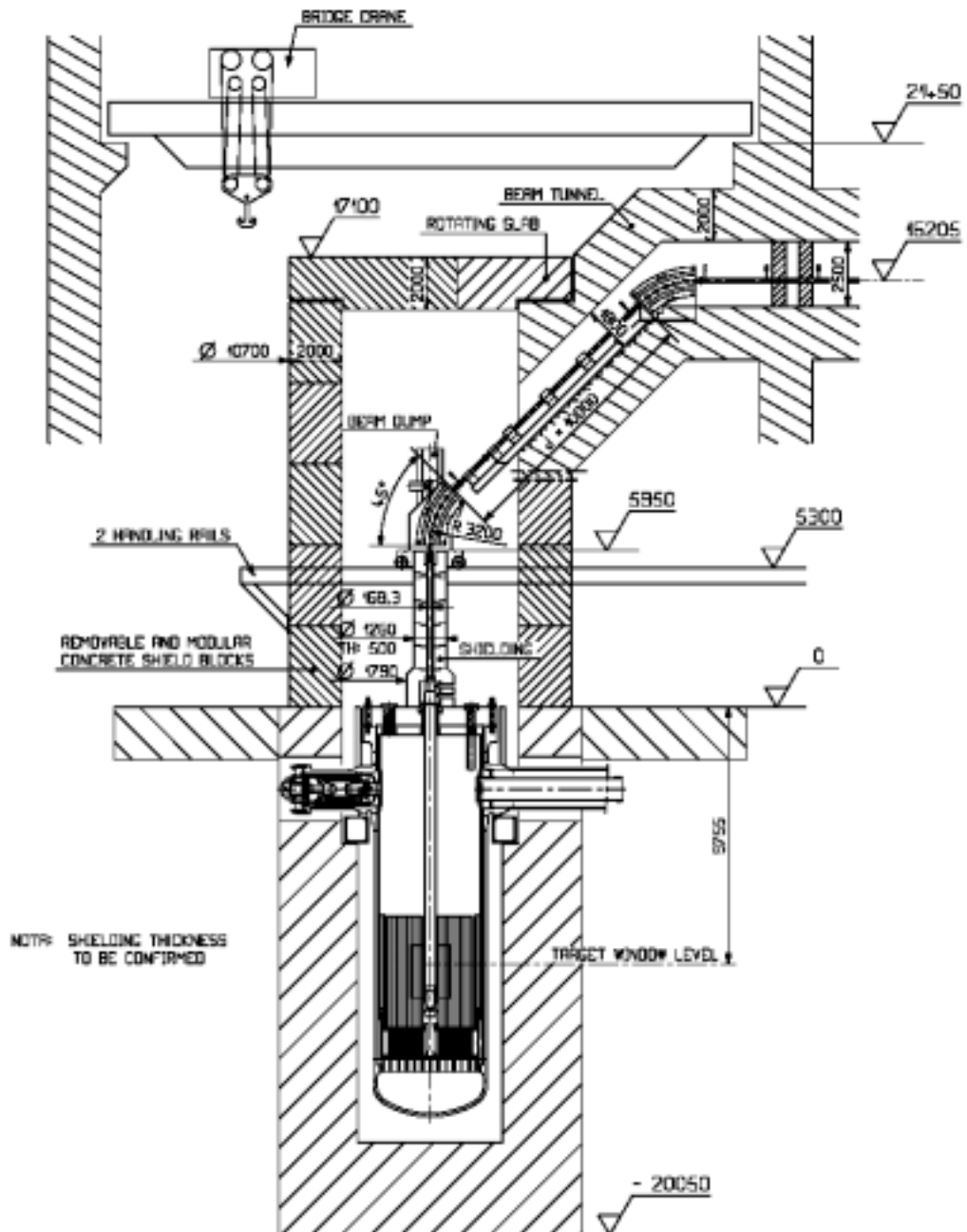


Figure 5 - Preliminary sketch of the arrangement of the reactor in operation.

To expand the beam onto the target, two approaches are available in principle. One technique involves defocusing the beam by means of additional quadrupoles, another is to

apply the so-called “raster scanning” method which consists in deflecting a pencil-like beam with fast ferrite magnets in a pre-selected pattern to paint the target area.

The first technique is foreseen for spallation source projects like ESS or SNS [13,14]. In these cases, the beam expansion does not require too strong defocusing quadrupoles because the emittance of the beam extracted from the accumulator rings is very large.

In our case, the emittance of the accelerator beam at 600 MeV is about one hundred times smaller. The defocusing method would therefore imply strong gradient quadrupoles carefully aligned and regulated. As a consequence, we have selected the second solution, which is based on already existing techniques validated by the R&D programs undertaken in the U.S. for the APT and ATW projects [15,16,17] and by the major achievement obtained at GSI in Germany for the treatment of cancer tumors with ion beams [18].

Another reason for choosing the raster scanning technique is that, in contrast with the first method, various types of beam distribution at the target are achievable by simply adjusting the rastering frequencies of the horizontal and vertical ferrite deflecting dipoles. To give just one example, Figure 6 shows the beam pattern and the resultant uniform distribution obtained for a circular beam footprint. In this case, the scanning magnets are operated at frequencies close to 500 Hz [19].

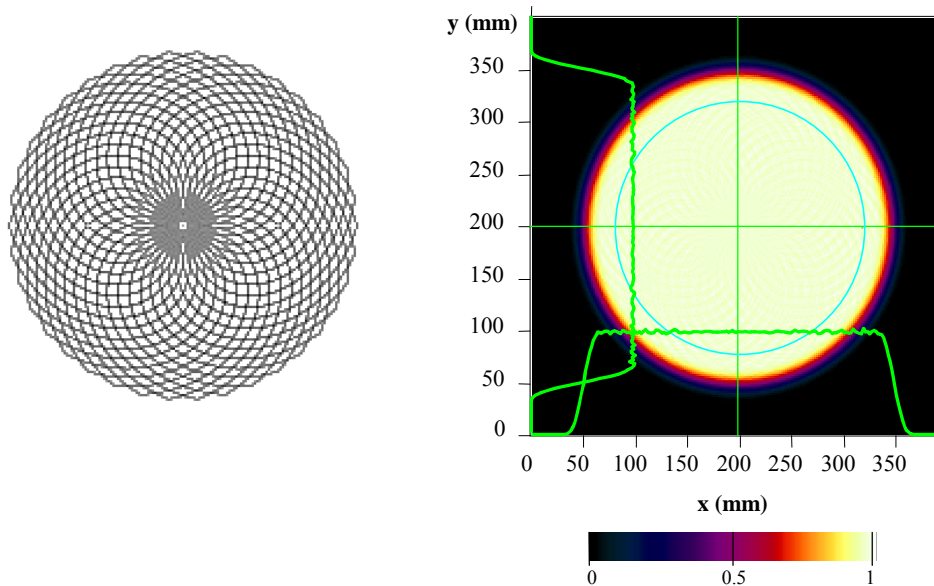


Figure 6 - Example of a circular beam scanning: pattern of the beam displacement (left) and power density deposited (right) in the target.

### 3.3.2 Proposed technical solution

The basic parameters used for beam optics calculations are summarized here under.

– Energy	600 MeV
– Normalized rms emittance <sup>2</sup>	0.33 $\pi$ .mm.mrad
– Non-normalized rms emittance at 600 MeV	0.25 $\pi$ .mm.mrad
– Maximum beam intensity	10 mA
– Last drift length	16 m
– Target diameter	0.16 m

<sup>2</sup> = 1.3 times the injector output beam emittance.

This achromatic 90 degrees deviation module is composed of two 45 degrees dipoles, three focusing quadrupoles and four raster magnets. It has to be noticed that these four raster magnets are operated synchronously and independently, so that the beam is always moved at the target if a failure occurs for one of them. As foreseen for the APT project, fault detection circuits will be used to switch off the beam if such a failure is detected.

All these elements can have rather small apertures because the proposed optical design involves small beam envelopes (see Figure 7 and Figure 8) and because the scanning dipoles are located as close as possible to the last bending dipole. As a consequence, the main characteristics of the beam transport line components could be as follows.

- Dipoles:
 

Deflection angle	45 degrees
Bending radius	3.2 m
Nominal field	1.27 T at 600 MeV
Gap height	0.1 m
Width	~ 1.1 m
Height	~ 0.8 m
Weight	~ 15 t
  
- Quadrupoles:
 

Length	0.4 m
Inscribed circle diameter	0.08 m
Maximum nominal gradient	5.8 T/m at 600 MeV
Width	~ 0.4 m
Height	~ 0.4 m
Weight	~ 0.3 t
  
- Scanning magnets:
 

Length	0.3 m
Maximum deflection angle	$\pm 3.5$ mrad
Maximum field	$\pm 0.048$ T

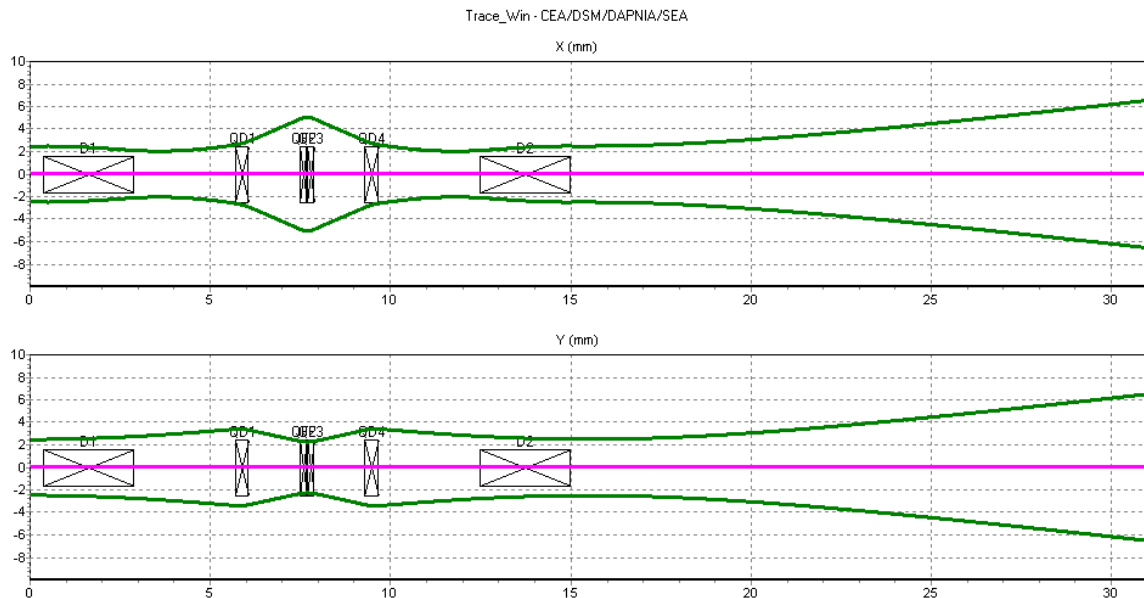
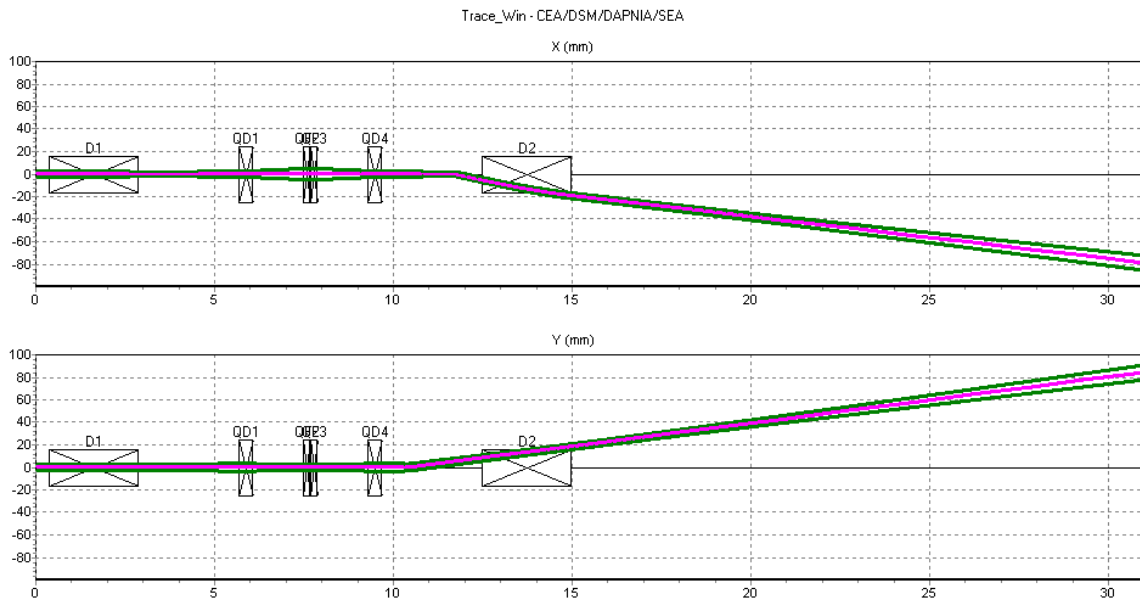


Figure 7 - Beam envelope along the beam line without deflection (length in meters).



*Figure 8 - Beam envelope along the beam line with maximum deflection.*

### 3.3.3 Additional considerations

Some additional issues and considerations have been pointed out during a working meeting organized between CNRS (WP3) and Framatome ANP (WP4.2) at IPN Orsay (April 5th, 2002). The problems, which will have to be solved in a future phase of the project, are the following:

- About the beam scanning on the target area: what is the desired power distribution on the spallation target (uniform, gaussian...)? This question should be linked with the studies made by WP4.3 on the target thermal properties. Note that in a preliminary study issued by WP4.3 in July 2002 [20], it is recommended to use an elliptical distribution of the beam current density at the beam window.
- About the last bending magnet: what are the positioning tolerances, and the sensibility to eventual vibrations? What should be the procedures of disconnection and repositioning during the fuel loading and the target handling?
- What is the level of radiation in the region of the last bending magnet?
- Do we need a beam dump above the last bending magnet in the vertical direction to intercept the neutron flux escaping from the reactor? That could imply a last bending dipole magnet with a “C” shape instead of an “H” shape.
- A “cold” double-window may be installed at the transition of the reactor confinement barrier: what should be its material and thickness?
- For the hybrid system commissioning, beam diagnostics should be needed after the last bending magnet: what kind of diagnostic can we plan to use in this harmful environment? Do we need a retractable beam-stop between this diagnostic and the spallation target to insure the accelerator commissioning without shooting on the target? Is a very low (about 1/1000 of the nominal power) pulsed operation acceptable for commissioning?

Of course, similar considerations need also to be done with WP4.1 and WP4.3 (See remarks made above for discussion).

## 3.4. The Spallation Target

### 3.4.1 Target Characteristics and Design Options

The proton beam line from the accelerator system is connected to the spallation target, which provides for the neutron source sustaining the subcritical core of the XADS. The target system constitutes the functional and physical interface between the accelerator complex and the primary nuclear system of the XADS.

The source neutrons are generated in the spallation target by the interaction of a high power proton beam with a high atomic-number medium (the Lead Bismuth Eutectic - LBE target material). The kinetics of the proton collisions with LBE nuclei and of the spallation reactions inside the compounded proton-nucleus system, as well as the dynamics of the proton beam itself, are prompt and ascribable, as far as the nuclear reactor control and its response are concerned, to the neutron prompt dynamics.

Any change, variation and/or perturbation of the beam characteristics either originating directly from the accelerator complex or induced along the beam line will instantaneously affect the coupling physics of the XADS. The nuclear power system and the whole plant can then potentially be subject to the effects of a very intense, hard flux and rapidly varying neutron source, which is directly converted in nearly one hundred megawatts of nuclear power with the same operational characteristics. This XADS feature may pose substantial issues for the primary and secondary cooling systems, under both operation and control perspective.

A number of key requirements need then to be defined for coupling a high power proton beam with a nuclear multiplying system, which mainly concern methods and procedures for beam injection and control, as well as for conditions on beam stability and quality.

The spallation target unit is the component that actually has to perform the coupling between two quite different systems, the accelerator complex and the nuclear power plant, and which actually "sees" and has to match with the high power proton beam directed from the accelerator-beam transport line and beam delivering system. A number of key aspects of the target unit are then worth to be reminded while defining the beam line-target coupling requirements.

When designing a spallation neutron source, two main undesirable effects of the spallation interaction must be taken into account:

1. The production of a large quantity of heat which is a consistent fraction (~ 70% for a 600 MeV proton beam) of the impinging beam power (typically some MW). This heat, which must be evacuated from the target, is concentrated in a small volume given by, roughly, the beam aperture cross-section area through the proton range in LBE. The first parameter depends as fixed by the beam delivery method for the given target design. The second is a direct function of the proton beam energy (~ 30cm depth for a 600 MeV beam);

2. The induction of an intense radiation damage in the structural materials due both to the dislocation of atoms in the material microstructure and to the formation of solid and gaseous spallation debris, which significantly affects the material properties, especially its mechanical toughness.

The best option for an efficient removal of a very high power density spallation heat is the use of a heavy liquid metal with the twofold function of spallation medium made from high-Z target nuclei (which enhances the spallation reactions yield) and of coolant vector that conveys the spallation heat directly from the spallation zone to a suitable heat exchanger. Due to its good spallation yield and neutronics properties, being besides endowed with fairly low

melting point and good thermal-physical properties, the heavy liquid metal chosen for the liquid metal version of the XADS is the **Lead-Bismuth Eutectic** (LBE). The use of the same coolant in the spallation target and in the primary system for cooling the fuel core allows a very good spatial continuity in the neutron physics of the LBE XADS: the target-fuel core neutronics coupling is in fact maintained at the highest efficiency with the most uniform diffusion of the neutron flux. Conversely, due to the inherently prompt physics of a subcritical system (for the fuel type and  $k_{\text{eff}}$  levels of interest, at least), such continuity is also kept in the functional aspects, as the delayed neutrons can play little or no role in decoupling the kinetics of the two systems.

Even using the same type of coolant, the LBE of the target is nevertheless kept separated from the primary LBE coolant in order to limit the pollution of the primary system from the spallation products generated by the high energy reactions of the accelerated protons. This separation is implemented for both the spallation target designs considered in the LBE XADS: the beam-**window target**, in which the spallation material is separated from the beam line tube by a thin sheath window, and the **windowless target**, where the free surface of the LBE is directly exposed to the vacuum, the proton beam directly impinging on the liquid.

Targets using a beam window have limited performance and duty lifetime due to significant thermal-mechanical stress under the spallation environment loading, damage of the window material under irradiation and potential LBE corrosion. While the windowless design is inherently immune to these problems, it nevertheless needs to fulfill some specific requirements for interfacing with the high vacuum conditions of the beam line.

In order to control the heating (power density) generated inside the window material by the ionization losses of the proton beam crossing the window sheath, the beam aperture needs to be conveniently enlarged to reduce the beam current density below  $50 \mu\text{A}/\text{cm}^2$ . The beam footprint on the extraction window may then be enlarged to a few hundred square centimeters, depending on the actual intensity of the beam current (see section 3.3.1). Conversely, in the windowless target configuration, the proton beam may be left at its original spot size (or just slightly enlarged to 1÷2 cm if the beam emittance is too low to produce a natural spread of that size) and linearly scanned over a 8 cm width. The constraint in the case of the windowless system is to avoid boiling inside the LBE spallation bulk and to maintain a moderate temperature at the LBE surface exposed to vacuum, in order to keep a moderate release of the LBE vapors and of other exhausts generated by the spallation process in the beam tube.

The two target options also differ for the removal of the spallation heat: the window target cooling can be based on a natural circulation system that uses an independent loop with a diathermic fluid as heat sink (with the heat exchanger located at the top of the target unit), whereas the windowless target needs to employ a forced circulation system for removing the spallation heat through a heat exchanger located below the fuel core, which evacuates the heat to the LBE of the primary system. An independent cooling loop is a necessary option for the window target, since the limitation of the window operating temperature requires to use a heat sink at temperature levels lower than the XADS primary coolant. Conversely, in the case of the windowless target, which is a configuration considered only for the Pb-Bi cooled XADS, the spallation heat can be removed by the primary coolant, as no window related issue is constraining any more.

### 3.4.2 The proton beam power

The maximum beam power level actually considered in the design of the target is 3.6 MW. A large fraction is converted into LBE spallation heating and must be evacuated through the target cooling system.



At low-moderate beam energy levels, the heat deposition path of the proton beam in the spallation target is substantially consistent with the expected range of the accelerated protons in the LBE, being the beam energy dissipated mainly by ionization losses.

However, as the energy of the colliding proton increases, the energy dissipation amount is progressively transferred from ionization losses in the electronic shells of the LBE atoms to hadronic interactions with LBE nuclei. When a higher fraction of heat is being released by interactions with the LBE nuclei, the range of the proton results shortening, in comparison with the ionization interaction path. Thus, while at 200÷400 MeV the heat deposition well matches the ionization range, at 1÷2 GeV the effective proton range fairly departs from the ionization assessments, due to the increasingly larger effects of hadronic interactions of the proton beam with the LBE nuclei. A variety of interactions are involved by proton-nuclei collisions (nucleus recoils, evaporation products, meson emission and decay, de-excitation gamma, etc.) and some may release heat far from the spallation zone. A substantial share of the proton beam energy, which do not directly contribute to heat generation, is also spent for extracting the neutrons from the LBE nuclei and is needed for supplying both nuclei binding energy and kinetic energy for the released neutrons.

Therefore, not all the power carried by the beam is deposited in the spallation target volume and, in the case of a 600 MeV beam, the energy released in form of heat is about 72% of the total. The remaining is shared between the particles escaping the system and the binding energy of the target nuclei. Therefore, for a 3.6 MW beam power, the heat directly released in the target and which needs to be evacuated by the target cooling system is 2.6MW [21]. This value is rounded to 3 MW in order to keep some margin on the heat generation to be evacuated from the spallation target.

The following table summarizes the main performance data of the target that, to the extent of applicability of this specific design, are substantially matching the general indications postulated in Deliverable D1 [1] and the technical specifications of D70.1.

Power of subcritical core	P = 80 MWth
Max. proton energy	E = 600 MeV
Max. proton beam intensity	I = 6 mA
Max. proton current density	~ 50 $\mu\text{A}/\text{cm}^2$ (Window target option)
Max. proton current density	~ 750 $\mu\text{A}/\text{cm}^2$ (Windowless target option)
Max. target power / beam power	P = 2.6 / 3.6 MW
Max. target design power	P = 3.0 MW
Target material	Lead Bismuth Eutectic (LBE)
Target life time	One fuel cycle (30 000 h, with 25 000 h at power)

*Table I – Target Specifications.*

### **3.4.3 Spallation Products Confinement**

As mentioned above, most of the proton kinetic energy is dissipated by ionization losses along the scattering path in the LBE target. The electronic shell dissipation and the intense nuclei repulsive fields require adequate proton energy for achieving efficient spallation rates in the LBE. Primary spallation neutrons, generated by proton collisions with the LBE nuclei, are instead unaffected by charge, so that they have a broad energy spectrum and can easily produce further spallation and secondary neutron cascades.

Conversely, the energy left in target nuclei by primary and secondary interactions steadily increases with the proton energy, so that the overall spallation yield may be seen not only under the perspective of a mere balance of neutrons throughput, useful to supply a neutron source for the XADS subcritical core, but also on how the overall proton kinetic

energy is used in the spallation process for generating these neutrons. Thus, high-energy protons, besides producing a substantial number of spallation neutrons, also tend to deliver high-energy contents to the target nuclei, increasing the probability of their splitting and leaving behind highly excited and unstable spallation fragments.

An assessment of the spallation products radiotoxicity trend vs. the proton beam energy, as dependent on the target material, may be found in [22]: a steep increase is shown above 600÷800 MeV for Pb-Bi and above 380 MeV for tungsten. In both designs (window or windowless target), the LBE of the target is kept separated from the primary coolant in order to limit the pollution of the primary system by the spallation products.

The beam transport line connected to the spallation target unit cannot in itself be credited (nor is intended for) to act as radiotoxicity safety barrier to outside environment (i.e. the third barrier in a nuclear power plant). Therefore, the segregation of the spallation products must be achieved in the part located inside the safety containment of the XADS. This requires the use of absorbing and trapping systems for the exhausts emanating from the spallation zone, which must prevent the migration of any radiotoxicity outside the reactor building. As for the second safety barrier in the windowless concept (which is not provided with a separation window), this may be seen as constituted by the combination of a number of components and systems:

- 1) The accelerator beam line itself as pertaining to the portion of the vacuum tube from the spallation target to the point where the isolation valves are located, i.e. close to the reactor containment building wall;

- 2) The isolation window(s) located in the portion of the beam line inside the reactor containment, between the fast isolation valves and the spallation target;

- 3) A fast-acting isolation system, valves, required to shut off the beam line after the detection of failure of either an isolation window or the high-vacuum exhausts evacuation system;

- 4) High-vacuum devices and LBE/spallation product exhausts trapping systems, which are able to maintain the required vacuum conditions of the accelerator beam line portion inside the reactor containment and prevent bulk diffusion of spallation products to impact and loading the isolation window(s).

Only the reactor containment can be credited for radiotoxicity ultimate barrier function as designed and qualified for that purpose. Any penetration of lines passing through its walls and in contact with the primary coolant or the containment environment (which constitute possible radiotoxicity by-pass) is required to be double-intercepted by fast-acting devices in case of potential leaking condition may occur. Where the beam tube is credited to perform any kind of low-level containment barrier function, this must be limited to the portion of beam tube inside the XADS containment and cannot prolong beyond the containment building walls. Appropriate measure must be taken in order to comply with this requirement (i.e. secondary isolation window(s) and fast-acting valves). Conversely, it may be observed that the high vacuum degree, which is necessary for an accelerator system to operate (even small losses are in fact reported to be able to prejudice its normal operation), may be considered to provide an effective safety barrier in itself. That is a sort of a functional active barrier, rather than passive solid mechanical, which can be credited under normal operating conditions. The portion of target-beam line delimited and characterized as per above, in connection with its “vacuum barrier controlling” purification system is assumed to be all under some vacuum conditions. But any possible exhaust leakage from these systems will be, in any case, eventually processed by the general purification system of the reactor containment, which is a slightly under-pressurized leak-controlled environment suitable and qualified for preventing radiotoxicity releases to the outside.

If, as mentioned, the separation of the target and primary coolants would allow, in principle, the segregation of the spallation products circumscribed to inside the target component itself, together with the connected beam tube portion and the purification system, nevertheless a small fraction of highly energetic secondary neutrons may come to end the spallation cascade in the LBE of primary coolant, outside the LBE contained in the target. In order to limit the radiotoxicity contribution in the primary coolant by these secondary spallation born outside the target, it is required that the design of the target component, which embodies a substantial portion of the last part of the beam line, can ensure the containment of more than a 90% of the spallation products totally generated by the spallation process.

#### **3.4.4 Target Cooling Requirements**

The basic conception of the target, where the LBE is presumed to flow opposite from the LBE-vacuum free surface downwards to a heat sink, is such to inherently hinder the exploitation of a natural convection design. The cooling of the LBE target can rely only on forced convection flow for circulating the hot LBE towards a heat exchanger, located about 1m under the core region, at the level of the fuel assemblies foot and which employs as secondary coolant the LBE primary coolant of the XADS fuel core. The flow pumping is actuated by means of two mechanical propellers that thrust the LBE from the heat exchanger towards the spallation region.

The target heat sink temperature is then fixed to the conditions of the LBE feed at the core inlet, i.e. at a temperature of 300°C, while the target LBE average flow speed is about 0.5m/s. The LBE flow inside the windowless target must be adequately designed to keep the maximum temperature below  $T_{\max}=450^{\circ}\text{C}$  at the LBE-vacuum free surface, in order to limit the vapor pressure and the evaporation rate of the LBE, as well as of other volatile spallation products, into the vacuum beam tube.

In the spallation region at the free LBE-vacuum surface, the LBE flows into a horizontal duct with rectangular cross-section, 12cm wide and 35cm deep. The shape of the duct is specifically designed so that the LBE flow is accelerated to a maximum speed in the middle of the duct (i.e. at the 12cm width) where the beam is transversally scanned. Whereas the maximum LBE flow at the free surface may be kept high enough in order to limit LBE temperature and evaporation rate, the potential corrosion drawbacks ask for limiting the maximum LBE flow below 2m/s.

The temperature level may be higher inside the LBE flow bulk in the spallation region due to the lower flow velocity profile and possibly a higher beam power density distribution at the end of the proton range in the LBE bulk (Bragg peak). The LBE maximum temperature through the beam spallation spike must be kept quite below the LBE boiling point, in order to avoid massive boiling and disruption of the spallation-cooling configuration in the beam-LBE interaction region. Nevertheless, the temperature levels of the target structures which are either in contact with the LBE or isolated from the flow should be maintained below limits which are compatible with the assumed target life time. Concerning the beam tube, it is foreseen, according to the actual windowless target design, to be immersed in LBE by-passed from the primary system, which would assure, by a smooth flow, some cooling of the tube walls. An adequate instrumentation shall be provided in order to monitor the temperature levels along the tube besides beam parameters and possible anomalies.

#### **3.4.5 Beam Distribution Requirements**

Owing to the peculiar LBE flow type which can be arranged at the free LBE-vacuum surface, there would not be, in principle, any need for widening the natural beam aperture in order to reduce beam density and thermal-mechanical loading on solid structures like beam

windows. Nevertheless, potential boiling out of the LBE must be accounted for high power concentrated beam spots impinging in the LBE spallation bulk, so that a wider distribution of the beam power is required for reducing the specific heat deposited by the beam per unit volume of LBE. This may be actually achieved by performing a simple scanning of the beam spot along a fixed line segment, 8cm wide inside the 12cm large LBE flow duct nozzle at the free LBE-vacuum surface. The beam scanning is transversal to the LBE flow direction in the duct, such to delimit the spallation region as a sort of flat slab 8x30cm wide, one beam spot thick, with an average power density of 12.5kW/cm<sup>3</sup> in LBE (assuming a beam average effective cross-section of about 1cm). At an average flow speed of about 0.5m/s, a 250 Joule heat would be deposited inside 1cm<sup>3</sup> of LBE. A 1.5 J/cm<sup>3</sup>K thermal capacity would give rise to an average LBE temperature increase of 167°C when crossing the spallation slab.

In order to assess the effective temperature levels in LBE crossing the spallation region, the actual beam intensity and resulting power density distribution need to be evaluated in connection with the actual LBE flow velocity distribution in the beam interacting slab. Moreover, the effects of possible beam spotting superposition at the scanning edges, where the to-and-fro beam motion is reversed, should be assessed to avoid potential LBE local overheating. Depending on the flow conditions, these could be controlled through the beam scanning frequency and, eventually, through adjustments of the beam spot width itself.

On the assumption of a beam spot width of the order of 1cm, which should include at least more than 99% of the beam intensity (at a 3÷4  $\sigma$  percentile of the beam intensity distribution, about 30kW beam power fringes are left – whose eventual effects on target parts are to be assessed), the beam scanning frequency, at the maximum flow speed of 2m/s at the LBE-vacuum surface, should be of the order of  $f = 1/\Delta t = 2_{m/s}/1_{cm} = 200\text{Hz}$ . This is the maximum frequency for assuring a continuous, 8cm wide, beam footprint at the LBE surface, without separation at the center of the beam zigzag path and some track overlapping at the scanning edges, towards the duct sides, which would be more enhanced in the deep bulk, where the LBE flow speed may be reduced. These effects are being assessed by design analysis. Simulated fluid mechanics tests on a target mock-up are planned to study the most suitable configuration for the LBE flow duct using diverters for shaping the flow profile according to the above-mentioned requirements.

### **3.4.6 Beam Operating Requirements**

The control of the XADS core power can be actuated either by beam or reactivity changes, as shown by differentiation of the core to beam power equation [23,24]:

$$\frac{\delta P_{th_{core}}}{P_o} \approx \frac{\delta P_{beam}}{P_{beam_o}} - \frac{\delta \rho}{\rho_o} \quad (1)$$

Since reactivity-controlling devices are not foreseen for operating the LBE XADS [21], changing only the beam current can control a core power change:

$$\frac{\Delta P_{th_{core}}}{P_o} = \frac{\Delta I_{beam}}{I_o} \quad (2)$$

Because of the prompt neutron kinetics of a sub-critical system, any beam current change from the accelerator, which directly drives the yield of the spallation target neutron source, is reacted almost instantaneously by the core multiplication, quite insensitive to delayed fission neutrons for enough large subcriticality margin  $\rho_0$ . The core neutron flux and fission power are subject to change at the same, potentially fast, rate of the beam intensity, which may constitute an actual drawback for the LBE XADS operability and safety. The

thermal time constant of the core and primary loop are in fact much slower (from a few to some hundreds seconds) in comparison with the fission power period ( $10^{-5}$ - $10^{-4}$ s) to which they are coupled. Thus, following any change of beam power or core reactivity, continuous recursive adjustments of the fast beam control could be needed for offsetting mismatched feedback and damping oscillations from the slow responding thermal system. Abrupt power changes may also apply major thermal-mechanical loading on the fuel and primary loop components, impairing either their toughness or endurance.

The absence of operating neutron absorbers in the LBE XADS may require controlling the beam injection rate to match, or envelope, the time constant of the coupling thermal systems. The condition for implementing in the XADS plant a homogeneous system dynamics during normal operating transients can then involve a crucial designing for the beam intensity variation rate, to make it suitable for the thermal inertia of the coupling systems. The beam intensity injection rate control can be fixed in emulation of the mechanically controlled absorbing rods and implemented by means of inherently safe electronics to prevent any malfunction, or misuse, in ensuring a reliable beam injection rate-controlling system.

In addition to fixing an adequate beam change rate at full XADS operating power, a flexible maneuvering procedure should also try to match at best the functional characteristics of the different coupled systems of the XADS plant (the accelerator complex, the spallation target, the core-primary system, the secondary system and Balance Of Plant) under the widest operational transient conditions, i.e. the system start-up and shut-down, which are shifting the core state between hot stand-by and full rated power. While arbitrary beam injection rates may peak the window temperature to damage at still moderate power levels [24], the need for matching smooth coupling in temperature changes between the primary and secondary system has also been shown [21]. A first tiny beam injection step may turn useful to initiate the beam power start-up sequence in order to trigger a small LBE flow in the spallation target in the case of the window design (for smoothing out the window temperature on the following beam power injection) and for smoothing the temperature mismatch between the primary-secondary loop (in any case). As the main rise to the nominal power level is being performed at a fixed ramp-rate, a 3-step sequence has been assumed [23] for the LBE XADS start-up to normal operation:

- a) **Turn-on step:** from hot stand-by zero power up to a  $1\pm 1.5\%$  of core rated power (i.e.  $\sim 1\text{MWth}$ );
- b) **Unrestricted ramp step:** from previous step up to  $10\pm 15\%$  core power (i.e.  $\sim 10\text{MWth}$ );
- c) **Fixed ramp-rate step:** at  $0.1\%/s$ ,  $0.0001(\Delta P/P)/s$ , power change rate from the  $10\pm 15\%$  level up to the rated core power of  $80\text{MWth}$ .

Hold-times may interleave the sequence, whenever needed, depending on accelerator-core or loops operation requirements. The aims for a 3-step sequence are:

- To set a flexible procedure for the joint start-up of quite different coupled systems (i.e. the chain formed by the accelerator, the target, the core, the primary system, the secondary system and the Balance Of Plant);
- To let a low power operation adequate for running high enough beam current to reliably stabilize the control of accelerator parameters prior to drive the whole system towards higher power levels;
- To limit the eventual need for running early beam rises at unrestricted rates to power levels that have limited impact on the driven complex.

The initial 1% power surge ( $30\pm 80\mu\text{A}$  beam; Beginning Of Life BOL- End Of Life EOL) may turn to be useful for providing a low-load feed for setting the accelerator system at low-power stand-by conditions. The XADS may thus be set at start-off to power conditions

without either major restrictions for the accelerator or impact for the driven system. This first small step may allow the following ramping to 10 MWth core power (i.e. up to 0.3÷0.8mA, BOL÷EOL) at a fairly unrestricted rate. This condition may apply to the core and primary loop system at least, while primary-secondary transients matching to avoid temperature instabilities in the secondary system would require slow rates [21]. Conversely, an unrestricted ramp rate option could be helpful for the accelerator complex to adjust and steady its control conditions at substantial power level (near to 1mA beam at EOL) so that the subsequent ramp to rated power may perform under most reliable conditions for the LBE XADS whole system. A converging option must then be eventually thought of, complying the plant operational transient requirements and the accelerator complex needs.

The third step of the start-up sequence is performed under fairly slow ramp-rate control of the beam intensity, which compares to the reactivity insertion controlled by absorber rods in fast reactors. The ramp-controlled step (with a rate of 8 kW/s) starts at a core power level of 10 MWth. It will take about 2.5 hours to get the nominal level of 80 MWth. It is noted that [24] if the core power were to rise driven by reactivity changes only, once the beam has been started and set to the nominal current level (2.5mA at BOL), a 30% control rod worth change would be released by neutron absorbers for accomplishing a 10÷100% power step. The beam current change is instead straightforwardly linear, but requires a beam intensity variation of a factor of ten. Nevertheless, while the addition of control rods to a small XADS may significantly increase the complexity of the primary system, the inherent liability to reactivity initiated accidents is also an unavoidable drawback of the control rods, i.e. movable neutron absorbing systems.

The choice of a 0.0001( $\Delta P/P$ )/s rate for the beam current ramping, which should address both the third step of the start-up and the XADS power changes at the nominal power level, is based on typical rates of reactivity insertion following inadvertent withdrawal (at its natural speed) of a control rod. A few cents/s, or  $\Delta k_{\text{eff}}=0.0001 k_{\text{eff}}/s$  are in fact assumed for a typical fast reactor fuel with  $\beta \approx 0.003\div 0.004$  [24]. When the 0.01%/s power rate is applied in the approximated equation (1) (applicable for small reactivity changes vs. larger subcriticality levels) equivalent rates can be alternately found at the BOL÷EOL subcriticality levels both for reactivity changes, which result as  $\Delta\rho \sim \Delta k=1.1\div 2.5\%/h$  for  $-\rho_0=3\div 7\%$  BOL÷EOL respectively, and beam current variations:

$$\frac{\Delta I}{I_o} / s = 0.01\% / s = \pm 0.25 \div 0.6 \mu A / s \quad (3)$$

The lower value of 0.25  $\mu A/s$  applies to fuel core under the highest reactivity conditions at BOL, when the core response is more sensitive to beam rate injections, and, in order to avoid mis-operation, is fixed as the lower bounding applicable one. Depending on various requirements as fuel conditioning, transients matching for different cooling loops, set points for operating condition check-out and overrun limitation, etc. the actual start-up control procedure of the LBE XADS may be managed to last as flexible as needed by interleaving ramp steps with time lapses at constant power.

As for the beam shut-off under normal operating conditions, these may just reverse the start-up control procedure. That allows a smooth fading of the high beam power and a soft relieve of the impact of the thermal-mechanical loading in the fuel core and primary system structures. The same beam rate of  $\pm 0.25 \mu A/s$  is also controlling the LBE XADS power changes at the nominal level in order to avoid both unstable control and abrupt thermal loading on the structures. Set points, adjustable along with core cycle, may also delimit maximum beam insertion for preventing control errors or mis-operation.

It is finally observed that the design flexibility of a control system based on electronic circuitry rather than on mechanical devices should allow to optimize the beam rate for best

operation of the LBE XADS under both performance and safety viewpoints. The reliability of a beam control system based as per above shall be assessed in connection with the XADS safety analysis in order to determine both type and probabilistic occurrence of possible malfunctions.

### **3.4.7 Beam Stability Requirements**

During normal operating conditions nuclear power plants generally account for limited instabilities of the power level, which are restricted to a few percent, i.e.  $\pm 2\%$  [24]. As an extension of equation (1), the differentiation of the XADS core power into source and multiplication terms is applied for assessing stability conditions:

$$\left(\frac{\delta P}{P}\right)_{core\ power} = \left(\frac{\delta S_n}{S_n}\right)_{neutron\ source} + \left(\frac{\delta M_f}{M_f}\right)_{system\ energy\ multiplicity} \quad (4)$$

So that, on a simple even sharing basis, a  $\pm 1\%$  variability range (or  $\pm 1.4\%$  by square-rooting) can be attributed to the neutron source and to the nuclear chain generation system. The allowance for source variability could be eventually extended to a larger range, e.g. to a full  $\pm 2\%$ , if the multiplying system variability could be assessed as fairly limited itself, e.g. to less than  $\pm 1\%$ . That results in a reasonable overall instability span at nominal power less than  $4\div 5\%$ . However, the actual XADS multiplying system variability has not been assessed yet, so that it may be rather arbitrary to speculate on its actual range. While in fact it could be expected to be somewhat limited, due to the absence of absorber systems (especially movable ones), the thermal-hydraulics-neutronics feedback is not straightforwardly forecasted. Consequently, a safe value of  $\pm 1.4\%$  accounting for both the source and the multiplying system is to be presently assumed. The neutron source variability is shown [24] to correlate to the beam energy and intensity as:

$$\left(\frac{\Delta S_n}{S_n}\right)_{rms} = \sqrt{w_{fE}^2 \left(\frac{\Delta E}{E}\right)_{rms}^2 + \left(\frac{\Delta I}{I}\right)_{rms}^2} \leq \pm 1.4\% \quad (5)$$

where  $w_{fE}$  is an energy dependent factor derived from the spallation neutron yield formula. Equation (5) can be then used to determine either the energy or the intensity variability limit once the complementary parameter is known, or has been otherwise assessed.

By applying a simple sharing basis between the two terms in the square root, equation (5) would provide a  $\pm 0.61\%$  and  $\pm 1\%$  variability ranges for the beam energy and current respectively. The allowable variability range of beam power would then be  $\pm 1.17\%$  (about 84% of the source variability), or  $\pm 42\text{kW}$  at the maximum beam power of  $3.6\text{MW}$ .

Quite different intrinsic stability characteristics are expected due to the distinct techniques in forming and controlling beam energy (connatural to accelerating devices) and current intensity (broad-range adjustable operating parameter). Therefore, some kind of criterion needs to be assessed for distinguishing constraints between beam energy and intensity. The most critical under the viewpoint of beam trajectory stability, i.e. the beam energy, needs to be apparently delimited, as this will eventually impact on the beam transport line requirements.

### **3.4.8 Beam Focalization Requirements**

A  $\pm 0.61\%$  beam energy stability figure, as assessed above by means of equation (5) on an even sharing basis between beam energy and current terms, may be assumed to transfer from the accelerator complex, through the beam transport line, to the spallation target without major additional variations. It is conversely assumed that the beam transport line be designed

with acceptance figures necessary to allow such beam energy instabilities. Since the beam line must be bent downwards to the spallation target, it is necessary to assess whether a given beam energy stability figure, as far as its impact on the beam path is concerned, is able to match the actual design of the spallation target unit.

This implies that, in practice, the beam stability figures shall be assessed by means of a focalization requirement that must be customized on the actual path of the beam line through the layout of LBE XADS [21]. The LBE XADS nuclear block arrangement allows a 15m proton beam “free-flight” distance between the beam line-to-target down bending magnet and the spallation zone in the core. As per the previously reported spallation target description, the beam is being scanned on the LBE-vacuum free surface along an 8cm line segment inside a 12cm wide LBE flow duct. This means that only a 2cm gap is available on both sides of the beam scanning for allowing possible over-scan due to either scanning or beam energy born instabilities. The 2cm allowance (that is actually theoretical, i.e. with a zero width spot beam size) has to be compared to the 15m free flight from the beam line-to-target bending magnet and its perturbing path on the beam energy instability.

The differentiation of the beam rigidity formula [24], where  $E_0=938\text{MeV}$  is the proton rest mass and  $E_{k0}=600\text{MeV}$  the nominal beam energy, allows to assess the relative variations of the beam bending radius,  $\Delta r/r$ :

$$\frac{\delta r}{r} = \frac{E_k + E_0}{E_k + 2E_0} \frac{\delta E_k}{E_k} - \frac{\delta B}{B} = 0.62 \frac{\delta E_k}{E_k} - \frac{\delta B}{B} \quad (6)$$

The beam shift at the target level, which would follow an energy swing  $\Delta E_k$  from the nominal value  $E_{k0}$ , perturbing the beam bending radius of  $\Delta r$  (from  $r_0$  to  $r_0'$ ) is given, on a geometric construction, by:

$$\Delta x \cong \frac{\Delta r}{r_0} [(1 - \cos\alpha)r_0 + L \sin\alpha] \quad (7)$$

where  $L=15\text{m}$  is the beam range to target and  $\alpha$  the beam-to-target bending angle and  $r_0$  the bending radius at the nominal energy of 600 MeV ( $r_0=2.71\text{m}$  for a magnetic field of 1.5T). In the case of a  $45^\circ$  beam-to-target bending and neglecting field perturbations  $\delta B/B$ , equations (6-7) allow to assess the beam shift as:

$$\left( \frac{\Delta E}{E} \right)_{rms} \approx \pm 0.28\% \Rightarrow \Delta E_{rms} = \pm 1.7\text{MeV} \quad (8)$$

The condition expressed by equation (8) is quite tight, more restrictive than the above estimated  $\pm 0.61\%$  based on an even beam energy-current sharing. This means that the allowance for the beam current intensity can be comparatively higher and, based on equation (5), it can be determined as:

$$\left( \frac{\Delta I}{I} \right)_{rms} \leq \pm \sqrt{(1.4\%)^2 - w_{fE}^2 \left( \frac{\Delta E}{E} \right)_{rms}^2} = \pm 1.32\% \quad (9)$$

It is noted that both beam energy and current variability values are assessed for a beam line-to-target bending of  $45^\circ$ , which is not the actual configuration considered in [21], where a  $90^\circ$  line-to-target bending is still considered instead (after a previous  $30^\circ$  line bending). The beam transport line assumed here with at least three bending sections of  $30^\circ + 45^\circ + 45^\circ$  shall be adequately designed to fit inside the reactor building and to accommodate the necessary beam conditioning and stabilizing optics between the  $30^\circ$  and the first  $45^\circ$  beam line bending and between the two  $45^\circ$  beam line bending. The substantial space needed for a beam bending system and its impact on the reactor layout and on the safety containment have to be kept in mind. No conditioning is assumed possible after the second  $45^\circ$  bending, which drives the beam directly downwards to the spallation target, in the free flight beam path.



Equations (8) and (9) show that, due to the quite restrictive requirement on the energy variability which is bound to the beam line transport to target configuration itself, the allowance for the beam current variability can be, in practice, as ample as the source variability is allowed to be.

It is finally noticed that in deriving equation (8) the contribution of the magnetic field variability term ( $-\delta B/B$ ) to  $(\delta r/r)$  in equation (6) has been neglected: this may be a reasonable assumption when the field is well inside the saturation region, for magnets with  $B=1.5\div 2T$ .

#### **3.4.9 Summary of Main Parameters for LBE-Cooled Primary System**

The main parameters considered for the windowless target and described in the previous sections are summarized in the following tables.

<i>Target Relevant Parameters</i>	
Power of subcritical core	P = 80 MWth
Max. proton energy	E = 600 MeV
Max. proton beam intensity	I = 6 mA
Max. target power / beam power	P = 2.6 / 3.6 MW
Max. target design power	P = 3.0 MW
Target material	Lead Bismuth Eutectic - LBE
Target life time	One fuel cycle (30000 h, with 25000 h at power)
Beam scanning footprint size	Beam spot width x 80 mm
Beam spot width (at 99.5%, 3.26 $\sigma$ or better)	10 mm (to be confirmed)
Beam scanning method	8 cm width, transversal to LBE flow
Beam scanning frequency	200 Hz
Current density profile of the beam spot	bivariate Gaussian (to be confirmed)
Maximum current density of the beam scanning	< 50 $\mu\text{A}/\text{cm}^2$ (Window Target)
Maximum current density of the beam scanning	< 750 $\mu\text{A}/\text{cm}^2$ (Windowless Target)
Vacuum level at the target LBE – beam interface	$\sim 10^{-6}$ Torr (to be confirmed)
Max. LBE temperature at the free vacuum surface	$\leq 450^\circ\text{C}$ (Windowless Target)
Target LBE velocity in the spallation zone <ul style="list-style-type: none"> <li>• flow average</li> <li>• maximum at the flow surface</li> </ul>	(Windowless Target) 0.5 m/s $\leq 2.0$ m/s
Geometry of the beam tube (Outer Dimensions) <ul style="list-style-type: none"> <li>• at the top of the target unit</li> <li>• at the beam extraction</li> </ul>	rectangular section 50 x 50 mm 80 x 120 mm
Beam line free magnet-to-target length	15 m
Beam tube thickness	5 mm (to be confirmed)
Geometry of the spallation zone: <ul style="list-style-type: none"> <li>Width of the LBE flow duct</li> <li>Beam scanning width</li> <li>Depth of the LBE flow duct</li> </ul>	(Windowless Target) 120 mm 80 mm 350 mm

*Table II – Main Target Parameters.*

<i>Beam Relevant Parameters</i>	
XADS Core gain factor G, BOL÷EOL	54 ÷ 22
Max. proton beam power	3.6 MW
Proton beam energy	600 MeV
Spallation neutron yield	~ 13 ÷ 15 neutrons/proton
Beam current, BOL÷EOL	2.5 ÷ 6 mA
$k_{\text{eff}}$ , BOL÷EOL	0.97 ÷ 0.93
Beam control rate at nominal core power level	± 0.25 $\mu\text{A/s}$
Beam start-up sequence	
a. Turn-on step	1 ÷ 1.5 % $P_0$
b. Unrestricted ramp step	10 ÷ 15 % $P_0$
c. Fixed ramp rate step	0.01 % $P_0/\text{s}$
XADS Plant power stability	± 2 %
Multiplication system stability	± 1.4 %
Spallation neutron source stability	± 1.4 %
Beam energy stability	± 0.28 % ± 1.7 MeV
Beam current stability	± 1.32 % ± 33 ÷ 80 $\mu\text{A}$ (BOL ÷ EOL)
Beam power stability	± 1.35 % ± 20 ÷ 49 kW (BOL ÷ EOL)

*Table III – Beam induced requirements from target.*

## 4. PROPOSED TECHNICAL SOLUTIONS

The layout of the two main options for the accelerator - the linear accelerator and the cyclotron - are described and discussed in this chapter. Some important technical solutions that may impact the overall design are presented in a more detailed manner in order to give a fairly precise idea of the technical difficulties. As indicated in the introduction part, more emphasis is given to the different linac possibilities and choices of RF structures than for the cyclotron option, given the definite advantages of using linacs for future XADS.

### 4.1. LINAC Option

The linac is divided in three major parts. The first part is the injector including the proton source and the Radiofrequency Quadrupole (RFQ). The second, called "intermediate

part", enables to accelerate the beam up to approximately 100 MeV. Finally, the last part is the high-energy part covering all energies above 100 MeV. While the injector and the high-energy parts are rather well determined from already known technology, the intermediate section is still under investigation and asks for additional R&D work.

#### 4.1.1 The Injector : Source and RFQ

##### 4.1.1.a The ECR Ion Source

###### 4.1.1.a.a Introduction

An ECR source should be the best choice to fit in with the high reliability - availability request of the XADS. This type of source does not need any filament or antenna inside the plasma chamber. The proton beam produced by the source can be injected in an RFQ cavity to be accelerated up to few MeV.

###### 4.1.1.a.b Source Description

The ion source operate at 2.45 or 3 GHz with an axial magnetic field providing two ECR resonance zones at both plasma chamber extremities simultaneously. The source and its ancillaries are installed on a 100 kV insulated platform to fit in with the RFQ entrance energy. The RF power is produced either by a 1.2 kW magnetron source or a klystron and fed to the source via standard rectangular waveguides. An automatic tuning system help to accommodate and adapt the RF load. The magnetic field is provided either by coils or permanent magnets. The small copper plasma chamber (0.5 liter) located at the center of the magnetic structure has to be water-cooled.

A single aperture extraction system has been designed with specific code. An intermediate electrode located in the accelerating gap can be tuned to minimize the distortions in the phase-space distribution. An electrode at  $\sim -2$  or  $-3$  kV is inserted between two water-cooled grounded electrodes to avoid the acceleration of electrons produced by ionization of the residual gas in the beam line. The electrode construction takes into account possible beam losses leading to damage.

shows a scheme of the French source SILHI [25] and accelerator column developed in the framework of the IPHI (High Intensity Proton Injector) project.

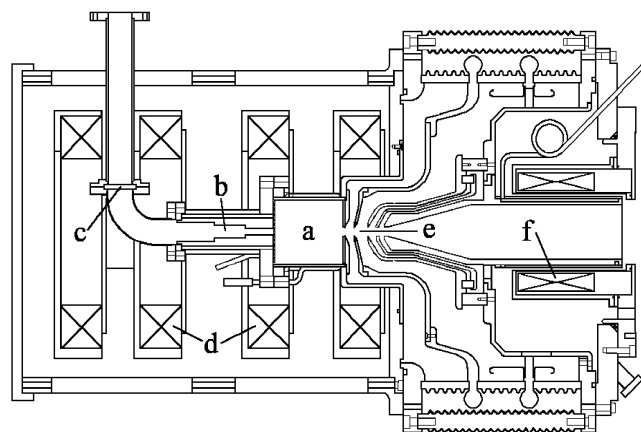


Figure 9 - Source and 95 kV extraction column: a) plasma chamber, b) RF ridged transition, c) quartz window, d) coils, e) 5 electrode extraction system, f) DCCT

The low energy beam transport (LEBT) line is designed to guide the beam into the RFQ acceptance, taking into account the variable space charge compensation (SCC). The SCC depends on the amount of free electrons due to beam losses on the walls or beam interaction with the residual gas. A small amount of heavy gas (Ar or Kr) in the LEBT allows a better space charge compensation. Intercepting diagnostics also lead to secondary electron production and locally modify the beam compensation. To allow an accurate beam matching to the RFQ, a precise knowledge of the beam characteristics is required at the cavity entrance. Presently the beam position and size could be obtained from CCD cameras. Faraday cup, beam stopper and toroids (DC and AC Current Toroid) allow beam current measurement and its high-frequency fluctuations. Insulated screens give information on beam losses and beam axis. Emittance at the RFQ entrance has also to be well known to minimize RFQ transmission limitation. To summarize, a lot of diagnostics items are needed to characterize the beam in the LEBT.

#### **4.1.1.a.c Optimization of performance**

To minimize possible breakdown and to optimize the reliability, different developments and technical choices have been adopted at Saclay. The next non-exhaustive list presents several topics able to improve the reliability, as already successfully tested with SILHI:

- Quartz window protected behind a water cooled bend
- Electrode shape optimization to minimize the electric field and the spark rate
- Large safety margins on every power supply (High Voltage and others)
- Optimization of power supply air or water cooling
- Separate cable path and shielding for signals and power
- Galvanic insulation of analogue and digital signals
- Use of EMI hardened devices especially for all sensitive electronics and PLC
- Development of beam current feedback
- Development of automatic start/restart procedures
- Development of specific beam diagnostics

Beam reliability – availability as high as 99.8 % (Figure 10) has already been achieved with SILHI, for a 90 mA proton beam (total extracted beam = 114 mA) during a 162 hours long run. The source was operating in a continuous mode, a feedback loop maintaining a beam stability of  $\pm 0.2$  mA. This loop would authorize a very precise adjustment of the extracted beam in case of the XADS commissioning for example. Figure 11 shows the SILHI extracted beam current as a function of the RF power. The SILHI source has been designed to inject a 100 mA proton beam in the IPHI RFQ. Developments are always in progress to minimize the number of beam trips and to reduce their duration.

Specific run tests for XADS (with lower current) will be performed to quantify the over design method efficiency in term of reliability.

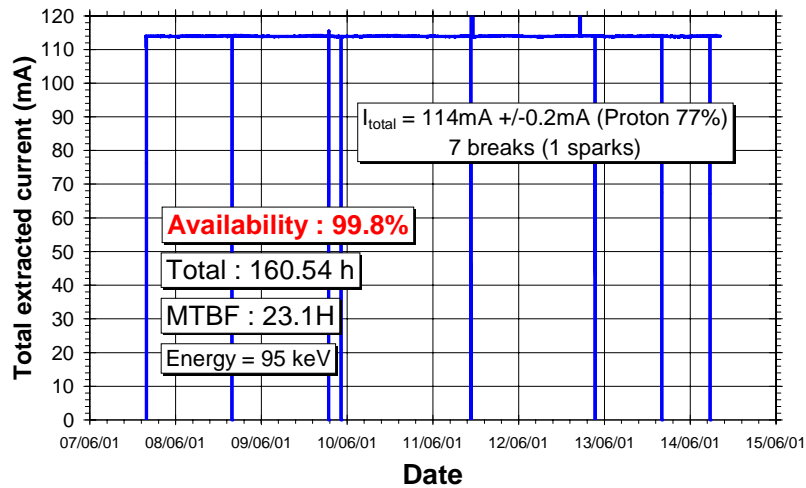


Figure 10 – A 162 hour long run reliability test performed with the SILHI source at CEA/Saclay.

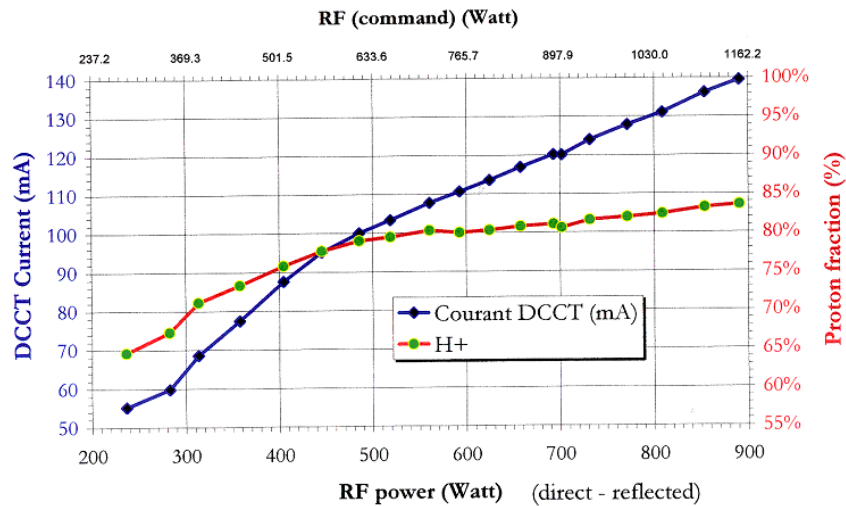


Figure 11 - Extracted beam and proton fraction vs RF power.

#### 4.1.1.b The RFQ (RadioFrequency Quadrupole)

##### 4.1.1.b.a Introduction

The ECR source, chosen for its well-known advantages, should deliver up to 10 mA at 95 keV to the RFQ. The existing test stand SILHI already currently produces a 130 mA, 95 keV proton beam with an emittance better than  $0.15 \pi \cdot \text{mm} \cdot \text{mrad}$  ( $r-r'$ , rms normalized) with a very high reliability. The following accelerating stage of the injector is a four-vane type RFQ [26].

Although this RFQ assembly could look somewhat delicate, recent progress were made in the field of long duty cycle (up to CW) 350 MHz four-vane RFQs and they are totally relevant to the proposed architecture. At Los Alamos National Laboratory, the construction of the 110 mA, 6.7 MeV, CW RFQ for the Low Energy Demonstration Accelerator (LEDA) [27] was commissioned at the design performance. The IPHI RFQ is under construction in France at CEA Saclay [28,29]. It already integrates some improvements, thanks to a close

collaboration with the LEDA team. In Italy at INFN-Legnaro [30] a third RFQ of this kind is under development. In this context, given the experience of the teams, a large number of the technical difficulties such as the cooling system or manufacturing tolerances are more easily addressed.

#### 4.1.1.b.b RFQ Design

The input energy of 95 keV results of a compromise between RFQ length, source reliability and space-charge control. The 5 MeV output energy results of a compromise between cavity length, feasibility of the next accelerating structure (DTL using EM quadrupoles or spoke cavities), and high beam transmission. The use of existing klystron at 352.2 MHz leads to an optimum size of the cavity. The design current of 100 mA is selected to reach a high reliability at the lower currents needed by the application. The expected normalized rms emittance from the source is  $0.2 \pi \cdot \text{mm} \cdot \text{mrad}$ . Nevertheless, a safety margin is taken using  $0.25 \pi \cdot \text{mm} \cdot \text{mrad}$  in beam dynamics calculations. The maximum field inside the RFQ, commonly measured in Kilpatrick units, is a parameter that strongly influences the length of the structure, its transmission and its robustness with regards to RF breakdowns. The maximum electric field has been limited to  $1.7 K_p$  ( $31.34 \text{ MV/m}$ ) taking into account experience with the CRITS Experiment at Los Alamos, the LEDA test stand in Los Alamos and RFQs operated at Saclay in the past.

At this stage, a longer RFQ designed with the view to guaranty the longitudinal field stability is preferred despite the small price increase of the overall project. With this choice of 1 or 2 extra meters of RFQ structure, the overall performance (lifetime and availability) will be improved. Great care has to be taken on lost particles in the RFQ cavity. The final design has to be selected to avoid localized and high-energy losses (activation problems), and to provide the highest transmission avoiding any bottleneck [26]. This way good availability might be achieved on the short term (spark down avoided by excellent transmission and low surface field) and long-term range (sputtering in the cavity, activation). Many beam dynamics computations including error studies will have to be done as for the French IPHI project, using several complementary existing codes (PARMTEQM, TOUTATIS [31,32], and LIDOS.RFQ [33]).

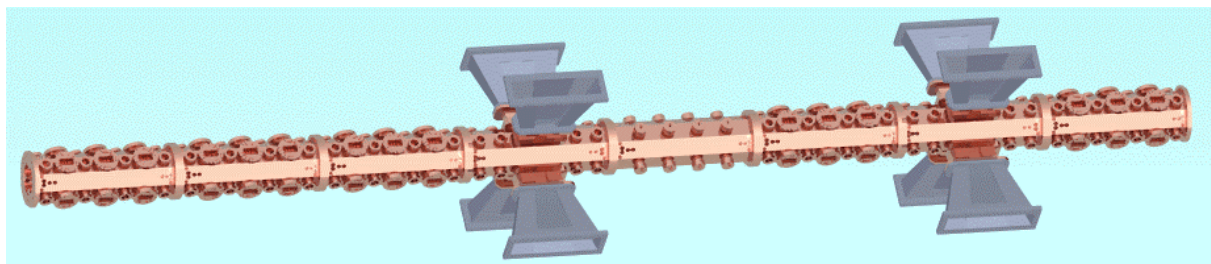


*Figure 12 – A sketch of the IPHI RFQ.*

#### 4.1.1.b.c RFQ Structure

In order to keep under control the cooling system, the cavity type has to be a 4-vane RFQ, much easier to cool. The structure is made up of 8 one-meter long sections accurately machined and brazed then assembled with resonant coupling every 2 meters (similar to the IPHI [29] and LEDA design [34]). The coupling plates allow a damping of the RF longitudinal parasitic modes and the introduction of fingers to push away the dipolar modes.

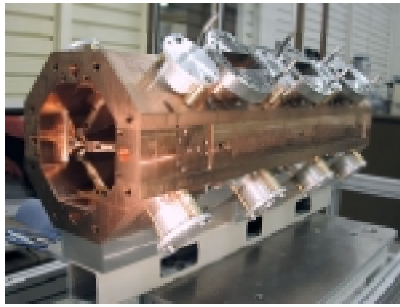


*Figure 13 - First meter of the IPHI RFQ before brazing.*



*Figure 14 - Radial matching section of the IPHI RFQ after brazing.*

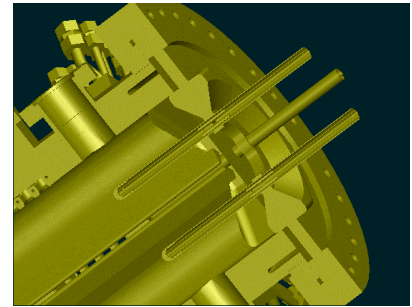


*Figure 15 - Drawing of the coupling plate.*

#### **4.1.1.b.d The RF system**

The RF design of the cavity requires intensive 3D simulations and developments [35] with cross-checking on cold model. The field will be tuned using 128 tuners equally distributed along the RFQ. Similar RF windows to those needed have been successfully tested up to 700 kW at LANL for LEDA [34].

Since the voltage law all along the RFQ has to be tuned with a high accuracy, it has been decided to use automatic tuning procedures [36] based on the bead pulling principle associated with a powerful mathematical formalism [37,38]. A six-meter long cold model was built to develop and validate these procedures [39], which were already successfully tested on two sections equipped with a coupling plate [40]. A procedure was also developed in order to check possible vane displacements during the brazing process [41], and allows the detection of a 20  $\mu\text{m}$  vane displacement.

#### **4.1.1.b.e RFQ Cooling System**

The cooling system of the RFQ must fulfil two essential functions: first to evacuate the 1.2 MW of dissipated power in the copper (independently of the current beam value) and then to maintain, by adjustment of the temperature, the resonance frequency of the cavity at the right value.

The slow frequency tuning will be done using the cooling system of the cavity based on the LEDA design [34]. The inlet water temperature is 10°C with a tunable water flow up to 6 m/s. An erosion/corrosion analysis is presently done to check the long-term effect.

#### **4.1.1.b.f RFQ Vacuum**

Great care has been taken in the optimization of the pumping system. Two of the 1-m long sections are dedicated to the RF feed while all the remaining sections are equipped with a total of 72 pumping ports carefully designed to maximize the pumping speed. Eight cryogenic pumps will provide through those 72 ports a vacuum lower than  $2 \cdot 10^{-5}$  Pa in the RFQ [42]. The port and manifold conductance have been optimized to obtain a pumping speed of 5700 l/s at the cavity level for 12000 l/s at the pump level.



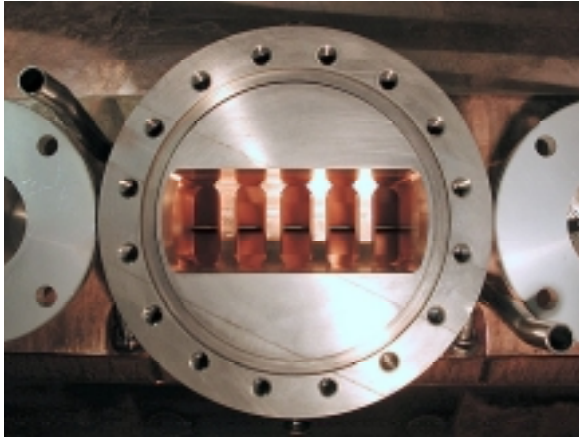


Figure 16 – Pumping port.

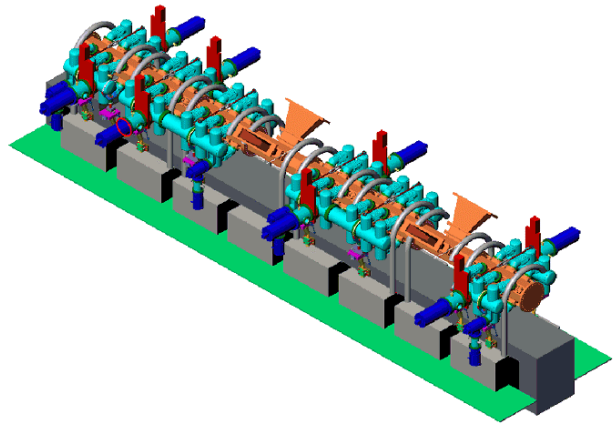


Figure 17 – Vacuum surrounding.

#### 4.1.2 Intermediate Section

As stated earlier, the intermediate part covering the 5-100 MeV range is still a wide-open domain. Because the proton energy is too low to be able to use typical elliptical cavities, a variety of new structures have been under study during the last decade that could achieve the required gradients. However, no ideal solution has yet been identified as the best one having no clear definite advantage. In order to show some of the possibilities, three completely different proposals are described, including one warm (normal conducting) option and two superconducting structures, namely the crossbar cavity and the spoke cavity.

##### **4.1.2.a Warm Option**

The intermediate part may be constructed using normal conducting copper structures. As a matter of fact, every high intensity proton accelerator design known today uses copper RF structures in this energy range. These structures are usually based on Drift-Tube Linac (DTL) with sometimes some variation or improvement, trying to optimize either RF fields, efficiency or reliability. As an example, the SDTL (Side Drift-Tube Linac) or CCDTL (Coupled-Cavity Drift-Tube Linac) fall in that category. Some detailed typical layouts maybe found in many accelerator designs (ESS, SNS, APT, TRISPAL, etc...)

In the intermediate section of the Spallation Neutron Source (SNS) under construction at Oak Ridge (Tn, USA), a DTL is foreseen just after the RFQ output at 2.5 MeV up to an energy of 20 MeV. Then, a short section with several tanks based on CCDTL structures will bring the beam up to 86.8 MeV. Finally, CCL (Coupled Cavity Linac) structures will follow up to 185 MeV prior injection in the superconducting high-energy cavities. In the APT project, only two types of structures (CCDTL and CCL) were planned to be used from 6.7 MeV (RFQ output) up to an energy of 217 MeV.

A DTL structure is convenient because it allows the use of focusing quadrupoles embedded inside, which is a good way for providing compact and strong focusing for low energy protons. At these energies, this structure offers a good power conversion efficiency from the radiofrequency to the beam (high shunt impedance). The CCDTL is a hybrid RF structure constructed of short DTL's contained in a cavity, alternate with quadrupoles magnets. Then, two adjacent cavities are linked together by side-coupling cells. That structure has been designed in order to combine the advantages of both the DTL and the CCL. The main advantage of the CCL is its high coupling strength and stability. It could therefore be

used as short individual accelerating cavities in between external focusing quadrupoles, just alike the SCRF high energy section. That is a great advantage when reliability is a strong issue, which is our case in a XADS type machine. In that way, the failure of a component can be easily handled without having to take apart the whole tank.

On the overall, the main disadvantage of the warm option is the need for a rather high RF power only to maintain the electromagnetic fields inside the structures. The RF to beam efficiency is therefore quite poor, especially for low intensity CW beams. On the other hand, there is a lot of experience on these structures since they have been (and will most probably continue to be) used for a long time. The associated risk in the choice of this option is extremely low. Also, very little development is required to demonstrate its performance adapted to the XADS case. In the frame of the following XADS program, a solution of the intermediate section based on DTL type structures will have to be looked at, and a detailed design worked out. Although no expensive R&D is required, it is quite important that this study should be finalized. It could be looked at as a baseline option to which the other new and promising superconducting designs described in the following would have to compare with.

#### **4.1.2.b Superconducting Cross-Bar Cavity**

##### **4.1.2.b.a Introduction**

This chapter describes one design option for the medium energy part of the XADS linac. The new CH structure (Cross-Bar  $H_{21(0)}$ -mode) is a promising candidate for that linac option. Investigations and extended particle dynamics studies for a Superconducting Cross-bar (SCCH) cavity showed the general capability of this resonator type for the acceleration and focusing of intense beams [43]. A superconducting CH layout for the medium energy XADS linac part is presented together with the corresponding beam dynamics calculations performed with the KONUS dynamics program LORASR [44]. A preliminary resonator layout made with MICROWAVE STUDIO [45] for the second tank of the proposed SCCH DTL linac has been done and the results are outlined. A ( $\beta = 0.1$ ) 19-cell prototype cavity has been designed and will be fabricated and chemically treated before autumn 2003.

##### **4.1.2.b.b Characterization of H-Type Drift Tube Structures**

H-type cavities were developed during the last 30 years successfully to serve for a large variety of applications in the field of ion acceleration [46,47,48,49]. Radio Frequency Quadrupole (RFQ) and Drift Tube Linac (DTL) versions were designed in the H11- (IH-DTL, like at GSI, CERN, TRIUMPF,...) as well as in the H21-mode (4-Vane-RFQ, standard structure at RF frequencies above 200 MHz). The Inter-digital H-type (IH) drift tube structure ( $H_{11(0)}$ -mode) is efficient for an energy range from 100 keV/u to 30 MeV/u, especially when combined with the KONUS beam dynamics. Effective voltage gains as high as 10.7 MV/m were demonstrated in pulsed RT operation. Because of its mechanical properties (very sensitive against lateral mechanical tank oscillations affecting the drift tubes capacity), the IH structure is not very well suited to realize superconducting versions.

However at beam energies between 5 MeV/u and 150 MeV/u the Cross Bar H-type (CH) drift tube structure ( $H_{210}$ -mode) shows a large potential as well for room temperature as for super-conducting designs. While the acceleration mode is identical to the one used to operate the 4-vane-RFQ, the dipole modes are shorted by the drift tube stems. Consequently mode separation is guaranteed in case of the CH-DTL, while in case of the 4-vane-RFQ special concepts had to be developed to push the dipole modes apart. Figure 18 shows an overview on H-Type linac structures.

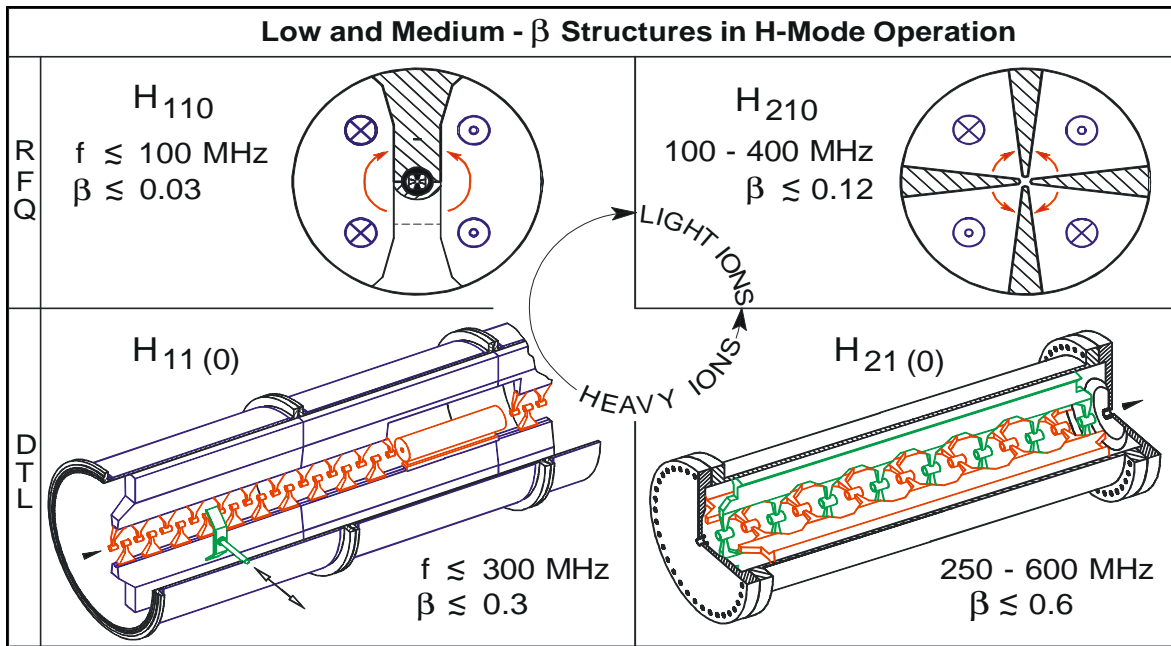


Figure 18 - Sketch of the H-type linac family.

#### 4.1.2.b.c The KONUS Beam Dynamics

The KONUS (Kombinierte Null Grad Struktur) beam dynamics is especially suited to exploit the full potential of H-DTLs: It is a periodic structure, which consists of quadrupole triplets and drift tube sections. Each drift tube section starts with a few rebunching gaps at negative synchronous phase ( $-35^\circ$  typically) followed by the main multigap acceleration section, where the bunches are injected at RF phases around  $0^\circ$  and gradually slip to negative rf phases towards the section end. This means that longitudinal focusing is located in front and behind of each quadrupole triplet, while the working point of the central part of each drift tube section is near the crest of the wave, where the acceleration efficiency is at its maximum, while the transverse defocusing RF forces are minimized. Figure 19 illustrates the KONUS concept in detail [50].

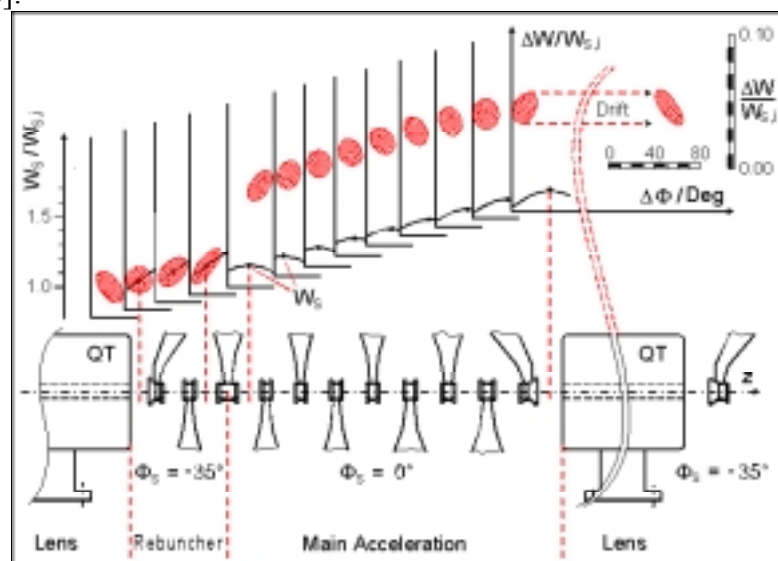


Figure 19 - Longitudinal bunch movement of one complete KONUS period.

After passing a quadrupole triplet the beam arrives defocused at the rebuncher section at a negative synchronous phase of usually  $-35^\circ$  and with synchronous energy. After passing this part the beam is focused and still on the synchronous energy. In the first cell of the following multi-gap  $0^\circ$  part the bunch has now 2-8 % more energy when compared to a synchronous test particle and starts near the crest of the wave, to minimize the radial defocusing forces, into the  $0^\circ$  section. The beam leaves the  $0^\circ$ -section longitudinally focused (because of slipping to-wards negative RF phases while passing that section) and enters the triplet lens where the bunch will be longitudinally defocused again.

As a consequence a maximum number of gaps at a given gap voltage and at a given aperture can be passed between two adjacent triplet lenses. This beam dynamics allows to build multi-cell cavities with drift tubes, resulting in high shunt impedance and high accelerating fields in case of H-type linacs. The lenses are completely separated from the cavities, resulting in slim drift tube geometry with small electrical capacities and with high acceleration field [51].

As the KONUS periodicity is not as smooth as the conventional concept, larger emittance growth is seen in KONUS designs at increasing beam current. On the other hand the concept of well aligned and robust triplet lenses, separated from the RF cavities, and the shorter total IH-linac length keeps the beam loss rate as well as the probability for misalignment low.

#### **4.1.2.b.d The CH-DTL**

At higher beam velocities one has to apply higher operating frequencies to get an efficient acceleration. The CH-cavity has a larger diameter at a given RF frequency when compared to the IH-cavity and by that way cavities with frequencies up to around 800 MHz can be realized.

The CH-cavity development can profit a lot from the experience gained on IH structures but needs some additional design effort. But the CH-structure has an enormous advantage: Its mechanical robustness, which is provided by the crossed stems. This opens the possibility to realize superconducting CH-cavities. Moreover all H-type structures have rather small transverse dimensions when compared to competing SC structures like 2 gap quarter wave and spoke-type or elliptical cavities at the same RF frequency [52].

At present the Institute for Angewandte Physik (IAP, J. W. Goethe-Universitaet Frankfurt) is equipping a cryogenic laboratory especially for the development of SCCH cavities. A design study of a 19-cell, 350 MHz prototype cavity with  $\beta = 0.1$  is nearly completed (see Figure 20). This cavity will be realized in close cooperation with industry. Besides the demonstration of attractive accelerating field levels, adequate RF couplers have to be developed for this structure. The RF tuning will be accomplished by a mechanical tuning of the cavity end walls, which means a variation of the end cell capacities.

In a next step XADS-specific cavities will be developed. It makes sense to investigate a SC large aperture cavity at 350 MHz and later on at 700 MHz. The manufacturer of the 350 MHz prototype cavity could transfer his experience towards XADS relevant cavity production even at 700 MHz.

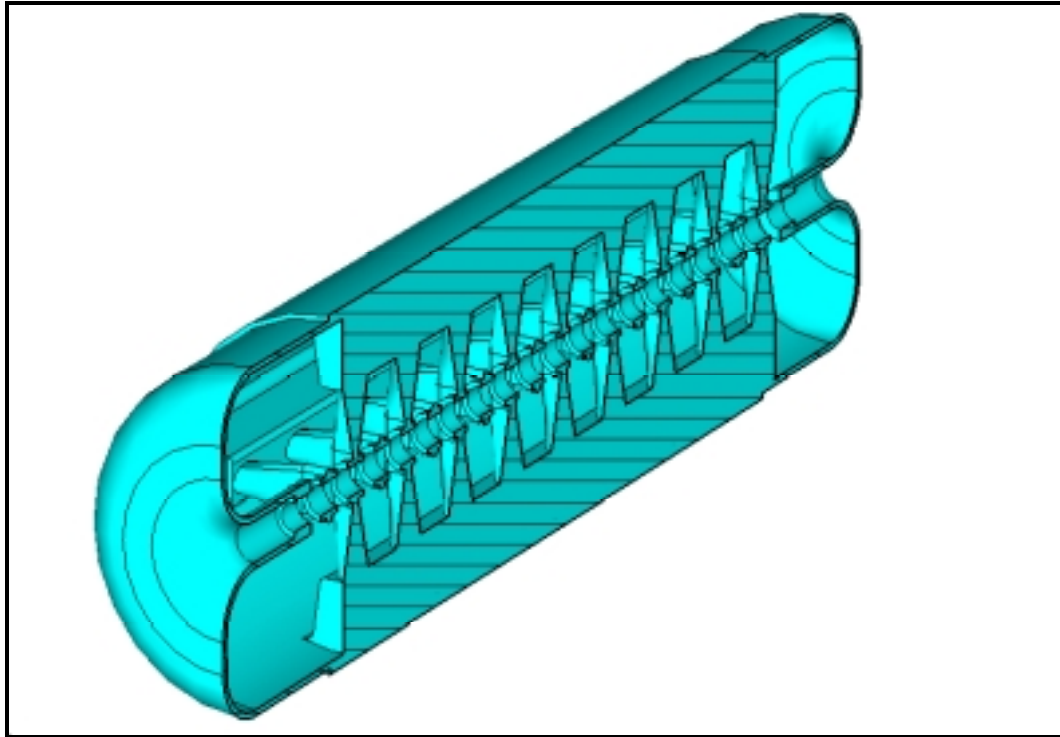


Figure 20 - Sectional view of a superconducting CH-cavity.

#### 4.1.2.b.e Layout and particle dynamics calculation of a SC CH-DTL

The low and medium energy part of a XADS linac design consists of a 350 MHz RFQ accelerator as front end (0.1 – 5 MeV) followed by a 350 and/or 700 MHz Drift Tube Linac from 5 to 100 MeV. The preferred CW operation favors a superconducting approach with shorter length, high efficiency and larger aperture, which gives a higher safety margin against possible particle losses and resulting structure activation. But the most important point is that the cavity RF power losses are reduced by about 5 orders of magnitude. One possible candidate in this energy region is the multi-gap SCCH structure, which combines high acceleration efficiency with comparatively small geometrical dimensions and mechanical robustness. In a first attempt a beam dynamics design has been studied: a chain of superconducting 350 MHz CH-sections up to an energy over 55 MeV was designed, then a frequency change to 700 MHz was made to increase the acceleration efficiency at higher energy (up to 100 MeV) and to prepare the beam for the transition into the 700 MHz high energy SC linac. Figure 21 shows a schematic layout of this XADS linac.

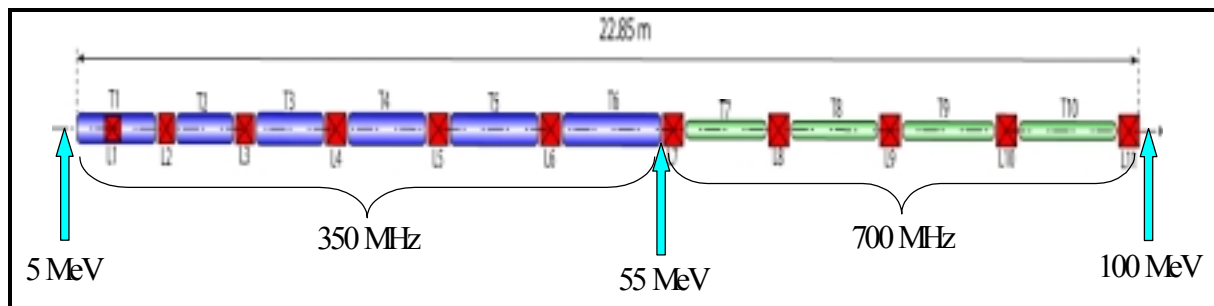


Figure 21 - Schematic layout of a SC 350/700 MHz CH-DTL for XADS. The first six tanks (blue) have a RF frequency of 350 MHz and the last four tanks 700 MHz (green).

The following Table IV shows the structure parameter of the medium energy linac for XADS generated with the multi particle program LORASR.

First design parameter	SC CH-DTL	Units
Mass to Charge Ratio (A/q)	1	
Design current I	40.0	mA
Frequency $f_{RF}$	350 / 700	MHz
Focusing structure	FDF - DFD	
Number of tanks	6 + 4	
Average tank length $L_T$	1.64	m
Average total RF power per tank $P_{tot/T}$	380.0	kW
Injection energy $W_{in}$	5.0	MeV
Extraction energy $W_{out}$	100.0	MeV
Total energy gain ( $W_{out} - W_{in}$ )	95.0	MeV
Effective energy gain per meter $W_{tot}/L$	4.15	MeV/m
Number of cells $N_c$	202	
Total linac length $L_{tot}$	22.85	m
Effective electric field amplitude $E_0T$	4.10 – 4.92	MV/m
Bore radius $r_0$	1.5 / 2.0	cm
Max quad gradient $G_{max}$	6.15	kG/cm
Max quad field $B_{max}$	1.23	T
Max Kilpatrick factor b	0.80	
Input / Output rms $\epsilon_{trans}^n$	0.3 / 0.385	mm.mrad
Input / Output rms $\epsilon_{long}^n$	0.53 / 0.97	keV/u.ns

Table IV - Structure parameter of a SC CH DTL design study for XADS.

The next figures show the results of a multi particle simulation calculated with the program LORASR and applying the KONUS beam dynamics concept. Space charge forces are calculated by the particle in-cell technique PIC. Each calculation was performed with 10000 macroparticles. As a starting distribution, we used a six dimension ellipsoid with a constant charge density in 3D space. Figure 22 and Figure 23 show the 100% beam size of the linac in the horizontal and vertical plane along the linac. No particle hits the structure and due to a large aperture factor, the safety margins in the high beta region of the accelerator are sufficiently large.

In Figure 24 and Figure 25, the longitudinal 100 % beam envelopes along the linac are plotted. There are also no longitudinal losses, which indicates a good beam profile in phase and energy. The shape of the curves shows the typical KONUS dynamics behavior. Plotted are the beam envelopes with respect to the synchronous particle of each structure section.

The energy and phase distribution at 100 MeV are plotted in Figure 26. One can notice that it is well suited for an injection into the high energy part of the linac as ( $\Delta E/E < 3.10^{-3}$  and  $\Delta\phi < \pm 8$  degrees).

Finally Figure 27 displays the relative transverse and longitudinal rms normalized emittance growth along the linac.

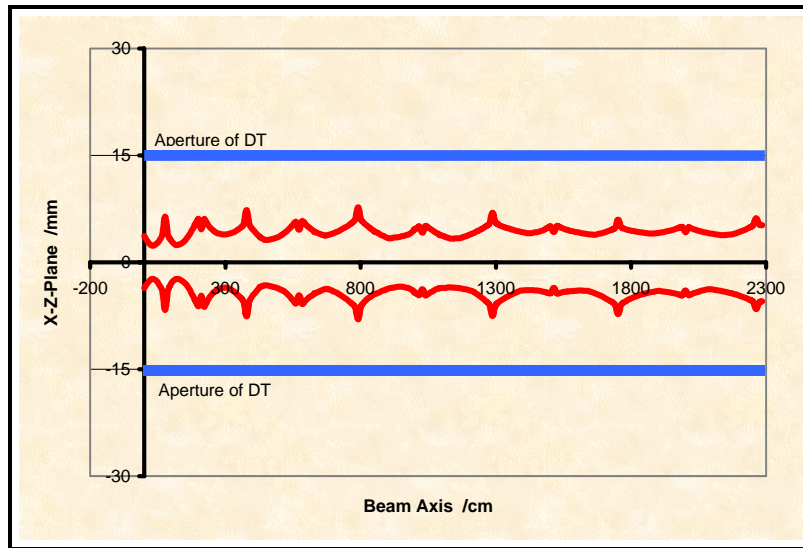


Figure 22 - Full transverse beam envelope of the SCCH linac of Table IV. The red line represents the 100 % beam envelope in the X-Z plane. Blue lines: aperture of the drift tubes.

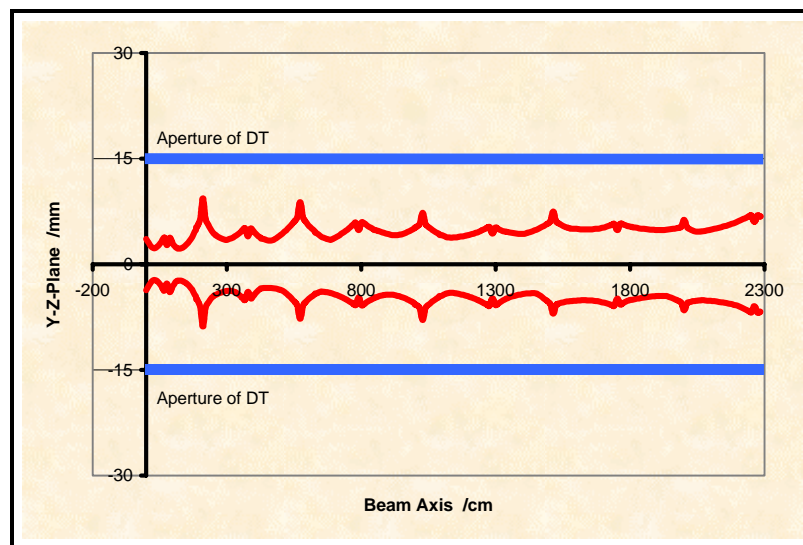


Figure 23 - Full transverse beam envelope of the SCCH linac of Table IV. The red line represents the 100 % beam envelope in the Y-Z plane. Blue lines: aperture of the drift tubes.

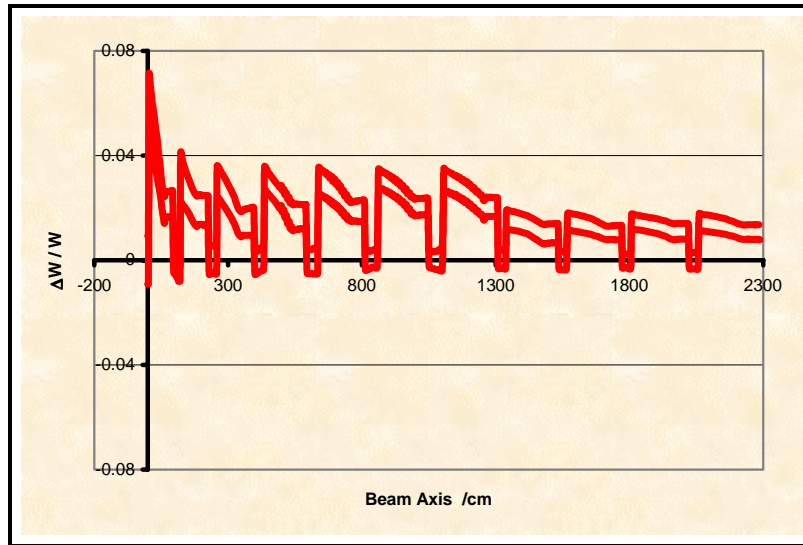


Figure 24 - 100 % effective energy width along the linac with respect to the bunch center.

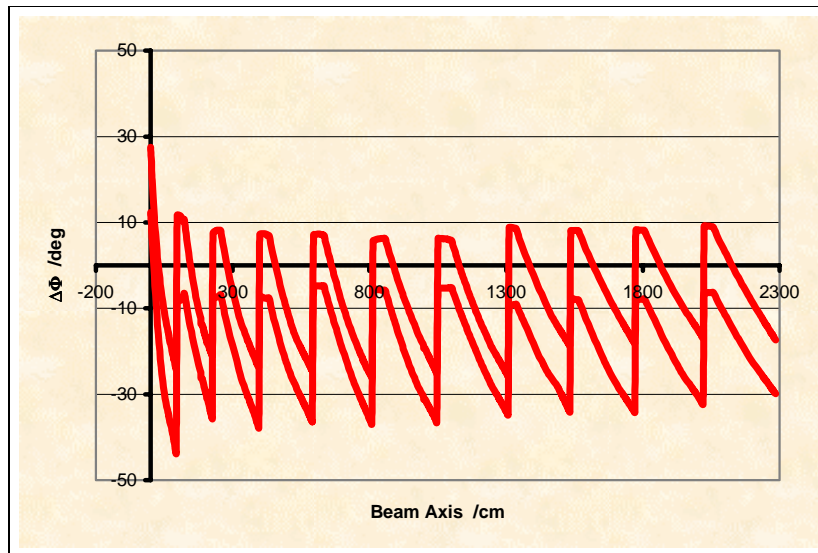


Figure 25 - 100 % effective phase width profile along the linac with respect to the bunch center.



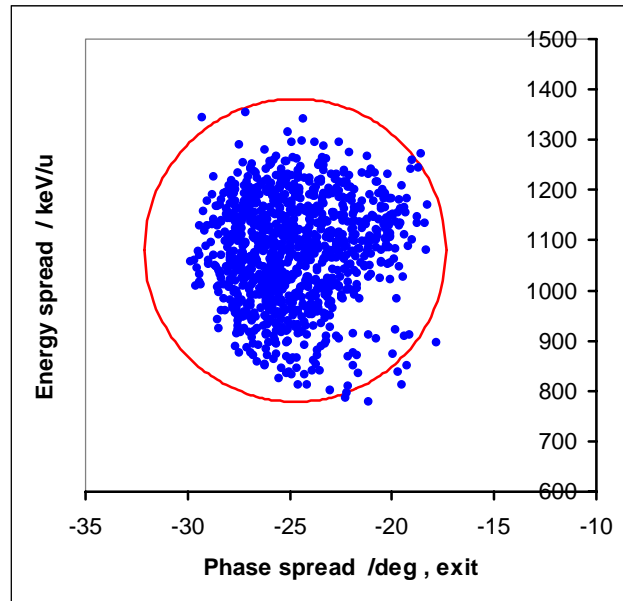


Figure 26 - Output beam distribution of the linac in the  $\Delta W$ - $\Delta\phi$  plane with 99 % emittance ellipse drawn for a beam current of 40 mA.

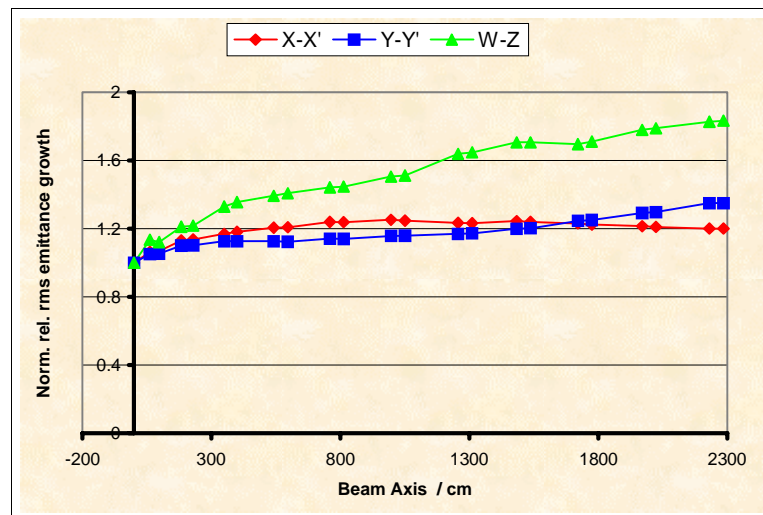


Figure 27 - Relative RMS normalized emittance growth along the linac.

#### 4.1.2.b.f Design of a superconducting 350 MHz CH cavity for XADS

After having determined the energy range, the aperture diameter of the drift tubes, the number of gaps and the acceleration gradient due to multi-particle simulations results done with the KONUS program LORASR, the RF behavior of the second resonator layout described above (see Figure 21) was studied with an analytical model that allows a first optimization step of the fundamental cavity parameters. The consequent numerical simulations of the resonators were done using the MICROWAVE STUDIO package. All parameters predicted with the analytical model were confirmed by MICROWAVE STUDIO within  $\pm 10\%$  deviation.

As a first step of the design process, only two accelerating gaps have been computed. Starting with a room temperature design the drift tubes and the shape of the stems were optimized. Special care was taken on the magnetic surface field trying to keep it well below

the critical field of niobium. By increasing the stem cross section, the magnetic surface field could be reduced by approx. a factor of two, reaching up only 44.6 mT in the actual design. This optimization process caused an increase in the capacitive load of the SC cavity. The maximum electric field (25.1 MV/m) has been found at the drift tube ends.

After this optimization step the whole cavity was computed to study the impact of the field flatness. As the magnetic flux bends from one to the neighboring sector at its ends one expects high magnetic surface field in this region. The girder undercuts, used in the room temperature IH-mode and 4-vane cavity successfully to create the zero mode, are not the right choice for a SC cavity. Therefore a careful redesign has been performed. The lowest surface fields were achieved by combining two modifications: The tank radius is increased by 17 % between the end flange and the first drift tube stem. To assure the field flatness, i.e. a constant accelerating field along the whole cavity, the local capacity at the cavity ends had to be further increased. This was attained by forming thicker stems. As a measure to reduce the surface currents at the cavity end flanges, half drift tubes were introduced [53]. Figure 28 and Figure 29 show the layout of the cavity for XADS in different views. Table V summarizes the results of the simulations.

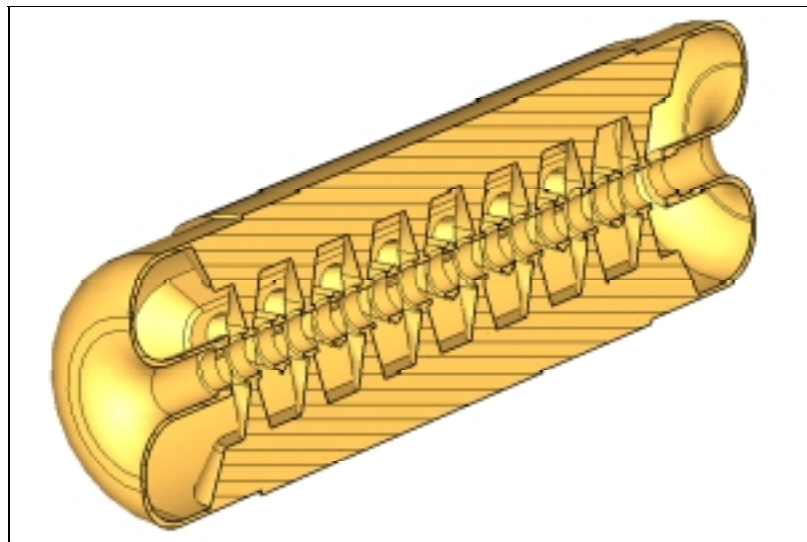


*Figure 28 - Sectional view of a superconducting 16-gap 350 MHz CH-cavity for XADS.*

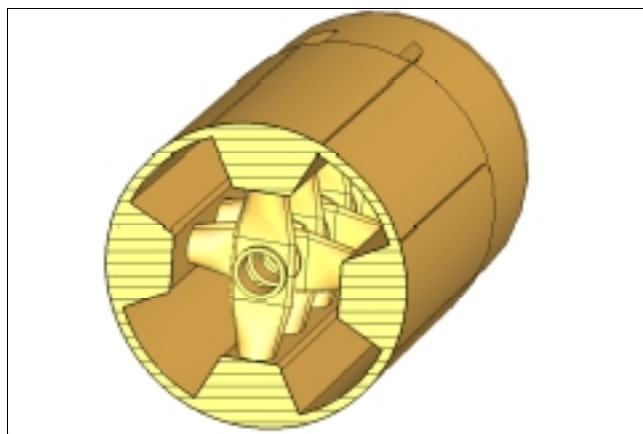


*Figure 29 - Middle-cut of a superconducting 16-gap 350 MHz CH-cavity for XADS.*

Cavity parameter	Tank 2 XADS DTL	Units
beta	0.1	
Frequency	350.43	MHz
$E_{\text{acc}}$	5.29	MV/m
Max electrical surface field $E_{\text{max}}$	25.1	MV/m
Max magnetic surface field $B_{\text{max}}$	44.6	mT
Tank length	0.936	m
Drift tube diameter	4.0	cm
Tank diameter	26.8	cm
Gaps	16	
$E_{\text{max}}/E_{\text{acc}}$	4.75	
$B_{\text{max}}/E_{\text{acc}}$	8.43	mT/(MV/m)

*Table V - Cavity parameter and peak fields of tank2 of the XADS SCCH-DTL.*

#### **4.1.2.b.g Conclusion**

A design of a chain of SCCH resonators with intertank focusing has been found which fulfills the requirements for a high intensity, low-loss medium energy DTL for XADS. The multi-cell SC CH resonators provide in this range very high RF and acceleration efficiency and due to its special cell geometry high mechanical robustness. The drift tube linac has a total length of  $\approx 23$  m only, with an energy gain of 95 MeV. The shortness of the structure is in comparison to 2-cell or 4-cell single-gap SC resonators a big advantage and reduces drastically building, real estate, operating and RF costs. The multi-particle simulation results showed a smooth beam behavior with moderate emittance growth and no particle loss. In addition a large aperture factor between beam and inner tank structure wall guarantees maintenance, reliability and availability of the facility. Therefore the results of particle dynamics calculations demonstrate the capability of the CH structure to handle high-current and high-intensity beams without particle losses. A preliminary resonator layout of the second XADS SC CH module with MI-CROWAVE STUDIO was made, to check the peak surface fields and the feasibility of the RF characteristics. The results were quite good. The maximum magnetic surface field (44.6 mT) and the maximum peak electric surface field (25.1 MV/m) are well below the theoretical niobium limits. A 350 MHz RF model for extended higher order mode and field flatness measurements is available at IAP. A technical design study in collaboration with industry was successfully done which points out technological solutions for all components. A call for tenders for the fabrication of a 19-cell,  $\beta = 0.1$  prototype CH-cavity is underway. Further extended tolerances and error studies are needed to test the overall stability of the SCCH linac against particle losses. In addition a cavity layout for the 700 MHz part should be done, to validate the RF and SC characteristics with respect to the smaller geometrical dimensions.

#### 4.1.2.c Superconducting Spoke Cavity

Superconducting cavities have been recently considered as a very promising technical solution for a use as accelerating devices in the intermediate section of high-intensity proton linear accelerators [54,55,56,57]. As a matter of fact, comparative study show that the use of superconducting cavities in this energy range, from 5 MeV up to 100 MeV, should provide many advantages compared with classical room-temperature structures: while the investment cost and the overall length for both solutions seem to be of the same order, the AC power consumption is much lower using SC cavities, that makes a huge difference in the operating cost. The savings are estimated to be in the order of 3 M€/year for a 10-mA CW proton beam. Moreover, the superconducting solution gives higher safety (larger beam tubes), and has great potential in terms of reliability and flexibility thanks to its independently-powered structures, which is a crucial point in the XADS context.

Considering the great potential of such a solution, R&D programs on very low- $\beta$  SCRF resonators, and in particular on spoke-type cavities, have been developed in various laboratories within the framework of several accelerators projects (AAA, ESS, RIA, EURISOL). Spoke-type cavities appear to be one of the most promising structures in this field. The first test of a spoke prototype was achieved successfully in 1992 [58], and the latest low temperature tests performed at Argonne [59,60,61] have showed very encouraging RF performances ( $E_{acc} > 12$  MeV/m and  $Q_0 > 10^9$  at 4 K).

Since 2001, a R&D program has also started at IPN Orsay on this type of cavities, with the design and construction of a first  $\beta=0.35$ , 2-gap spoke prototype [62] (see Figure 30) that should be tested before end 2002. IPN Orsay also proposed a design for a 5 – 100 MeV high-intensity proton linac using spoke cavities [57] that fits with the XADS accelerator specifications. This spoke linac design, which is described here, is based on the following choices:

- Energy range from 5 MeV (RFQ output) up to 80–100 MeV (high-energy section input)
- Operation at 352.2 MHz and 4.2 K (or 2 K).



Figure 30 - 352.2 MHz,  $\beta=0.35$ , 2-gap spoke cavity prototype (IPN Orsay – CERCA).

#### 4.1.2.c.a Reliability Considerations

This study has been done keeping in mind the extremely high reliability required for the XADS accelerator, which is necessary to achieve an operation with less than 5 beam trips per year. In this sense, the choice of the spoke technology for the intermediate-energy section appears to be a good choice, since spoke SC cavities show specificity with some real potential in terms of reliability and safety: very large beam aperture, good mechanical stability, negligible steering effects and modularity.

Moreover, comfortable margins have been taken in account during the linac design, so as to try to ensure both a reliable operation of the accelerating structures and of RF components (that should lead to an intrinsically redundant design), and a high robustness of the focusing design, with some fault-tolerance capability. These margins leads especially in limiting, in a reasonable way, the minimum beam apertures, the fields in the cavities, the phase advances along the linac, the sensibility to beam mismatch, or the possibility of halo creation due to phase-space distortions.

#### 4.1.2.c.b Accelerating Structures

A preliminary optimization of the linac shows that, using 2-gap SC spoke cavities, only two different  $\beta$ -values are needed to cover the required energy range: “ $\beta=0.15$ ” spoke cavities are used from 5 MeV up to 17 MeV, and “ $\beta=0.35$ ” cavities from 17 MeV up to 100 MeV. The use of 2-gap cavities was motivated by the fact that they have large energy acceptance, and remain quite easy to fabricate as compared with multi-gap structures. An alternative design would be to use 3-gap or 4-gap cavities, but one can show that this configuration is not very attractive because first, 3 different  $\beta$ -values are needed, and second, the gain in terms of overall length and cavity number is not significant, due to the very strong longitudinal phase advance in this energy range and the subsequent limitations on the accelerating field.

The 2-gap spoke cavity design optimization has been done for each  $\beta$ -value [63,64] so as to minimize the peak surface fields in the cavities during operation ( $E_{pk}<25$  MV/m), while reaching good RF and mechanical properties, and keeping large beam apertures. Optimizations led to the final shape shown in Figure 31, exhibiting a cylindrical spoke base (minimum  $B_{pk}/E_{acc}$  value), a racetrack spoke center (maximum transit time factor), and a spoke center thickness of 1/3 the iris-to-iris length.

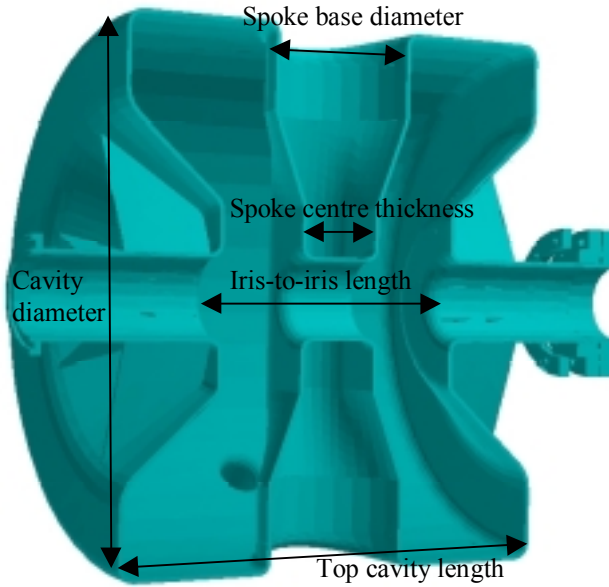


Figure 31 - Cross-section of the " $\beta = 0.35$ " 2-gap spoke cavity.

The main characteristics of these two 352.2 MHz, 2-gap cavities are summarized in the table below.

	" $\beta=0.15$ " cavity	" $\beta=0.35$ " cavity
Geometrical beta $\beta_g^*$	0.135	0.314
Optimum beta	0.194	0.363
Cavity diameter	354 mm	408 mm
Top cavity length	217.5 mm	354 mm
Spoke base diameter	72.5 mm	118 mm
Spoke center thickness	28 mm	67 mm
Iris-to-iris length	85 mm	200 mm
Beam tube aperture	50 mm	60 mm
Shunt impedance $r/Q^{**}$	101 $\Omega$	220 $\Omega$
Geometrical factor G	72 $\Omega$	101 $\Omega$
$E_{pk}/E_{acc}^{**}$	3.56	3.06
$B_{pk}/E_{acc}^{**}$	7.59 mT/(MV/m)	8.28 mT/(MV/m)
$E_{acc}$ @ $E_{pk} = 25$ MV/m $^{**}$	7.02 MV/m	8.18 MV/m
Maximum voltage $^{**}$	0.60 MV	1.64 MV
Quality factor @ 4K	$1.4 \cdot 10^9$	$1.9 \cdot 10^9$

\* Defined here as  $\beta_g \lambda / 2 = \text{gap-centre-to-gap-centre length}$

\*\* Given for  $\beta=0.15$  &  $\beta=0.35$  protons respectively;  $E_{acc}$  is normalized to the iris-to-iris length.

Table VI – Spoke cavity parameters.

#### 4.1.2.c.c Focusing Design

Different philosophies have been investigated for the conception of the linac architecture (see Figure 32). A first one (1) consists in using long and compact cryomodules with short focusing lattices. This approach is very attractive because it leads to a very short linac, but the main drawback is that the lattice length continuity is broken at each warm transition between modules: in this case, a specific beam matching is required at each transition, that could induce some “weak points” as far as the robustness of the focusing design is concerned. For this reason, a second approach (2), which consists in keeping the lattice length continuity in the whole linac, was preferred. This solution leads obviously to an increased overall length of the linac, but it may be the price to pay to ensure a fault-tolerant focusing design. Moreover, the cryomodules are very simple and modular, that could be an argument in terms of reliability and flexibility.

In order to obtain a focusing design as robust as possible, the following choices have been made:

- Superconducting focusing elements are used to minimize the lattices’ length, ensuring certain continuity between the RFQ and the high-energy section. The quadrupole gradient is always kept below 35 T/m.
- The synchronous phase is ramped from  $-65^\circ$  to  $-30^\circ$  in the first focusing lattices for a good longitudinal capture of the beam without any phase space distortion.
- The emittance growth is minimized keeping the zero-current phase advances per focusing lattice below the envelope stability at  $90^\circ$ , which leads to upper limits for the energy gain per focusing lattice (and consequently on the accelerating fields) and the beam size. Longitudinal and transverse phase advances never cross, so as to avoid any resonant collective instability that could imply some emittance exchange between the longitudinal and transverse planes.
- The phase advance per meter is kept continuous through the linac to have a good matching between the structures, to decrease the sensitivity to current variations, and to minimize the halo formation.



Figure 32 - Different linac architecture philosophies.

#### 4.1.2.c.d Proposed Accelerator Layout

The proposed spoke linac covers the energy range from 5 MeV up to 95 MeV, which corresponds to the optimum energy transition with the 700 MHz high-energy section. It is composed of 96 spoke cavities, for an overall length of about 100 meters. The main characteristics of the linac are summarized in the table below. More information about a preliminary technical design of the cryomodules can be found in [63].

<i>Beam intensity: 10 mA CW</i>	<b>“<math>\beta=0.15</math>” section</b>	<b>“<math>\beta=0.35</math>” section</b>
Energy range (MeV)	5 – 17	17 – 95
# Cavities	34	62
# Cavities per focusing lattice	1	2
Focusing lattice length (m)	1.3	1.9
Synchronous phase	- 65° to - 30°	- 30°
Energy gain per real meter (MeV/m)	0.06 – 0.38	0.31 – 1.58
Beam loading RF power (kW/cavity)	0.8 – 5.0	4.1 – 15.0
Quadrupole gradient (T/m)	17 – 24	24 – 35
Overall length (m)	44.2	58.9

*Table VII – Main characteristics of the spoke type cavities.*

#### **4.1.2.c.e Beam Dynamics Simulations**

Beam dynamics simulations have been performed using codes developed at CEA Saclay (GenLin, TraceWin, Partran). The calculations include space charge effects (PicNic routine), and multi-particle simulations are done using 50 000 particles. In all cases, the IPHI RFQ exit beam characteristics are used as the input beam for the spoke linac. The matching between the two spoke sections is achieved adjusting slightly the cavity phase and the quadrupole gradients at each side of the transition.

In the case of a matched beam, the simulation results show (Figure 33) very smooth envelopes, and an emittance growth below a few percent with no phase space distortion.



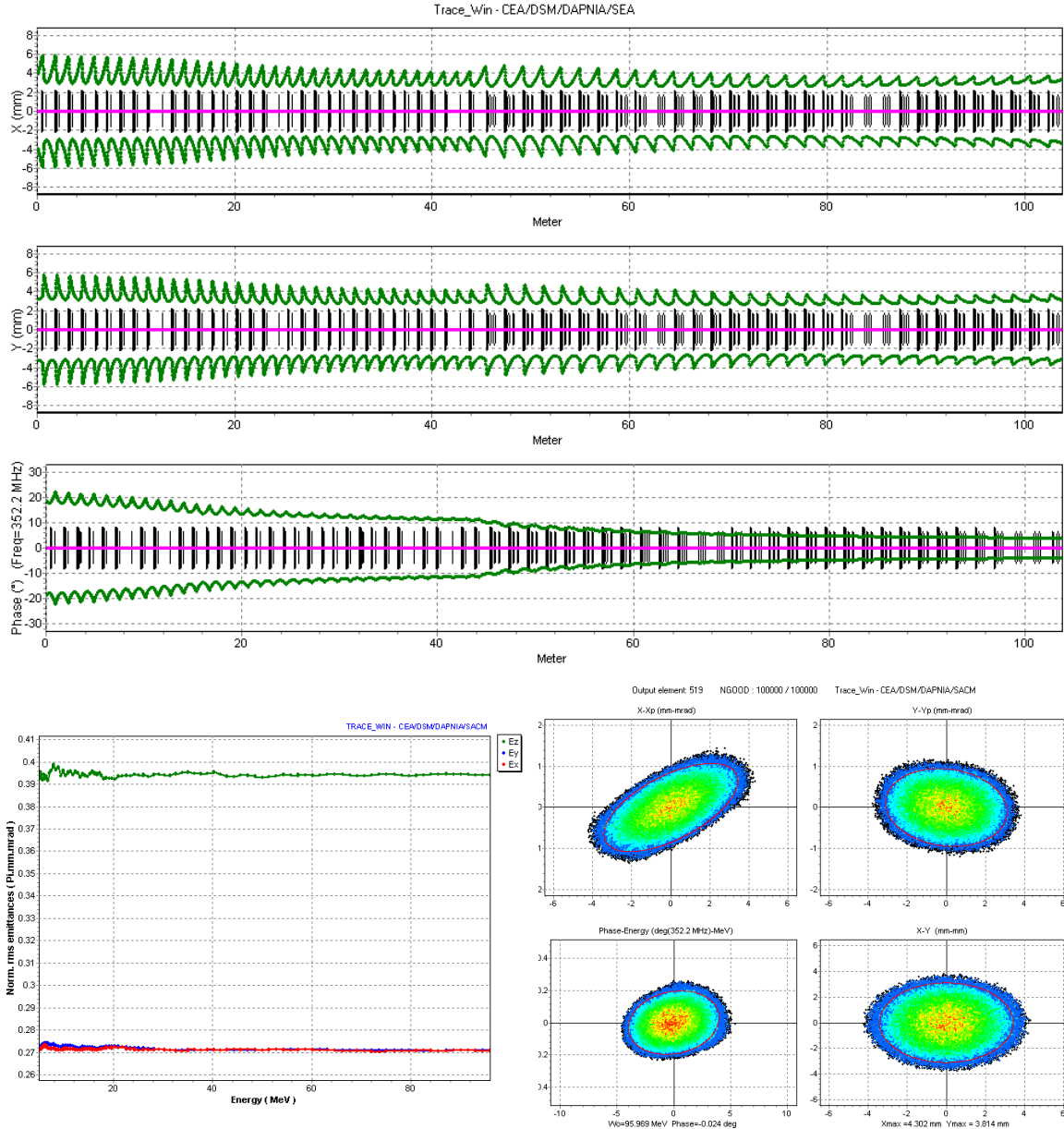


Figure 33 - Simulation results for a matched beam: real beam envelopes, rms emittance evolution, and beam distribution at the linac exit (95 MeV).

#### 4.1.2.c.f Additional Considerations

The main issue of this study is to design a highly reliable linac; in this context, a thorough analysis of possible fault scenarios is a crucial point, since the aim of the study is to reach a final design where the failure of most of the components can be allowed during the accelerator operation. Some first simulations indicate that our design should be quite fault-tolerant, both in the case of mismatched beams, and in the case of failures of components. Finally, one has also to point out the limits of such a design using only spoke cavities. Indeed, it appears that such a linac is not very efficient in terms of real-estate gradients in the extremely low energy part, from 5 MeV to roughly 25 MeV. It is only after approximately 25 MeV that the real-estate energy gain grows above the 1 MV/m level. It is therefore advisable to identify alternative solutions to the spoke technology in the region from 5 MeV

to 20/30 MeV, like a warm DTL section or a different structure (e.g. the superconducting CH-DTL proposal – see section 4.1.2.b). If such a solution is found, the spoke linac would cover only the 25 MeV – 95 MeV energy range, and would be composed of only  $\beta = 0.35$ , 2-gap (or 3-gap) spoke cavities.

### 4.1.3 High Energy Section

A worldwide R&D effort for high power proton linacs is in progress since a few years and the high potentiality of these machines has been proven by an intense prototyping activity. Different programs have driven this effort: tritium production (APT), spallation sources (SNS, ESS) and ADS (AAA, TRASCO, ASH). The well-developed and high efficient superconducting radiofrequency technology that has been greatly improved during the last ten years by the TESLA/TTF [65] International Collaboration has been chosen in all design above beam energies of 100-200 MeV. In this type of accelerators the cost per MeV is decreasing with energy up to 1 GeV and after this value it stays practically constant, with only a marginal decrease. Moreover, a superconducting linac has an intrinsic high modularity, which increases with energy and favors the implementation of redundancy schemes.

Starting from beam energies in the range of 85-100 MeV the use of SC multi-cell elliptical cavities appears the most efficient and cost-effective solution. Due to the varying velocity of the moderately relativistic protons, the superconducting multi-cell cavities need to operate over a given range of beam velocities. Thus, the high-energy part of the XADS linac is divided in three sections, each covering an energy range with a single type of structure. The geometrical  $\beta$  values of these structures are 0.47, 0.65 and 0.85, respectively. The transition energies between the sections are set to approximately 200 and 490 MeV, and the last family of cavities, bringing the beam to the nominal energy of 600 MeV, could operate to approximately 2 GeV without great losses of efficiency. Three sections are anyhow needed to efficiently cover the required energy range up to 600 MeV. In the present design the highest beta section is marginally used, but gives a large margin for further upgrades, eventually required for the final plant. Moreover the proposed scheme is consistent with the R&D work ongoing on the lowest beta cavities and the fine-tuning of the three betas does not affect the technology achievements.

The released version of Deliverable 1 [1] has provided the accelerator requirements for the XADS, namely a 6 mA intensity at the energy of 600 MeV. However, we have to recall that the mission of the PDS-XADS study is to provide, at the end of the three-year study, an indication for the extrapolation of the accelerator technologies to an industrial-size transmuter (deliverable D80). It is already clear that an industrial application will require higher energies than the one set by the XADS specifications. Furthermore, the technology of elliptical cavities allows designing sections of increasing efficiency as the energy increases (approaching that of the electron machines as the beam approaches the speed of light). The TTF Collaboration has fully demonstrated that this technology is mature, and the fabrication, processing, cleaning and handling procedures in order to achieve high accelerating fields have been set.

In order to cover the desired energy range from 90/100 MeV (output of the intermediate section) to the nominal energy of 600 MeV, it would be possible to shift the geometrical cavity  $\beta$  in order to finely adjust the accelerator design. However, from our experience in similar studies (ASH, TRASCO, SNS) we believe that we should include in the design the  $\beta=0.85$  section, which, in principle, could be lengthened to extend the XADS linac capabilities up to energies greater than 1-2 GeV at a very high efficiency. This section, that, for the case of a nominal design of 600 MeV is of very short length (only 3 lattice length for

the case discussed in the table below), would achieve a real estate gradient greater than 5.5 MV/m in the energy range between 600 MeV to 2 GeV.

The transverse focussing lattice is provided by a periodic array of quadrupole doublets, and the SC cavity cryostats are placed in the long drifts between quads. Table VIII summarizes the main parameters in the high-energy section.

	Section number		
	1	2	3
Input Energy [MeV]	95	200	490
Output Energy [MeV]	200	490	600
Cavity Technology	Elliptical		
Structure $\beta_g$	0.47	0.65	0.85
Number of cavity cells	5	5	6
Number of cavities	28	48	12
Focusing type	NC quad doublet		
Cavities/Lattice	2	3	4
Synchronous Phase [deg]	-25		
Lattice length [m]	4.2	5.8	8.5
Number of lattices	14	16	3
Section Length [m]	60.8	92.8	25.5
Real estate gradient [MV/m]	1.8	3.1	4.3

*Table VIII - Main parameters of the high-energy linac sections.*

#### 4.1.3.a Elliptical cavities design and prototypes

The SC cavity design was performed in close collaboration in the context of the Italian TRASCO [66] program and the French ASH [67] program, sharing the R&D and prototyping efforts [68]. In particular, while most of the effort of the French group has been concentrated on the work on  $\beta = 0.65$  cavity prototypes, the Italian group was dedicated to the development of  $\beta = 0.5$  cavities. The groups decided to focus the R&D and prototypical efforts on the two shortest beta sections, due to the fact that the technological challenges increase lowering the geometrical beta of the structure.

The baseline cavity design geometry have been chosen using a procedure that takes into account all the electromagnetic and mechanical performances of the cavities, and choosing the most suitable compromise for the required application. The operating cavity parameters in the linac design have been set to conservative values in terms of peak surface field, in according with the derating/over-design criteria needed for the linac reliability. In particular peak surface magnetic fields of 50 mT and surface electric field of 30 MV/m has been used as upper limits on the cavity operation, while the TTF cavities have been successfully operated up to more than 100 mT and 50 MV/m on the TTF linac. Furthermore, the first three cavity prototypes of the SNS  $\beta=0.61$  multi-cell cavities have been tested reliably up to 90 mT and 45 MV/m in a test linac cryomodule. The vertical tests of the SNS  $\beta=0.61$  and  $\beta=0.81$  cavities reached even better performances [69].

Up to now, several prototypes of the single cell cavities have been built and tested, both in France and Italy, and the results were up to the design specifications. Prototypes of full multi-cell cavities equipped with the ancillary equipment needed for operation are underway for both geometry.

<b>Geometrical Parameters</b>			
Cavity geometrical beta	0.47	0.65	0.85
Number of cells	5	5	6
Cell geom. length [mm]	100	140	180
Full Cavity Length [mm]	830	1050	1460
Iris diameter [mm]	80	90	100
Tube $\varnothing$ at coupler [mm]	130		
Internal wall angle, $\alpha$ [ $^{\circ}$ ]	5.5	8.5	8.5
Equator ellipse ratio, R	1.6	1	1
Iris ellipse ratio, r	1.3	1.3	1.4
<b>Full cavity electromagnetic Parameters</b>			
Max. $E_{peak}/E_{acc}$	3.57	2.60	2.37
Max. $B_{peak}/E_{acc}$	5.88	4.87	4.07
Max. Operating $E_{peak}$ [MV/m]	30.4	26.7	29.1
Max. Operating $B_{peak}$ [mT]	50		
Cell to cell coupling [%]	1.34	1.10	1.28
R/Q [Ohm]	159	315	598

*Table IX - Parameters of the SC cavities.*

Figure 34 Shows picture of two of the  $\beta=0.47$  single-cell cavities fabricated for the TRASCO program in Italy.

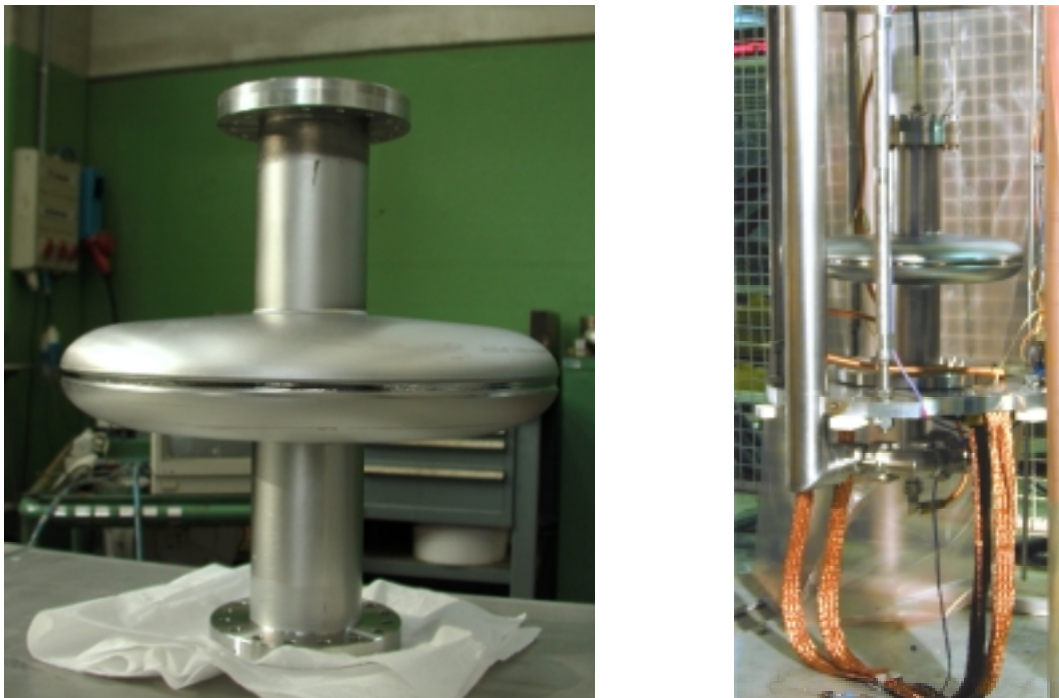


*Figure 34 - Two of the  $\beta=0.47$  cavities built for the TRASCO program in Italy, after fabrication (left) and on the test insert before cryogenic measurements (right).*

Figure 35 show the result of the tests of all the four  $\beta=0.47$  single cell cavities. The curve of the cavity quality factor as a function of the accelerating field (and of the peak operating fields) is displayed and compared to the design specification. All cavities outperformed the design goals, both in terms of quality factor and of fields.

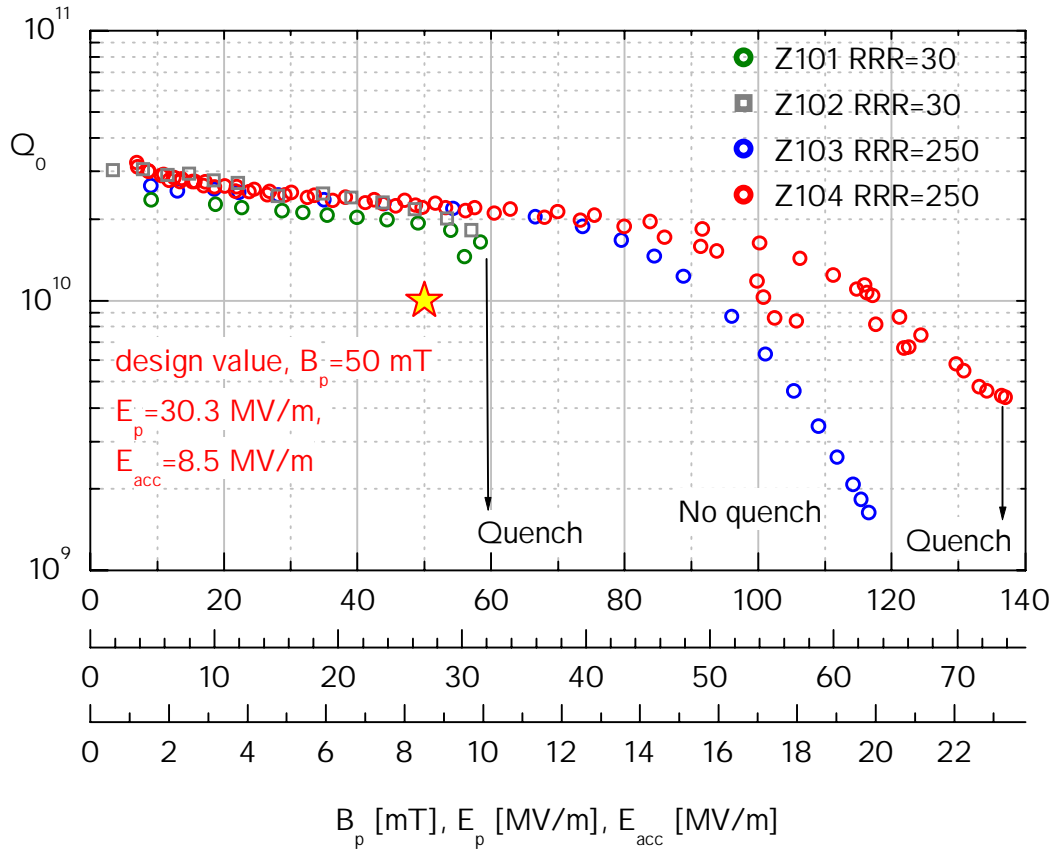


Figure 35 –  $Q$  vs.  $E_{acc}$  curves of four single-cell  $\beta = 0.47$  cavities.

#### 4.1.3.b Beam dynamics simulation

Beam dynamics simulations of the full beam line showed that no showstoppers for the superconducting linac exist. Indeed a beam line from 5 MeV to the final nominal energy is feasible and looks promising from many points of view (possibility of intrinsically redundant design, modular structure, simplicity, fault tolerance, etc.). Note that comfortable margins on critical values have been chosen in this study to ensure a design as robust as possible. These margins leads especially in limiting, in a reasonable way, the minimum beam apertures, the field in the cavities, the phase advances along the linac, the sensibility to beam mismatch, or the possibility of halo creation.

Moreover, the high current beam physics is well understood. The linac has been designed in order to satisfy the necessary smoothness criteria in order to avoid beam quality degradation and to avoid the possibility of particle losses. The structure and the intensity of the focusing lattice are smooth, and the matching between the sections has been carefully studied. The design stays clear from all types of resonance: structure resonance (by means of phase advance limitations), envelope-particle parametric resonance (by means of limitations of tune depression) and resonance between planes (by avoiding resonance between the different planes).

The following figures show the main characteristics of the linac design and the results of beam dynamics simulations for the whole beam line, from the output of the RFQ, through the spoke cavity beam line (discussed in section 4.1.2.c) and into the high energy elliptical cavity section.

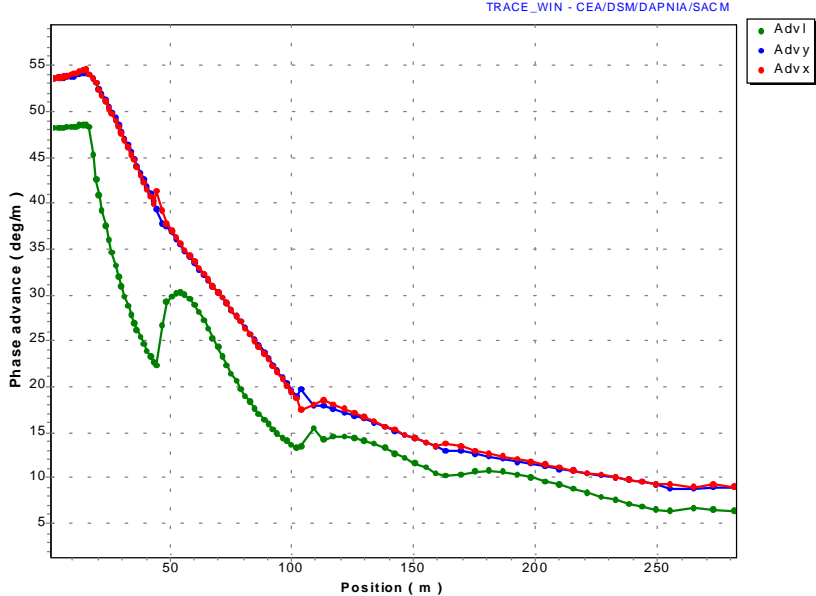


Figure 36 - Phase advances for the full 600 MeV linac.

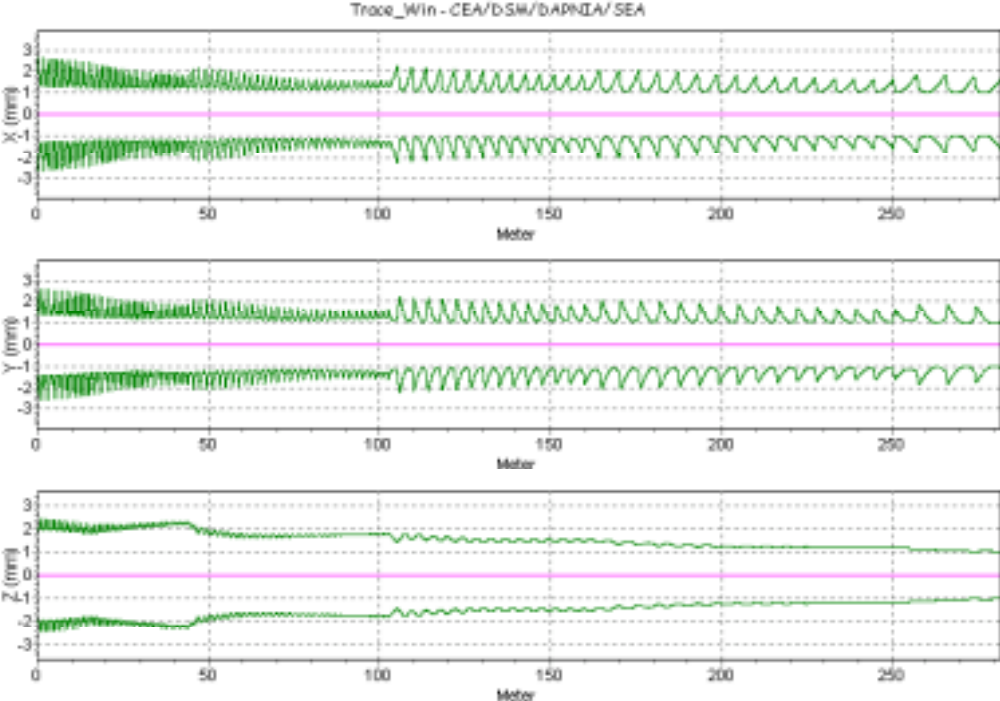


Figure 37 - Beam size (rms) along the whole linac.

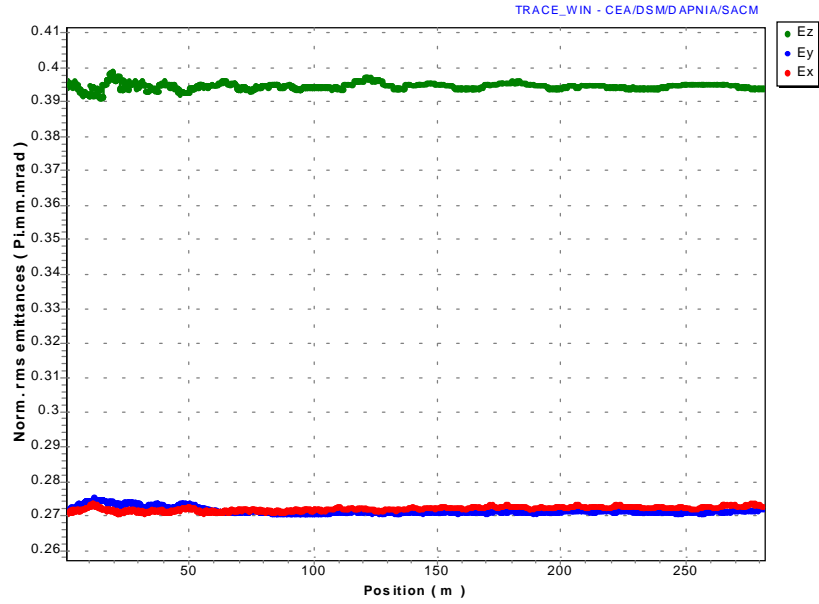


Figure 38 - Evolution of the rms beam emittance in the whole linac.

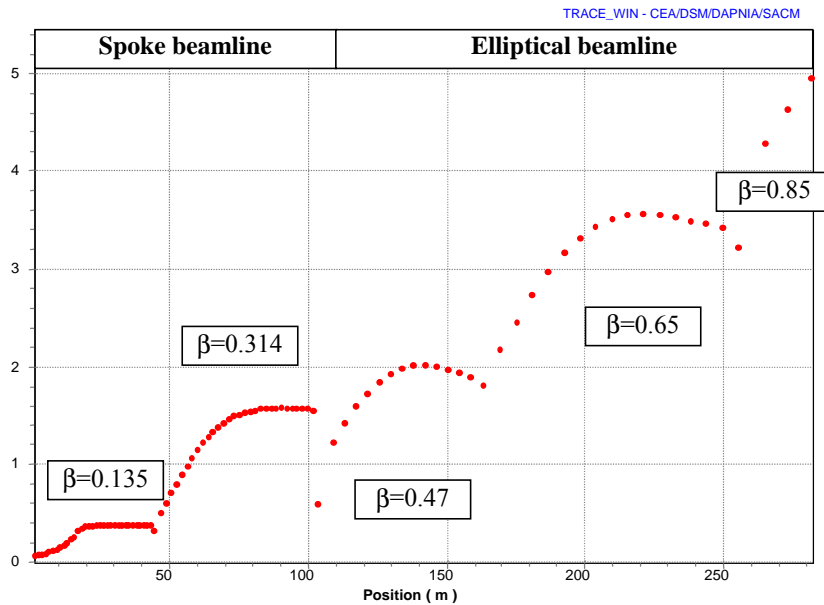


Figure 39 - Real Estate accelerating gradient along the whole linac.

## 4.2. Cyclotron Option

### 4.2.1 Relevant requirements

Requirements for the XADS accelerator [1] specify a 600 MeV / 10 mA (hence 6 MW) CW machine, able in addition to deliver pulses (at a rate to be defined), with very stringent requirements for beam availability and easily expandable to 800 MeV. If a 600 MeV final energy is well established for a cyclotron [70], it is felt in the cyclotron community, largely based on PSI experience, that a value of 5 mA should be considered as safely

reachable but extrapolating up to 10 mA is more questionable so that, should this intensity be necessary, a complex of at least two cyclotrons will be required, the two beams being funneled together. A cyclotron cannot be expanded in energy, so that boosting the energy from 600 to 800 MeV would require the full replacement of the final and main stage, an absolutely not cost effective operation. In addition a cyclotron is basically a CW machine and the requirement to provide pulses for neutronics measurements is a major difficulty for a cyclotron of such power.

#### 4.2.2 Cyclotron design

Different possibilities are open for the ion to be accelerated:

- $H^-$  as at TRIUMF [71]: the rate of electromagnetic dissociation will be such that the level of radioactivity will be unmanageable, so that this solution should be abandoned,
- $H^+$  as at PSI [70]: based on the performances of the present PSI ring a 5 mA intensity should be easily reached: the space charge limit could be pushed up to 10 mA, but losses on the deflector septum are unpredictable at that level, so that a 5 mA intensity is considered as a safer value. The main drawback of this design for ADS is the number of short beam interruptions (trips) due to the high voltages (electrostatic deflectors and RF cavities). Should this number be unacceptable, acceleration of the  $H_2^+$  molecule must be considered,
- $H_2^+$  : extraction is accomplished by stripping and the condition of very high acceleration voltages can then be relaxed, and in addition the accelerated electrical current is divided by a factor 2. The disadvantage of such a machine is the size,  $B\rho$  being 8.1 T.m: this large size is however not a reliability issue. Superconducting coils could be considered in order to reduce the size but at the expense of reliability. The extraction path can be difficult to define and if probably not a major difficulty, would require the delicate transport of 3 MW beams in a series of small magnets [72]. Based on present experience the lifetime of the stripping foil should not be an issue and a robotized foil exchanger can be built. Nevertheless the injector would require an electrostatic deflector and the question of beam trips remains, though at a lower level. In any case, funneling is mandatory in all cyclotron solutions, and this will be considered below.

#### 4.2.3 Funneling

Funneling of two 3-MW beams on the same beam line toward the target can be accomplished by a series of septum magnet, Lambertson magnet and finally of a RF cavity. TJNAF magnets have been taken as reference [73] and do not show any technological problem. The cavity is the most delicate point: considering a ESS like RF cavity [74] led to the conclusion that a 3-5 meter long CW cavity could be built to obtain the required funnel angle. Altogether a 20 m long space should be reserved for funneling where focussing is difficult to implement. In addition running MW beams in a series of narrow elements should be carefully studied: monitoring of the stability of the position of the beams would probably lead to a large number of alarms (true or false), inducing beam trips. The technical feasibility of such a funnel remains to be demonstrated, even if each element looks feasible.



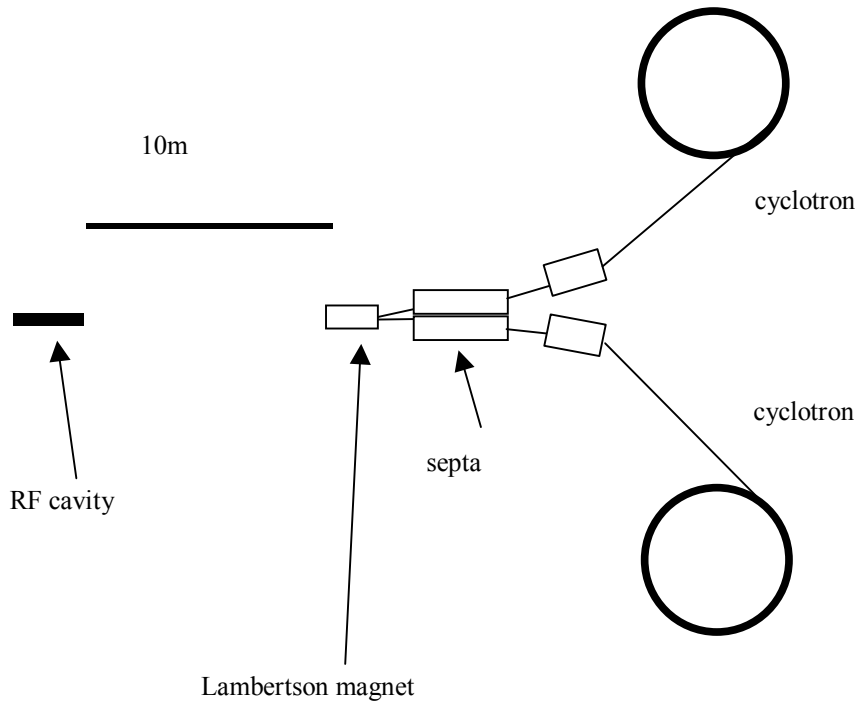


Figure 40 – Overall Layout for the Cyclotron XADS option.

#### 4.2.4 Conclusion

In conclusion, the cyclotron solution for a XADS presents a number of difficulties if not impossibilities: funneling, pulsing, beam trips, double-machine scheme, intrinsic current limitation, energy upgrading that precludes this solution despite its advantages such as lower price, proven technology at the MW level as demonstrated by PSI, compactness...

## 5. TECHNICAL FEATURES

### 5.1. Assessment of Availability/Reliability

The assessment of the accelerator availability and reliability is the object of a separate deliverable, D57, due at the end of January 2003.

As we stated in section 2.5, the reliability analysis of a complex system is an iterative process that starts from a preliminary design of the whole system and its components. This phase is then followed by the development of the Reliability Block Diagram (RBD) and the gathering of data from a component database, as required by the deductive, top-down approach of the RBD, that takes into account the nature of connection of the system components.

In parallel, the FMEA/FMECA methodology can be implemented, following an inductive, bottom-up approach in order to identify the failure modes of the system, and their criticality.

This path should be iterated to review the system and component design, in order to meet the required system availability and reliability.

The whole procedure is described pictorially in the following figure.

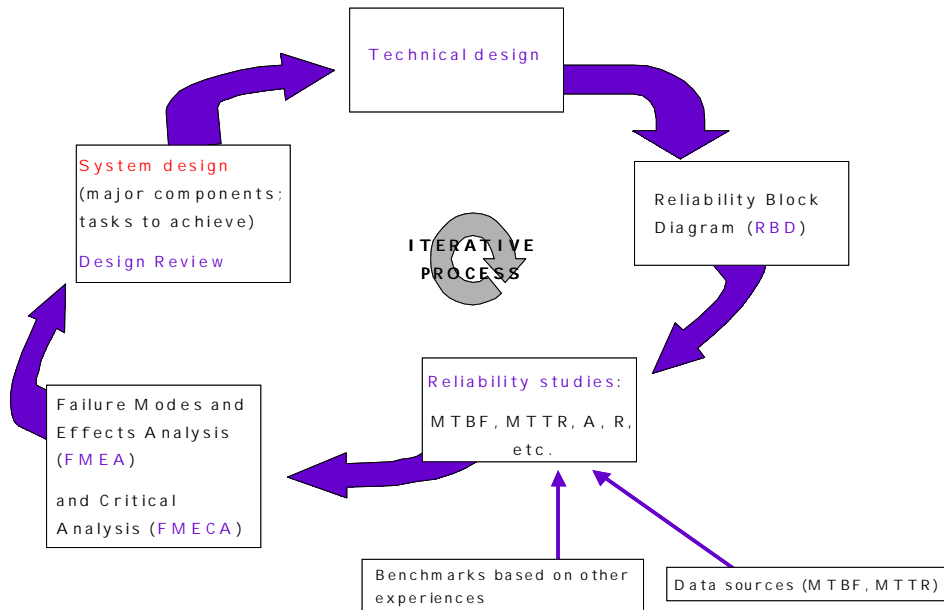


Figure 41 - Iterative process for the reliability and criticality assessment.

However, in order to devise the RBD needed to perform the reliability evaluations and FMEA analysis, a reference accelerator solution (or at most a few options) needs to be set as soon as possible, with an initial choice of the main components. All the accelerator components should be listed here schematically, possibly indicating their function and failure modes, and the nature of their connections among them.

Furthermore, in order to assess the effect of the failure of each component in the beam line, it is necessary to identify its failure modes and include them in the beam dynamics simulations of the linac to determine its criticality. Since, at least for the linac case, the beam line consists of several hundreds of components, this process leads to a heavy simulation activity, that can be efficiently performed only after one (or at most a few) reference solution has been chosen.

Since the collaborating Partners of the PDS-XADS has not yet proposed a reference solution neither for the linac nor for the cyclotron option, in the following paragraphs we can make some general comments on the implementations of the reliability criteria described in section 2.5 in the overall design of the accelerator.

### **5.1.1 Beam trip duration induced by a faulty component**

According to the requirement of D1 and to the discussion outlined in section 2.5, the XADS system performance is not hindered by short beam trips with duration of up to a second. So, as a general strategy, a careful accelerator design (including diagnostic and control systems) should be aimed to bring, when possible, the duration of the most frequent beam trips below this time scale.

Furthermore, beam dynamics simulations and FMEA analysis of the whole accelerator need to identify the effect of single component failure. Components that have failure modes that potentially lead to a long (i.e. > 1 s) beam stop should be:

- Designed with great attention, with a considerable margin of over design (derating) where possible;
- Assigned strict procedures for equipment testing and acceptance before installation;
- Assigned proper scheduled maintenance plan during the shutdown;
- Monitored during operation with diagnostic systems.

These components need to have the highest achievable possible reliability.

Components that have failure modes that leads to beam stops with duration of less than a second (possibly due to redundancy) should have, if possible, the highest accessibility in order to be replaced while the beam is on. As an example, this could suggest, for the linac option, the possibility of having a double tunnel scheme, where ancillary components (power supplies, RF generators, control electronics...) can be placed in a free-access tunnel, separated from the beam tunnel. By doing so, the number of some needed redundant components, as power supplies, could possibly be reduced with respect to the choice of using a single tunnel (with no access during beam operation).

From the accelerator operational experience, sparks on high voltage components drive the highest fraction of beam trips. These events can generally be detected and handled in a small fraction of a millisecond, keeping the beam on. Again, due to their limited duration, these beam trips are not counted among the allowable number of beam trips.

Another aspect that is worth mentioning - concerning the criteria to implement hot (switched on and on-line) or cold (switched off, and on-line) parallel redundancy - is the operational procedure used to switch the beam on. In principle a fast beam switch can be implemented to allow the use of redundancy and spares on line in a time of the order of a second.

Finally, the chosen degree for over design and redundancy is a direct function of the duration and frequency of the scheduled shutdown for reactor maintenance.

#### **5.1.2 The role of control electronics**

In order to bring the highest number of possible beam trip events within the maximum allowed duration of 1 second, an “ad hoc” fast digital electronics must be implemented, based on the redundancy criteria that have been already applied in other fields.

The control of beam power as a function of time, as required by D1, looks easy at the percent level. An even better control can be possibly achieved through a feedback loop from a reactor signal.

As a general criterion, redundant fast electronic systems need to be designed to avoid, in principle, the intervention of the last beam protection (robust beam shutdown), which will be anyhow required for safety reasons.

#### **5.1.3 Constrained optimization of the design**

The different design options that are being studied at present should be more deeply analyzed and compared in term of their potential degree of modularity, reliability of the used technology and cost. This is indeed the intention of deliverable D57. Possibly in the iterative design and reliability assessment procedure described in Figure 41, constraints on the system cost should be added in order to achieve a final design.

#### **5.1.4 Safety issues**

It is a general opinion of accelerator experts that the safety rules for the accelerator and the reactor need to follow separate procedure. From the accelerator side, no major concerns have been expressed for the needed safety issues, because of the low level of expected beam losses.

As in all operational accelerators, the machine interlocks will be based on redundant active systems.

The beam handling, once in the reactor building, will follow the reactor safety regulation.

## 5.2. Assessment of Investment Cost

### 5.2.1 Introduction

In the last WP1 released document [1] about the missions and recommendations of the XADS project, the first estimate given in the Roadmap of April 2001 [75] is considered as a starting point to be confirmed by a complete cost analysis to be performed during the PDS phase. For the Accelerator (Linear accelerator with an energy of 600 MeV and a beam current of 20 mA), this estimate was given as:

- |  |                    |
|--|--------------------|
| ▪ Linear Accelerator System Engineering Design | 50 M€              |
| ▪ Linear Accelerator Components Cost           | 100 M€             |
| ▪ Civil Works and Infrastructure               | 80 M€ <sup>3</sup> |
| ▪ Site Engineering and Commissioning           | 70 M€ <sup>3</sup> |
| ▪ Indirect Costs                               | 50 M€ <sup>3</sup> |

It is also considered that the necessary R&D must be accomplished during the 6th European Framework Program.

It is difficult today to identify the contribution of the accelerator to the Civil Works, Site, and associated costs. We propose to start detailing the cost assessment of the first two items covering the design study, the procurement and the integration of the accelerator components.

### 5.2.2 Analysis of previous projects costs

Several similar major projects from the 1999-2002 period, like the SNS project [76] (which is now in its construction phase) and several others projects like ADTF [77], ESS-Concert [78], EURISOL [79] and SPL [80] that have extensively detailed their cost have been taken as our reference basis.

The SNS project is currently in the construction phase. The initial commissioning of the linear accelerator is planned in 2005. This project has developed a very detailed and well documented cost analysis, the accelerator architecture is very close to the first proposals for XADS, and it represents a very useful tool for our estimates.

The total cost of the SNS project is **1290 M\$** (not including a 125 M\$ for contingencies). This cost includes all the expenses concerning the components, the civil works, the instruments, and the manpower (design and management). The cost of the linear accelerator alone is **540 M\$** (including R&D, components, infrastructure, tunnel, buildings, commissioning and project support). For the linear accelerator, the total cost is approximately half shared between the hardware procurement (52 %) and the manpower (48 %).

If one tries to go further in detailing the associated costs of the major components of the linear accelerator (Table X), one finds two major items : The accelerating structures and the RF power system account together for almost 2/3 of the total investment cost.

---

<sup>3</sup> This budget includes all facilities: accelerator, sub-critical system, technical buildings, ...

<b>Item</b>	<b>Cost</b>	<b>Percentage</b>
Front End (Injector)	21 M\$	7.8 %
RF Accelerating Structures	70.3 M\$	26.3 %
RF Power System	102.2 M\$	38.3 %
Cryogenic Plant	16 M\$	6 %
Beam Diagnostics	14.3 M\$	5.3 %
Focusing	3.1 M\$	1.1 %
Beam Transfer Line	10 M\$	3.7 %
Control System	30 M\$	11.2 %
<b>Main Linac Components</b>	<b>266.9 M\$</b>	<b>100 %</b>

Table X - Linac components breakdown cost for the SNS Linear Accelerator.

### 5.2.3 XADS Characteristics

The present reference characteristics of the XADS Linear Accelerator, as given in the last WP1 released document are recalled in the previous sections of this document (See section 2). The final proton energy is 600 MeV and the maximum beam intensity for the design is 10 mA.

From the current WP3 study following many discussions in recent meetings, the main XADS characteristics are summarized at the end of this document (Table XII). Some features concerning the linac sections can be extracted in the following Table XI.

	<b>INPUT Energy</b>	<b>OUTPUT Energy</b>	<b>Technology</b>	<b>Length</b>
<b>Injector</b>	90 keV	5 MeV	IPHI, TRASCO,...	20 m
<b>Intermediate Energy Section</b>	5 MeV	90 MeV	SC (or RT) resonators (Spoke, QWR, SCCH,...)	50 ...100 m
<b>High Energy Section</b>	90 MeV	600 MeV	SC (elliptical cavities)	180 m

Table XI – XADS preliminary linac sections.

Different simulations have shown that the intermediate energy section of the linac could be build with superconducting resonators of different type, as well as with room temperature structures. Some projects, like for example SNS, because it is a pulsed machine with a rather low (6%) duty cycle, have chosen room temperature cavities for this energy section. In this preliminary cost analysis it has been assumed that the intermediate part is using superconducting resonators [81].

### 5.2.4 First XADS cost estimation

Starting from previous estimates (Roadmap, ASH and EURISOL projects) completed by more recent analysis of some components, as it was proposed in recent WP3 meetings (i.e. introduction of SC structures for almost all the accelerator), a more detailed estimate can be proposed including all the components procurements and the associated manpower costs for design and assembly.

▪ Injector + Low Energy Beam Transport	15 M€
▪ Low Energy Section (SC resonators)	40 M€ <sup>4</sup>
▪ High Energy Section (SC cavities)	132 M€ <sup>5</sup>
▪ Medium Energy Beam Transport	3 M€
▪ High Energy Transfer Line	10 M€
▪ Control Systems	10 M€

---

**Total            210 M€**

The Roadmap of April 2001 [75], gives an estimation for the design and construction of the linear accelerator of 50 M€ + 100 M€ = 150 M€ (not including civil works, commissioning and indirect costs). In the present state of our estimation, a total cost of **210 M€** corresponds to a more complete list of components after reevaluation of their cost and taking in account the studies made by other projects. In this proposal, the major components of the low and high energy sections (RF structures and RF power systems) amount for 128 M€ (representing 61% of the total investment). The cost of the RF structures (54 M€ including cavities, couplers and fully equipped cryomodules) leads to an average cost per energy unit of 90 k€/MeV which is very comparable to all other projects. For the RF power system, a total RF available power of 10 MW has been considered with a cost of 74 M€ (including power tubes, circulators, high voltage power supplies, waveguides, low level RF controls,...). This installed power could give enough safety margin in regard of the full power needed for accelerating the beam (6 MW). This time, direct comparison with other projects is not quite possible as performance, power margin, and operation mode (CW or pulsed) of the different projects are quite different, leading to a large spread in the corresponding investment cost.

What has been discussed here above concerns mainly the linac components system cost. In order to supply a more complete estimation of the total cost of the linear accelerator several important items must be added :

- the associated R&D
- the civil works (accelerator tunnel and buildings)
- the site engineering
- the commissioning
- and other indirect costs

### 5.2.5 Conclusion

Some basic comments can be easily deduced from this preliminary analysis.

- 1) The need for a preliminary definition of the scope covered by this study, i.e. R&D costs in the initial phase of the project, civil works, beam commissioning, ...
- 2) The need for a more elaborated analysis of the major components of the accelerator, i.e. available RF power sources, industrial survey for the fabrication of RF structures, consequences of reliability performances in terms of redundancy, power margins,...

---

<sup>4</sup> include RF power systems, RF structures, focusing system, diagnostics, vacuum, interfaces and RF controls.

<sup>5</sup> same as above but also includes the cryogenic plant which is estimated to amount to 20 M€.

3) It is particularly urgent to define a.s.a.p. a WBS (Work Breakdown Structure) for the XADS project. It could help for a better analysis of the components and manpower cost. It could also facilitate that different contributors could compare its estimates on different components.

### 5.3. Potential for Other Applications

Over the past few years, great consideration was given to the feasibility of a new generation of high power proton accelerators (HPPA), capable of delivering beam powers ranging from a few MW to a few tens of MW, to be used as a driver to produce intense fluxes of protons impinging on a heavy target and producing by the spallation mechanism a high flux of neutrons and other particles.

Besides the specific application in ADS systems for transmutation of nuclear waste, other potential applications that could benefit from the availability of a proton beam of high intensity and energy in the hundreds-of-MeV belong to a wide range of fields such as fundamental and applied research in Materials Science, Fuel and Reactor Physics research, fundamental Particle and Nuclear Physics and Applications in Medicine and Biology. Some of these applications are:

- Spallation neutron sources
- Materials irradiation tools
- Production of radioisotopes (for medical, industrial and research purposes)
- Medical applications
- Muon and Neutrino factories
- Radioactive Nuclear and Ion Beams generation

All possible links and synergies between different R&D efforts, projects and initiatives going on at the international level in those areas should be considered in order to avoid duplication of efforts and to optimize resources. Common R&D is already being developed and this project is already benefiting from development of other projects.

It is important to stress that the feasibility of this XADS system can be of valuable use for a future neutron irradiation facility, eventually at the same location site. In fact, the same kind of accelerator and the same type of spallation target could be used to deliver an intense high flux neutron source. The neutron source can be easily adjusted (by adjusting the accelerator beam intensity). Also the neutron spectrum can be adequately chosen.

An interesting proposal addressing the same physics theme followed by the present XADS European strategy is the MYRRHA project [82] proposed jointly by the Belgium nuclear research center (SCK-CEN) and the company Ion Beam Accelerators (IBA, Belgium). This project of a neutron source for R&D applications is aiming at research in the field of waste transmutation based on a liquid lead-bismuth eutectic cooling a 20 to 30 MWth subcritical core.

However, the possibility of having a shared driver accelerator operating a multipurpose facility is not considered a priority, as this will introduce a higher level of complexity, and might significantly degrade reliability and availability. The corresponding cost-benefit implications should be carefully assessed and estimated, as well as other significant factors such as the consequences for the different types of facilities arising from the abnormal operation of the high power accelerator.

## 6. PRELIMINARY REQUIRED R&D

In the present preliminary phase of the XADS project, the needs in R&D are closely linked with the demonstration of the technical feasibility of the main components of the accelerator, and with the evaluation of their reliability. Three main items have been identified for the preliminary required R&D:

- The reliability study of the injector section, operated with beam.
- The full-demonstration of the technology for the high-energy section
- The building and testing of the first cavity prototypes for the intermediate section.

The first item deals with the injector section, the feasibility of which has been already demonstrated in the frame of several projects either partly, like in the IPHI (France) and TRASCO (Italy) projects, or completely, like in the LEDA project (Los Alamos, USA). But the high reliability required by the XADS accelerator implies to start a thorough campaign to test the reliability of every component of the injector. It is especially foreseen to check the availability of the whole injector under real operation, which requires a proton beam of at least 10 mA (a higher value would be preferable for safety margin) operated over a long period of time (a continuous run of six months for example).

Concerning the high-energy section (second item), R&D is already going on since a few years in Europe on superconducting elliptical cavities at a frequency of 700 MHz. Nevertheless, the demonstration of the full technology is not yet accomplished, and needs a few more years of additional work. As a matter of fact, it is important, besides the development of the bare superconducting cavity, to build prototypes of each auxiliary system needed for the cavity operation in a real environment (power coupler, RF source, power supply, RF control system, cryogenic system, cryostat...). This full demonstration requires the construction of a real prototype of an accelerating module in which, besides the superconducting cavities, all these elements have been included (see Figure 42).

The construction of such an integrated module at a given beta value (for example  $\beta = 0.65$ ) would thus be considered as a proof of principle of the technology, not only for that particular beta, but also for all others since many similarities exist between them. Moreover, such a module could allow some real scale demonstration with RF tests at nominal power (although without beam), and could be used for specific studies dealing with the XADS reliability issue, like the completion of the RF control system procedures in case of a cavity failure.



**Proof of principle:** cryomodule, RF power, cryogenics  
 (R & D Program for the High and Intermediate Energy Sections)

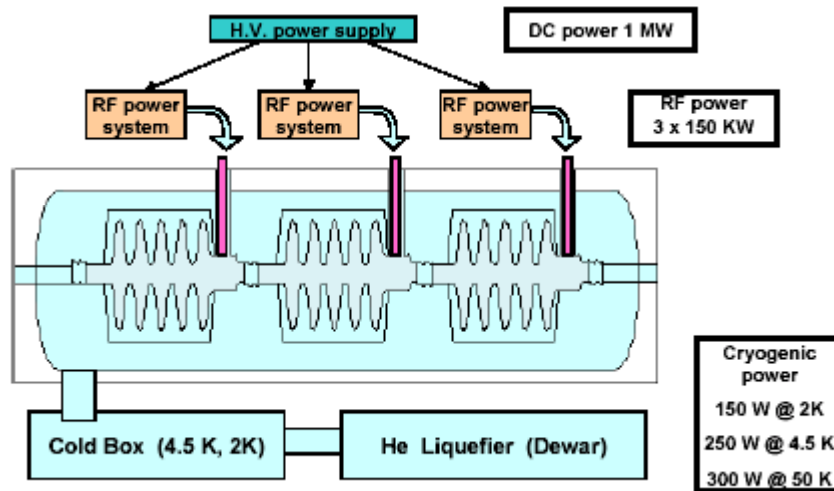


Figure 42 – Scheme of a complete cryomodule containing all the different elements needed for demonstration: cavity, RF coupler, RF system and cryogenics.

Finally, the third and last item concerns the intermediate section for which basic R&D is required in order to assess a solution which is as much reliable as possible and also of interest from an economical point of view. For these reasons, the participating institutes of WP3 share the vision that superconducting components should be used starting at the lowest possible energy. Indeed, compared to the classical room temperature copper structures, the proposed superconducting resonators are short and modular. That enables a better and more efficient approach for the implementation of the reliability strategy. As an example, separate independently phased RF transmitters could drive spoke-type or reentrant-type cavities. First cavity prototypes for the intermediate section are presently built and tested with quite a success. It is therefore important to actively pursue these developments. New cavity prototypes (in particular spoke and CH structures) equipped with their helium tank and power coupler are needed in that R&D phase. In parallel, the warm option has to be carefully studied and finalized for two reasons. First, it could very well be required for the injector section (a short DTL structure maybe needed if the RFQ output energy turns out to be not high enough to allow proper injection into the intermediate section). Second, although the RF losses are quite high for the warm option, its development risk is low, relying on an old but well established technology. In fact, the warm option could as well be considered by the other superconducting new structures proposed here as a baseline option to be compared with.

It should be stressed that the final aim of all these developments would be to allow the best technical option choice for the intermediate section of the XADS accelerator based on established demonstrated performance.

## 7. CONCLUSION

In summary, the main features of an XADS accelerator have been identified. In general, there is confidence that the technical feasibility of the proton machine is achievable within present technology as no hard showstopper has been found. However, in order to properly and safely move towards the construction phase of such an accelerator, some remaining points need to be worked out. Among the identified issues that would require more attention are the reliability assessment, the technology development of the intermediate section and the specific diagnostics items. Due to its acknowledged importance, the reliability topic will be addressed in a separate deliverable (Deliverable 57). It is therefore recommended to support a generic R&D that would help moving ahead in the know-how of an XADS type system.

Finally, the most important technical figures of the proton accelerator are summarized and reported in Table XII.

<b>General</b>	<b>Range or Type</b>	
Energy	350 – 600 MeV	± 1.0 %
Intensity (average)	0 – 6 mA	± 2.0 %
RF Duty Cycle	CW operation	
Beam Duty Cycle	0 – 100%	
Normalized rms emittance	< 0.4 $\pi$ .mm.mrad	longitudinal & transverse
<b>Accelerator type</b>	LINAC	
Ion Source	ECR type, 90 keV	
RFQ	4-vane, 352 MHz, 5 MeV	
Intermediate Section	TBD	Superconducting? Spoke? SCCH?
High Energy Section	Superconducting Elliptical Cavities, 704 MHz	
<b>Reliability</b>		
Beam trips > 1 s.	< 5 / year	
Beam trips < 1 s.	Not accounted for	
Availability	TBD	
Maximum Beam Loss	TBD	
Beam Dump Power	TBD	100 kW ?
<b>Target interface</b>		
Injection scheme	From top lid	
Footprint on target	4 rastering magnets	
Beam current density	< 50 $\mu$ A/cm <sup>2</sup>	(Window Target)
Beam current density	< 750 $\mu$ A/cm <sup>2</sup>	(Windowless Target)

Table XII – Main XADS Accelerator Characteristics.

## List of Figures

Figure 1 – Schematic layout of the XADS accelerator in the linac option.....	3
Figure 2 – Proposed beam time structure for the XADS accelerator. ....	7
Figure 3 – Schematic of the accelerator overall operation. ....	17
Figure 4 - Conceptual view of the XADS plant. ....	18
Figure 5 - Preliminary sketch of the arrangement of the reactor in operation.....	19
Figure 6 - Example of a circular beam scanning: pattern of the beam displacement (left) and power density deposited (right) in the target. ....	20
Figure 7 - Beam envelope along the beam line without deflection (length in meters). ....	21
Figure 8 - Beam envelope along the beam line with maximum deflection. ....	22
Figure 9 - Source and 95 kV extraction column: a) plasma chamber, b) RF ridged transition, c) quartz window, d) coils, e) 5 electrode extraction system, f) DCCT .....	36
Figure 10 – A 162 hour long run reliability test performed with the SILHI source at CEA/Saclay. ....	38
Figure 11 - Extracted beam and proton fraction vs RF power. ....	38
Figure 12 – A sketch of the IPHI RFQ.....	39
Figure 13 - First meter of the IPHI RFQ before brazing.....	40
Figure 14 - Radial matching section of the IPHI RFQ after brazing.....	40
Figure 15 - Drawing of the coupling plate. ....	40
Figure 16 – Pumping port.....	41
Figure 17 – Vacuum surrounding.....	41
Figure 18 - Sketch of the H-type linac family. ....	43
Figure 19 - Longitudinal bunch movement of one complete KONUS period.....	43
Figure 20 - Sectional view of a superconducting CH-cavity.....	45
Figure 21 - Schematic layout of a SC 350/700 MHz CH-DTL for XADS. The first six tanks (blue) have a RF frequency of 350 MHz and the last four tanks 700 MHz (green). ....	45
Figure 22 - Full transverse beam envelope of the SCCH linac of Table IV. The red line represents the 100 % beam envelope in the X-Z plane. Blue lines: aperture of the drift tubes. ....	47
Figure 23 - Full transverse beam envelope of the SCCH linac of Table IV. The red line represents the 100 % beam envelope in the Y-Z plane. Blue lines: aperture of the drift tubes. ....	47
Figure 24 - 100 % effective energy width along the linac with respect to the bunch center.....	48
Figure 25 - 100 % effective phase width profile along the linac with respect to the bunch center.....	48
Figure 26 - Output beam distribution of the linac in the $\Delta W$ - $\Delta\phi$ plane with 99 % emittance ellipse drawn for a beam current of 40 mA.....	49
Figure 27 - Relative RMS normalized emittance growth along the linac. ....	49
Figure 28 - Sectional view of a superconducting 16-gap 350 MHz CH-cavity for XADS. ....	50
Figure 29 - Middle-cut of a superconducting 16-gap 350 MHz CH-cavity for XADS.....	50
Figure 30 - 352.2 MHz, $\beta=0.35$ , 2-gap spoke cavity prototype (IPN Orsay – CERCA).....	52
Figure 31 - Cross-section of the " $\beta = 0.35$ " 2-gap spoke cavity.....	54
Figure 32 - Different linac architecture philosophies.....	55
Figure 33 - Simulation results for a matched beam: real beam envelopes, rms emittance evolution, and beam distribution at the linac exit (95 MeV). ....	57
Figure 34 - Two of the $\beta = 0.47$ cavities built for the TRASCO program in Italy, after fabrication (left) and on the test insert before cryogenic measurements (right). ....	60
Figure 35 – $Q$ vs. $E_{acc}$ curves of four single-cell $\beta = 0.47$ cavities. ....	61
Figure 36 - Phase advances for the full 600 MeV linac.....	62
Figure 37 - Beam size (rms) along the whole linac. ....	62
Figure 38 - Evolution of the rms beam emittance in the whole linac.....	63
Figure 39 - Real Estate accelerating gradient along the whole linac.....	63
Figure 40 – Overall Layout for the Cyclotron XADS option. ....	65
Figure 41 - Iterative process for the reliability and criticality assessment.....	66
Figure 42 – Scheme of a complete cryomodule containing all the different elements needed for demonstration: cavity, RF coupler, RF system and cryogenics. ....	73

## **List of Tables**

<i>Table I – Target Specifications.</i>	25
<i>Table II – Main Target Parameters.</i>	34
<i>Table III – Beam induced requirements from target.</i>	35
<i>Table IV - Structure parameter of a SC CH DTL design study for XADS.</i>	46
<i>Table V - Cavity parameter and peak fields of tank2 of the XADS SCCH-DTL.</i>	51
<i>Table VI – Spoke cavity parameters.</i>	54
<i>Table VII – Main characteristics of the spoke type cavities.</i>	56
<i>Table VIII - Main parameters of the high-energy linac sections.</i>	59
<i>Table IX - Parameters of the SC cavities.</i>	60
<i>Table X - Linac components breakdown cost for the SNS Linear Accelerator.</i>	69
<i>Table XI – XADS preliminary linac sections.</i>	69
<i>Table XII – Main XADS Accelerator Characteristics.</i>	74

---

## References

- 1 "PDS-XADS : Technical Specifications, Missions of XADS, Recommendations for the Main Characteristics", Deliverable 1, WP 1, PDS-XADS Report
- 2 J. Sherman & al., "A 75 keV, 140 mA proton injector", Rev. Sci. Instrum., Vol. 73, n°2 , p. 917, 2002
- 3 R. Gobin & al., "High Intensity ECR ion source ( $H^+$ ,  $D^+$ ,  $H^-$ ) developments at CEA/Saclay", Rev. Sci. Instrum., Vol. 73, n°2 , p. 922, 2002
- 4 "Motivation note for the choice of the EURISOL driver beam operating mode – CW or Pulsed ?-", H. Safa, J.L. Biarrotte & T. Junquera, EURISOL report
- 5 "A European Roadmap for Developing Accelerator Driven Systems (ADS) for Nuclear Waste Incineration", The European Technical Working Group on ADS, chaired by C. Rubbia, April 2001
- 6 P. Ausset and al., "Beam diagnostics for high intensity accelerators", Utilization and reliability of high power proton accelerators Workshop Proceedings – Aix en Provence, France, 22-24 November 1999
- 7 "Operational Experiences at Existing Accelerator Facilities", in Proceedings of the Workshop on the Utilization and Reliability of High Power Proton Accelerators. Mito-Japan, 1998
- 8 Spallation Neutron Source Beam Loss Policy, SNS Draft, April 2001
- 9 P. Pierini, Communication to the WP3 Genova Meeting, April 2002
- 10 "Technical Assessment of different Proton Beam Penetration Directions for the Target Unit", (XADS/WP4.3/D4), P. Rathjen, Framatome ANP report FANP NGES3/02/0007, XADS-DEL02-004, February 2002.
- 11 "Preliminary design of a vertical beam injection into the reactor (gas-cooled primary system)", A. Tkatchenko, J-L. Biarrotte, B. Giraud and G. Stalport, PDS-XADS report n° DOC02-130, April 2002.
- 12 See [http://people.web.psi.ch/rohrer\\_u/tesinq.htm](http://people.web.psi.ch/rohrer_u/tesinq.htm)
- 13 "European spallation source study", volume III, 1996
- 14 "The SNS ring to target beam transport line", D. Raparia, J. Alessi, Y.Y. Lee and W.T. Weng, Proc. of the PAC, New York, 1999
- 15 "A 200A, 500Hz, Triangle Current-Wave Modulator and Magnet used for Particle Beam Rastering", C. Rose & R.E. Shafer, Proc. of the PAC, Vancouver, 1997
- 16 "Development of a raster electronics system for expanding the APT proton beam", S. Chapelle & al., Proc. of LINAC, Chicago, 1998
- 17 "Testing of a Raster Magnet System for Expanding the APT Proton Beam", M.E. Schuze & al., Proc. of the PAC, New York, 1999
- 18 "Magnetic scanning system for heavy ion therapy", Th. Haberer, W. Becher, D. Scharadt and G. Kraft, NIM A330 (1993), 296-305
- 19 "Etude préliminaire du balayage circulaire d'un faisceau de forte puissance sur une cible", N. Pichoff, D. Uriot, DAPNIA/SEA 99-80
- 20 P. Rathjen, "Window target: proton current profile of the beam footprint", PDS-XADS document n° DOC/02/144, issued by WP4.3 & Framatome ANP GmbH, July 2002
- 21 L. Cinotti et al., "XADS Pb-Bi Cooled Experimental Accelerator Driven System – Reference Configuration – Summary Report", ANSALDO ADS1SIFX0500, Rev.0, June 2001
- 22 A. Stankovsky et al., "Radiological Issues of Accelerator-Driven Transmutation of Fission Product  $^{126}\text{Sn}$ ", OECD-NEA Workshop on Utilization and Reliability of HPPA's, Aix-en-Provence, France, 22-24 November, 1999
- 23 A. Negrini, "Design Specification – Performance Requirements for an Accelerator to couple with a Subcritical System", ANSALDO Internal Report ADS1SNPX0191, Rev.0, June 2000
- 24 A. Negrini, "Operating Requirements for a Proton Beam Accelerator to Couple with a Subcritical System", 3rd OECD-NEA Workshop on Utilization and Reliability of HPPA's, Santa Fe - New Mexico (USA), 12-16 May, 2002
- 25 P-Y. Beauvais, "Status report on the construction of the French high intensity proton injector (IPHI)" Proceedings of EPAC 2002, Paris, France
- 26 R. Ferdinand et al, "Optimization of RFQ design", EPAC 1998, 1106, Stockholm, Sweden
- 27 D. Schrage et al., "CW RFQ Fabrication and Engineering", Proc. Linac 99, Chicago, 1998, p. 679
- 28 R. Ferdinand et al., "Status Report on the 5 MeV IPHI RFQ", Proc. Linac 2000, Monterey, 2000
- 29 P-Y. Beauvais, "Status report on the construction of the French high intensity proton injector (IPHI)" Proceedings of EPAC 2002, Paris, France
- 30 A. Pisent et al., "TRASCO RFQ", Proc. Linac 2000, Monterey, 2000
- 31 R. Duperrier, "Dynamique de faisceaux intenses dans les RFQs – Toutatis", PhD thesis n°6194, Université Paris-sud ORSAY, France, July 2000

- 
- 32 R. Duperrier et al, "Toutatis, the Saclay RFQ code", Proc. Linac 2000, Monterey, 2000
- 33 B. Bondarev, A. Durkin, S. Vinogradov "Multilevel Codes RFQ.3L for RFQ designing", Moscow Radiotechnical Institute, Proc of Computational Accelerator Physics Conference (Virginia, USA, 1996)
- 34 J. D. Schneider, "Operation of the Low-Energy demonstration Accelerator: The proton injector for APT", PAC99, New York, pp 503-507
- 35 P. Balleyguier, "3D Design of the IPHI RFQ Cavity" Proc. Linac 2000, Monterey, 2000
- 36 "A Fully Automated Test Bench for the Measurement of the Field Distribution in RFQ and Other Resonant Cavity", F. Simoens, F. Ballester, A. France, J. Gaiffier, A. Sinanna, Proceedings of EPAC 2002, Paris, France
- 37 "Theoretical Analysis of a Real-life RFQ Using a 4-Wire Line Model and the Spectral Theory of Differential Operators", F. Simoens, A. France, CEA Saclay, Gif-sur-Yvette, France
- 38 "Electromagnetic Characterization of the First IPHI RFQ Section" F. Simoens, A. France, J. Gaiffier, Proceedings of EPAC 2002, Paris, France
- 39 "Simulations vs. Measurements on the IPHI RFQ Cold Model", P. Balleyguier & F. Simoens, Proceedings of EPAC 2002, Paris, France
- 40 "A New RFQ Model applied to the Longitudinal Tuning of a Segmented, Inhomogeneous RFQ with Highly Irregularly Spaced Tuners", F. Simoens, A. France, J. Gaiffier, Proceedings of EPAC 2002, Paris, France
- 41 "A New RFQ Model Applied to the Estimation of Mechanical Defaults Distribution", F. Simoens, A. France, J. Gaiffier, Proceedings of EPAC 2002, Paris, France
- 42 "Status of the Vacuum System for the IPHI Project", N. Rouvière & D. Francis, Proceedings of EPAC 2002, Paris, France
- 43 A. Sauer, R. Tiede, H. Deitinghoff, H. Klein, U. Ratzinger, R. Eichhorn, "Beam dynamics design of a superconducting 175 MHz CH-linac for IFMIF", EPAC 2002, Paris, France, June 2002
- 44 U. Ratzinger, Habilitationsschrift vorgelegt beim Fachbereich Physik der Johann Wolfgang Goethe-Universität Frankfurt, "Effiziente Hochfrequenz-Linearbeschleuniger für leichte und schwere Ionen", Frankfurt, Germany, July 1998
- 45 CST MICROWAVE STUDIO, Software for electromagnetic analysis and design in the high frequency range, CST Computer Simulation Technology
- 46 J. Klabunde, "The High Charge State Injector for GSI", Proc. of the 1992 LINAC Conf., Ottawa, AECL-10728, p. 570
- 47 H. D. Haseroth, "Pb Injector at CERN", Proc. of the 1996 LINAC Conf., Geneva, CERN 96-07, p. 238
- 48 U. Ratzinger, "RNB-specific Linac development", Nucl. Physics A 701 (2002), p. 641c-646c
- 49 U. Ratzinger, "Commissioning of the new GSI high current Linac and HIF related RF Linac aspects", Nucl. Instr. and Methods A 464 (2001), p. 636-645
- 50 U. Ratzinger, "Commissioning of the new GSI high current Linac and HIF related RF Linac aspects", Nucl. Instr. and Methods A 464 (2001), p. 636-645
- 51 J. Broere, "High Power Conditioning of the 202 MHz IH Tank 2 at the CERN LINAC3", Proc of the 1998 LINAC Conference, Chicago, p. 771
- 52 R. Eichhorn, "RF structures for linear acceleration of radioactive beams", PAC 2001, Chicago, USA
- 53 R. Eichhorn, U. Ratzinger, "Superconducting H-Mode Structures for Medium Energy Beams", LINAC 2000, Monterey, USA, Vol. 2 Page 926
- 54 R.W. Garnett & al, "Conceptual design of a low- $\beta$  SC proton linac", PAC 2001, Chicago, June 2001
- 55 P. Pierini & al, "Status of the high current proton accelerator for the TRASCO Program", EPAC 2002, Paris, June 2002
- 56 J-L. Biarrotte & al, "High-intensity driver accelerators for EURISOL", EPAC 2002, Paris, June 2002
- 57 J-L. Biarrotte & al, "High-intensity proton SC linac using spoke cavities", EPAC 2002, Paris, June 2002
- 58 J.R. Delayen & al., "Design and test of a superconducting structure for high-velocity ions", LINAC 92, Ottawa, August 1992
- 59 T. Tajima & al., "Evaluation and testing of a low- $\beta$  spoke resonator", PAC 2001, Chicago, June 2001
- 60 T. Tajima & al., "Results of low temperature tests on ANL spoke cavity (340 MHz,  $\beta=0.291$ )", LANL Report, LA-UR-01-3161
- 61 T. Tajima & al., "Test results of the LANL 350 MHz,  $\beta=0.175$ , 2-gap spoke resonator", LINAC2002, Gyeongju, Korea, August 2002
- 62 G. Olry & al, "Design and industrial fabrication of  $\beta=0.35$  spoke-type cavity", EPAC 2002, Paris, June 2002
- 63 G. Olry & al, "R&D on spoke-type cryomodule", EPAC 2002, Paris, June 2002
- 64 G. Olry & al, "Study of a spoke cavity for low-beta applications", SRF2001, Tsukuba, September 2001
- 65 TESLA Technical Design Report, March 2001, Desy Print, DESY 2001-011
- 66 The TRASCO\_AC Group, "Status Of The High Current Proton Accelerator For The TRASCO Program", INFN Internal Report INFN/TC-00/23, December 21, 2000

- 
- 67 "A Superconducting Proton Linear Accelerator for Waste Transmutation", H. Safa & al., Proceedings of the 3<sup>rd</sup> International Conference on Accelerator Driven Transmutation Technologies and Applications, Praha, Czech Republic, June 1999
- 68 J.L. Biarrotte, H. Safa, J.P. Charrier, S. Jaidane, H. Gassot, T. Junquera, J. Lesrel, G. Ciovati, P. Pierini, D. Barni, C. Pagani, 704 "MHz Superconducting Cavities For A High Intensity Proton Accelerator", in Proceedings of the Ninth Workshop on RF Superconductivity, Santa Fe, NM USA, 1999
- 69 G. Ciovati, P. Kneisel, K. Davis, K. Macha, J. Mammosser, Superconducting Prototype Cavities For The Spallation Neutron Source (SNS) Project, in Proceedings of the EPAC 2002, Paris, France, p. 2247
- 70 "The feasibility of high power cyclotrons", Th. Stambach et al., Nuclear Instruments and Methods in Physics Research B 113 (1996) 1-7
- 71 "Recent performances of the TRIUMF cyclotron and status of the facility", G. Dutto et al. Proceedings of the 14th International Conference on Cyclotrons and their Applications, Cape Town, South Africa, 8-13 October, 1995, Editor John Cornell, World Scientific
- 72 "A superconducting ring cyclotron to deliver high intensity proton beams", L. Calabretta et al., 2000 European Particle Accelerator Conference, Vienna, Austria
- 73 CEBAF Project Review (1988)
- 74 N. Pichoff et al., "The ESS-CONCERT funnel line", 2001 Particle Accelerator Conference, New York City
- 75 "European Roadmap for ADS" April 2001. Published by ENEA, Rome (Italy)
- 76 "The SNS Superconducting Linac System" C. Rode et al., PAC2001. Chicago (USA), June 2001. Project Web site: <http://www.sns.gov/project/info>
- 77 ADTF Project Web Site : <http://apt.lanl.gov/>
- 78 "SC Proton Linac for the Concert Multi User Facility" PAC2001, Chicago (USA), June 2001. Project Web Site : <http://essnts.ess.kfa-juelich.de/TheESSProject/>
- 79 Project Web Site : <http://www.ganil.fr/eurisol/>
- 80 Project Web Site : [http://ps-div.web.cern.ch/ps-div/SPL\\_SG/](http://ps-div.web.cern.ch/ps-div/SPL_SG/)
- 81 J.L. Biarrotte et al., "High Intensity Proton SC Linac using Spoke Cavities", EPAC 2002, Paris (France) June 2002
- 82 H. Aït Abderrahim & al., "MYRRHA: A Multi-Purpose Accelerator Driven System for Research and Development", Nuclear Instruments and Methods in Physics Research, A, **463**, p.487 (2001)